CRANFIELD UNIVERSITY

SCHOOL OF ENGINEERING

PhD THESIS

A novel laser diode wavelength stabilisation technique for use in high resolution spectroscopy

Academic Year 2014-2015

Abdullah Shah Asmari

Supervisors: Dr Jane Hodgkinson, Prof Ralph. P. Tatam

This thesis is submitted in partial fulfilment of the requirements for the degree of Doctor of Philosophy

Abstract

Tuneable diode laser absorption spectroscopy (TDLAS) based gas sensors are widely used for trace gas detection for their high selectivity and sensitivity. The laser source used in TDLAS requires a narrow line width in the order of 10s of MHz, with a wavelength stability multiple orders lower than the molecular absorption line width, which is, for example, 4.1GHz (38pm) for an air broadened methane line.

TDLAS requires the use of a laser diode with a long term wavelength stability of better than 10% of the absorption line width of the target gas species. The wavelength stability of the laser is highly temperature dependent as the wavelength increases with increasing temperature. Therefore, control of the temperature of the laser diode is vital for stabilising the laser emission wavelength.

In this thesis, a novel method has been proposed to measure and stabilise the temperature of a laser diode. The laser diode emission wavelength was stabilised by using its measured junction voltage in a control feedback loop. In order to determine the junction voltage, a series resistance correction term was identified, which was the novel part of this wavelength stabilisation technique. The laser diode junction and forward voltages were calculated from the forward voltage drop of the laser diode at measured at various operating temperatures. The laser diode series resistance was measured dynamically and was subtracted from the forward voltage to calculate the junction voltage. Both the forward voltage and series resistances were found to be temperature dependent.

This method was investigated for its short term (~ 5minute) and long term (~ 1 hour) wavelength stability and was compared with other available methods. The laser diode wavelength stability attained using this method has been also investigated at various ambient temperatures (10-40 °C).

The laser diode had a long term wavelength stability of ±0.7pm (±80MHz) and wavelength drift of 0.03pm /°C with ambient temperature using the junction voltage control technique. On the other hand, the conventional thermistor based control technique had a long term

wavelength stability of ±2.2pm (±240MHz) and a wavelength drift of 3.8pm /°C with varying ambient temperature. The wavelength stability attained using junction voltage control was also compared with wavelength stability attained using the forward voltage technique. For this project, the forward voltage method was technique proposed initially to stabilise the laser diode wavelength. However, when this technique was used to stabilise the laser diode under variable ambient temperature, the laser wavelength drift was found to be ±4.5 pm/ ºC, almost double the conventional thermistor-based method. The long-term wavelength stability of the laser diode achieved using this technique was ±1.3pm (±145MHz), better than the conventional thermistor-based method.

A further objective of this project was to develop a compact method for stabilising the laser diode and implement it in TDLAS based wavelength modulation spectroscopy (WMS) for detecting methane gas (CH_4). Therefore, junction voltage control was used to stablise the laser diode wavelength in WMS, which had a wavelength drift of 0.24pm / ºC (26MHz / ºC) with ambient temperature, as compared to that achieved using the conventional thermistor-based control, which was 2.6pm / ºC (295MHz / ºC).

In WMS, the laser emission wavelength is locked conventionally to molecular absorption line. This wavelength locking technique gives wavelength stability in the range of 1.6 kHz-40 kHz over a duration of few seconds. However, this wavelength technique is complex and requires careful optical alignment. The wavelength locking technique is also sensitive to the optical path length of the reference gas cell and to the concentration of the reference gas. The junction voltage control is insensitive to optical alignment and uses electrical means to stabilise the laser diode wavelength. In addition, the locking technique is simple and could be implemented within the laser package.

The junction voltage control technique has also been investigated for light emitting diodes with initial results suggesting that this method could also be extended for their temperature stabilisation.

Acknowledgements

I would like to thank my academic supervisors Jane Hodgkinson and Ralph Tatam for their continuous support and guidance throughout my PhD.

I would specially thank Steve Staines for his technical help during my PhD. Steve went an extra mile to help me with my electronics and gave me excellent suggestions.

I would like to thank everybody in the laboratory area for helping and being patient with me for hoarding equipment in my lab during the last few months of my PhD, while I was finishing my experimental work.

Finally I would like to thank my parents and my wife for their continuous support and encouragement during my PhD.

This work was supported by an EPSRC (Engineering Physical Sciences Research Council) grant (EP/I002278)

Table of contents

List of Figures

List of Tables

Notations

α	Lorentz halfwidth
α , β	Varshni parameters
α_a	The temperature coefficient (eV/K) of band gap energy
α_e	Expansion coefficient
A	Absorbance
A_d	Area of a diode
A_{mod}	Modulation amplitude
A_j	Junction area
b_c	Pressure broadening coefficient
B	Frequency dependency of the laser excess noise
C	Concentration
e	Charge on electron
E_a	Dopant activation energy
E_c	Conduction band
E_g	Band gap energy
E_V	Valence band
E_{FC}	Quasi Fermi level of the conduction band
E_{FV}	Quasi Fermi level of the velance band
f_m	Modulation frequency
F	Line shape
F_e	Finess of Fabry-Perot etalon
h	Plank's constant
I_{dark}	Photodiode dark current
I_f	DC injection current
i_T	Thermal current
i_s	Shot current
I_s	Saturation current of a diode
I_o	Intensity of light
I_{th}	Threshold current of laser diode
$I(\nu)$	Transmitted intensity
K	Force constant
k_b	Boltzmann's constant
k_o	Absorption coefficient
$k(\nu)$	Absorption cross section
Δf	Detection bandwidth
$l_r = nl$	Cavity length of laser
L	Absorption medium length
λ_m	Transmission peak wavelength of Fabry -Perot etalon
λ_{mod}	Centre wavelength
λ_0	Average wavelength of laser

λ_p	Peak lasing wavelength
$\delta\lambda_m$	Size of wavelength shift of a laser diode
M	Atomic weight
M_m	Molecular mass
n	Refractive index
η	Laser diode slope efficiency
$\Delta\eta$	Change in laser diode slope efficiency
η_i	Intensity modulation index
η_{ideal}	Ideality factor
η_{pd}	Efficiency of the photo detector
ΔN	Change in carrier density
p	Gas pressure
P	Transmitted power
Pj	Power dissipated when the laser operated in CW mode
P_o	Laser diode output power
R_c	Ohmic contact resistance
R_d	Detector resistance
R_p	Parallel resistance
R_s	Series resistance
R_{sh}	Shunt resistance
R_{th}	Thermal impedance
$\Re$	Responsivity of photodiode
ρ_B	Resistivity of the metal-semiconductor substrate
S	Line strength
S_T	Temperature dependence of the carrier mobility
Δt	Time constant of the lock-in amplifier
τ	Ring down constant
T	Temperature
T_j	Junction temperature
ΔT_{hs}	Heat sink temperature
T_{ref}	Reference temperature
T_0	Characteristic temperature
$T(\lambda)$	Etalon transmission
T_{max}	Peak etalon transmission
ΔT	Temperature rise in the active region of a diode
μ	Reduced mass of the system
v_o	Frequency at the line centre
$V_{dc,f}$	Dc forward voltage
$\bar{v}$	Natural frequency of vibration of a bond
δv	Half-width of the absorption line
Δv_D	Doppler broadened linewidth
Δv_L	Lorentzain linewidth

Δv_v	Voigt linewidth

1 Introduction

Tuneable diode laser absorption spectroscopy (TDLAS) based sensors are reliable, compact and gas specific. Laser diodes in TDLAS are single mode, with output wavelengths that match absorption features of the target gas, typically in the mid-infrared region. Sensors based on TDLAS have wide applications, including in atmospheric measurement, where high sensitivity is required, and in aircraft or gas flux measurement, where a fast response time is essential. The gas absorption lines have narrow linewidths and to achieve high resolution spectroscopy, the linewidth of the laser diode has to be narrow. Therefore, the laser diode should have sufficiently narrow line width and high wavelength stability to meet the requirements of TDLAS. The laser diode output characteristics, such as wavelength and output power, are temperature dependent. Therefore, a laser diode used in TDLAS will require a robust temperature controller to achieve suitable wavelength stability.

In addition, the laser diode wavelength drifts with time due to heat generated by the laser diode injection current and variation in the ambient temperature in the absence of a wavelength control system. Therefore, some means of laser wavelength control will be required to maintain the laser diode's central wavelength.

This chapter sets out the background to the application, the objectives and outlines the structure of the thesis.

1.1 Back ground to laser diode wavelength stability techniques

Laser diode central wavelength drifts over time with fluctuation in operating temperature and injection current. To reduce the drift in the laser diode wavelength, several techniques have been developed that can be divided into the following categories [1]:

- Interferometers
- Molecular absorption lines
- Atomic transitions

Laser wavelength locking systems based on interferometers such as Fabry-Perot (FP) etalons and waveguide resonators are used widely due to their simple implementation and wide tuning range. The laser diode central wavelength is locked to the FP etalon. The first

derivative of the FP etalon transmission curve can be used in the feedback loop for the wavelength stabilisation of the laser diode [1][2].

FP based wavelength locking systems provide good short-term wavelength stability. However, the cavity length of the FP cavity fluctuates with temperature and will require an absorption reference to maintain its cavity length, complicating its use for ensuring long-term wavelength stability [1].

Molecular and atomic absorption lines are the other techniques where the laser central emission wavelength is locked to the atomic or molecular absorption lines such as rubidium (RB), cesium(Cs), methane (CH_4) and ammonia(NH_3). These atomic and molecular absorption lines provide good long term wavelength stability. However, absorption line locking provides wavelength locking at discrete wavelengths (due to the absorption lines at specific wavelengths) limiting its application [3].

The above three categories and the variety of wavelength locking techniques could be adopted in TDLAS . The target gas of this thesis is methane. Methane was selected as it has inference free, strong gas absorption lines in the near infra-red region, it as a narrow line width and TDLAS is used widely for its detection.

1.2 Application to gas sensing

Gas detection in TDLAS is carried out by scanning the narrow emission line width of a laser diode across the target gas absorption line. The narrow line-width and absorption-specific emission wavelength allows for selective, high-resolution detection. TDLAS gas sensors have high signal to noise ratio (SNR), fast response times and accuracy. To achieve high resolution spectroscopy, the laser diode wavelength has to be known accurately and its wavelength fluctuation should be smaller than the line width of the target gas absorption line [4]. This stringent requirement of wavelength stability much better than the line width of the gas absorption line necessitates a very stable laser diode in TDLAS.

The laser diode emission wavelength drifts with temperature and has a large temperature coefficient. Therefore the temperature control of the laser diode is vital for TDLAS.

The common method for stabilising the laser diode emission wavelength may be achieved by locking the laser diode to a gas absorption line. While this method has the advantage of high

wavelength stability, it requires highly sensitive and difficult optical alignment and an additional measurement channel.

This thesis will investigate alternative methods for stabilising the laser diode temperature, with the requirement that the technique simple, has a wide tuning range for use in TDLAS and other laser diode based applications where stringent laser diode wavelength stability is required. In addition, the project will aim to develop a compact wavelength stability technique (without the requirement of a wavelength locking reference) using an all-electronic method.

1.3 Thesis objective

This thesis is focused on stabilising the operating temperature of a laser for use in high resolution TDLAS. The main objectives of thesis are outlined below:

- Investigate the performance of laser diode wavelength stability with temperature using conventional thermistor and thermoelectric cooler based system
- Investigate methods and techniques to measure the operating temperature of the laser diode
- Investigate the feasibility of using the voltage drop measured across the laser diode terminals as a temperature sensor and for use in stabilising wavelength of the laser diode
- Implement this scheme in tuneable laser diode absorption spectroscopy
- Extend this scheme to other light sources, such light emitting diodes

The developed wavelength stablisation approach will be exploited in a TDLAS system to detect methane. The scheme could be applied more generally to the detection of other gases.

1.4 Thesis outline

Concise literature review is presented in Chapter 2, covering the issue of laser diode wavelength stability and reviewing the laser diode wavelength stabilisation techniques that have been used gas absorption spectroscopy systems. Gas detection using the optical

absorption spectroscopy technique Wavelength Modulation Spectroscopy (WMS) is discussed in detail. In addition, factors that limit the performance of WMS, such as interference fringes and residual amplitude modulation (RAM) , are also reported. The primary objective of this thesis is to develop a wavelength stabilisation technique for use in wavelength modulation spectroscopy that will provide an alternative to the conventional technique of locking to the wavelength of a gas absorption line, which is affected by factors like RAM and interference fringes. The Literature review identified the need for a simple and robust laser diode wavelength stabilisation technique for use in TDLAS

Chapter 3 covers theoretically the effect of temperature on the laser diode threshold current, output power and emission wavelength. Different methods for measuring the laser diode operating temperature are also investigated and compared. The effect of the laser diode series resistance is also considered. Diode series resistance measurement methods are theoretically and experimentally investigated and compared. The experimental verification the theoretical analyses in chapter 3 is carried out in the next chapter

Chapter 4 starts with a theoretical analysis of the effect of temperature on the forward voltage of the laser diode. This is followed by experimental work to develop suitable techniques for measuring the forward voltage of a laser diode. Different light source such as a distributed feedback (DFB) laser, vertical cavity surface emitting laser and LED were investigated to determine the effect of temperature on their forward voltages and the use of their forward voltages as a measure of their junction temperature. An alternative method known as the *power averaged wavelength technique* is also investigated for measuring the junction temperature. In the following chapter forward voltage method is investigated for calculating the laser diode junction temperature and then using it to stabilise its emission wavelength.

Chapter 5 deals with a modified technique whereby the actual junction voltage of a laser diode is determined by taking into account the series resistance and correcting the measured forward voltage. A theoretical model is followed by experimental investigation into the wavelength stability achieved using the junction voltage method implemented in a control feedback loop. Finally, the use of the junction voltage method is investigated for stabilising the laser diode by means of an optical spectrum analyser and molecular absorption line. In the next chapter the application of junction voltage based wavelength control in TDLAS technique is investigated

In chapter 6, a WMS based system is setup with a conventional temperature controller and is used for probing different concentrations of methane gas. The conventional temperature controller is replaced with the newly developed temperature control method and the system again used to detect methane gas. In the final setup, the influence of variations in ambient temperature on the performances of the system employing the conventional temperature controller and of that using the newly developed method is compared.

Chapter 7 concludes this thesis with a summary and consideration of future work.

1.5 References

[1] T. Ikegami, S.Sudo and Y.Saki, Frequency Stabilization of Semiconductor Laser Diodes, Boston: Artech House, 1995

[2] R. W. P. Drever, J. L. Hall, F. V. Kowalski, J. Hough, G. M. Ford, A. J. Munley, andH. Ward, "Laser phase and frequency stabilization using an optical resonator", Applied Physics B , vol. 31, no. 2, pp. 97-105, 2007.

[3] S. Schilt, R. Matthey, D. Kauffmann-Werner, C. Affolderbach, G. Mileti, and Luc Thévenaz1, "Laser phase and frequency stabilization using an optical resonator", Applied Optics , vol. 47, no. 24, pp. 4336-4344, 2008.

[4] W. Demtroder, Laser Spectroscopy Vol.1 : Basic Principles, Springer-verlag Berlin Ltd, 2008.

2 Introduction to optical gas detection

This chapter discusses the issues raised by the wavelength stability required of laser diodes used in TDLAS. The aim of this chapter is to review laser wavelength locking references and methods for use in absorption spectroscopy.

The basics of optical gas detection will be discussed along with the reasons for the choice of the target gas, methane. This will be followed by a detailed explanation of WMS, which is used experimentally in chapter 6. The noise sources that affect WMS and techniques to eliminate or reduce their influence on the detection sensitivity of WMS are also discussed in this chapter.

2.1 Wavelength stability of laser

The stability of the laser wavelength is vital for the resolution of narrow band molecular transitions in the probed species. The wavelength of the laser drifts due to geometric changes in its cavity length induced by thermal, mechanical and acoustic noises. The temperature and carrier density can also affect the refractive index of the laser diode cavity. The change in operating temperature and current can therefore change the optical cavity length of the laser diode, which in turn changes the wavelength output from the laser. The change in resonant frequency due to the change in the laser cavity length can be represented the in the following equation [1]

$$\frac{dv}{v} = \frac{dl_r}{l_r} \tag{2.1}$$

Where v is the lasing frequency and $l_r = nl$ is the cavity length. Taking into account the thermal expansion of the cavity length and the thermal induced refractive index change, the change in the cavity length of the laser diode in response to a change of temperature, dT_{av} can be expressed as

$$dl_r = nl\left(\alpha_e + \frac{\partial n}{n\partial T}\right)dT_{av} \tag{2.2}$$

Where α_e is the thermal expansion coefficient, n is the refractive index of the cavity and T is the operating temperature of the laser. Inserting equation (2.1) in equation (2.2), the thermally induced change on the laser wavelength can be expressed as

$$\frac{dv}{dT} = -(\alpha_e + \frac{\partial n}{n\partial T})v \qquad (2.3)$$

In the next section different wavelength locking reference and techniques used to stabilise the laser diode emission wavelength will be reviewed

2.2 Basic principle of stabilising laser diode emission wavelength

The laser diode emission wavelength is often stabilised by comparing its wavelength to the wavelength of reference wavelength source and an error signal is fed back to the laser diode driver as shown in Figure 2.1.

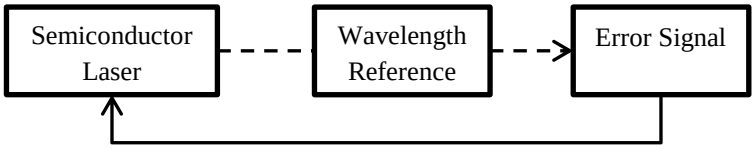

Figure 2.1 Basic concept of laser diode wavelength stabilisation. Adapted from [2]

Several types of wavelength references, such as Fabry-Perot (FP) etalons and gas molecules absorption lines have been used to stabilise the laser diode wavelength and are described below.

The laser diode wavelength can be stabilised using an external wavelength reference by adopting two basic methods, as shown in Figure 2.2. In one method, a narrow wavelength reference is used for wavelength stabilisation of the laser diode [2]. The derivative of the spectral curve of a wavelength reference such as an FP interferometer or gas absorption line is acquired and is used for wavelength stabilisation. Alternatively, a narrower wavelength spectrum can be obtained from an external reference source such as a Doppler-free line of gas molecular absorption. The derivative of this line is then acquired. The zero crossing point between the derivative curve at the horizontal axis is used as the reference wavelength [2].

Both methods require accurate acquisition of the centre wavelength of the referenced spectrum.

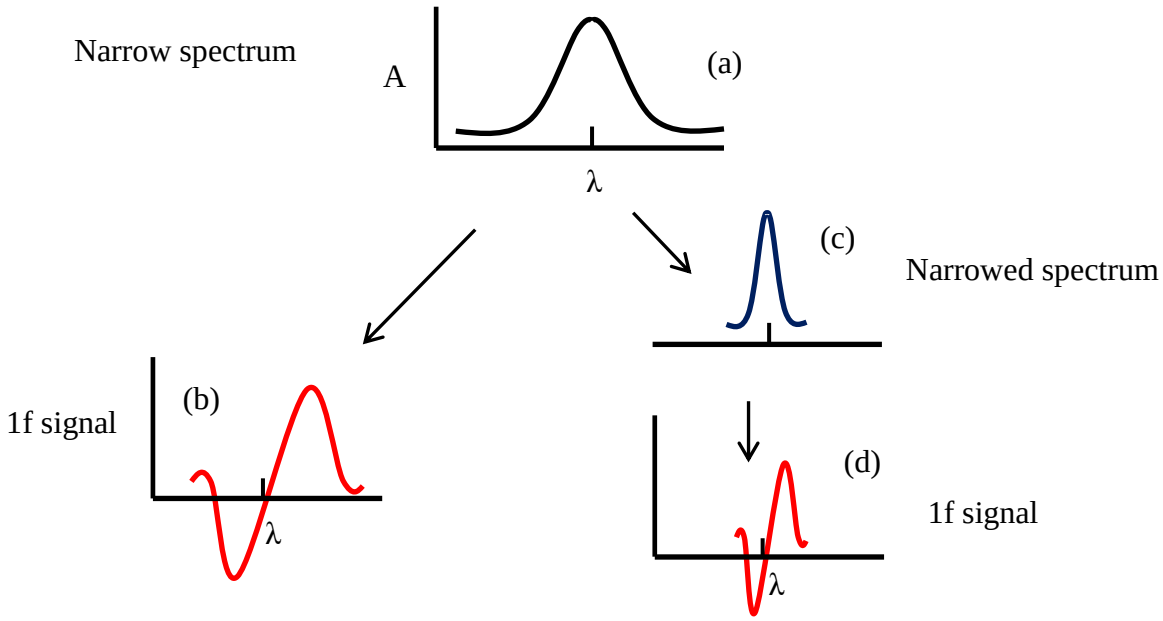

Figure 2.2 (a) The use of narrow spectrum itself as a wavelength reference (b) and the used of the narrower spectrum obtained from the original spectrum. Redrawn from [2]

Table 2.1 summarises the wavelength locking techniques and references used in stabilising laser diode wavelength.

Table 2.1 Categories and types of wavelength references Taken from [2]

Category	Type	Materials
Interferometers	Fabry-Perot Wave guide resonator	Air, quartz, glass
Atomic transition	Normal absorption, Optogalvanic effect	Rb, Cs, Na, K, Ba, Bi etc
Gas molecular absorption	Diatomic molecules	I_2, Cs_2, Na_2, K_2, Rb_2, O_2, HF, HI
	Poly atomic molecules	H_2O, NH_3, HCN, C_2H_2, CH_4, H_2CO

The wavelength stability of the laser diode cannot exceed the line width of the wavelength reference, so that the choice of the wavelength reference should reflect the requirements of the wavelength stability. A good wavelength reference should be independent of external perturbations such a temperature, pressure, electric and magnetic fields [3]

In the next section, the wavelength techniques tabulated in Table 2.1 are reviewed in detail.

2.2.1 **Interferometer based wavelength references**

The interferometer is the most common and oldest method used for laser diode wavelength stabilisation. Interferometers such as waveguide resonators and FP etalons are easy to implement and have wide tuning ranges [4].

The 1st derivative of the FP transmission curve is used for locking the laser diode emission wavelength. When a laser diode is modulated with a sinusoidal signal, the laser diode wavelength modulation λ can be described by the following equation [2]

$$\lambda = \lambda_o + \lambda_{mod}\sin(\omega t) \tag{2.4}$$

Where λ_0 is the average wavelength of the laser diode, λ_{mod} is the wavelength amplitude modulation, ω is the frequency modulation, and *t* is the time.

The transmission, $T(\lambda)$, of the FP etalon is given by [2]

$$T(\lambda) = \frac{T_{max}}{\left[1 + 4\left\{\left(\frac{F_e}{\pi}\right)\sin\left[\frac{(\lambda_{mod} - \lambda_m)\pi}{FSR}\right]\right\}\right]} \tag{2.5}$$

Where T_{max} is the peak etalon transmission; *FSR* is the free spectral range of the FP etalon, F_e is its finesse, and λ_m is the transmission peak wavelength of FP etalon.

If the argument of the sinusoid in equation (2.5) meet the following condition

$$\frac{(\lambda - \lambda_m)\pi}{FSR} \ll 1 \tag{2.6}$$

then equation (2.5) can be expanded in a Tayler series about the average wavelength λ_0 , resulting in a first approximation

$$T(\lambda) = T(\lambda_0) + T'(\lambda_0)\sin(\omega t) \tag{2.7}$$

$T'(\lambda_0)$ is the first derivative of the Fabry-Perot etalon transmission curve with respect to the laser wavelength . In equation (2.7), the amplitude and the sign of sin(ωt) are directly proportional to the first derivative of the etalon transmission curve

For a tightly locked system, the difference between the average wavelength and etalon transmission peak wavelength is much less than the etalon pass band width, $\lambda_0 - \lambda_m \ll \frac{FSR}{F}$.

Therefore, the etalon transmission function and its derivative can be approximated as

$$T(\lambda) = T_{max} \tag{2.8}$$

$$T'(\lambda_0) = \left[-\frac{8(\lambda_0 - \lambda_m)}{\left(\frac{FSR}{F}\right)^2} \right] T_{max} \tag{2.9}$$

The first derivative of the etalon transmission becomes zero when $\lambda_0 = \lambda_m$ i.e. the laser wavelength is locked.

Byovskii *et al* [2], in 1970 for the first time implemented a wavelength stability scheme using an FP etalon. The laser had a frequency tuning coefficient of -0.9 GHz/mA, and the authors modulated the injection current of the laser diode. They obtained the 1st derivative of the F-P transmission and, by using this derivative curve as a wavelength reference, they attained a frequency (wavelength is directly related to wavelength) stability of 40MHz over a duration of several minutes.

Picque and Poizen obtained an improved frequency stability of 4MHz by enhancing the cooling system for the GaAs laser diode [5] by using helium gas.

A practical FP-based scheme for the wavelength stabilisation of a laser diode was developed by Okoshi *et al*. [6]. Figure 2.3 shows the block diagram of their wavelength stabilisation scheme. In this scheme the laser diode wavelength was stabilised by feeding back the error into Peltier cooling system.

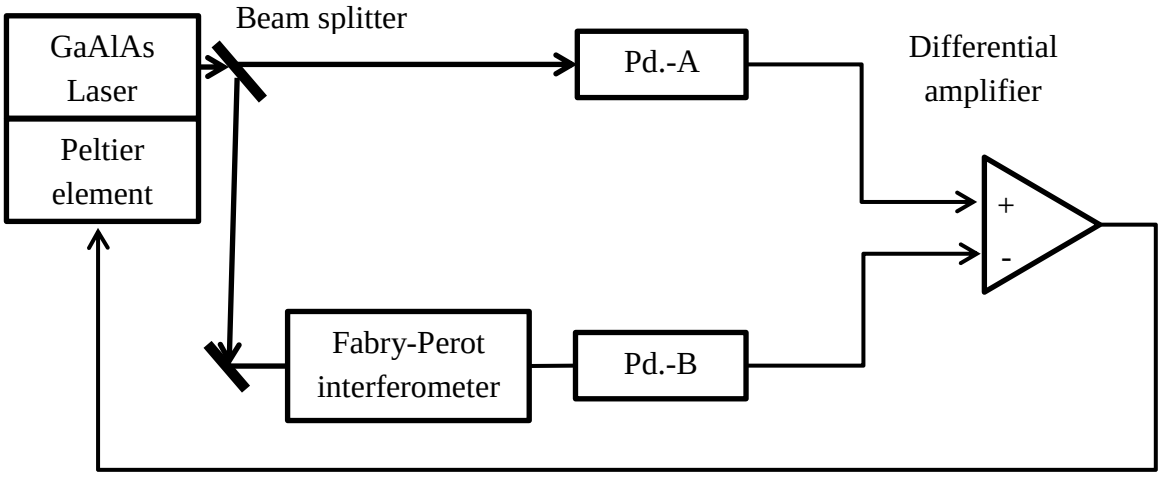

Figure 2.3 Wavelength stability scheme based on Fabry-Perot interferometer, designed for use in practical application. Redrawn from []

The unmodulated output of the GaAs laser, at an operating wavelength of 0.828μm, was divided into two parts and fed separately into a photo-detector A (Pd A) and, via a Fabry-Perot interferometer, to photo-detector (Pd.B). The pass band of the Fabry-Perot was adjusted using a piezoelectric tuning element, so that the laser emission wavelength coincided with the maximum – slope of the transmission spectrum of the FP. The detected voltages of the photo diodes were sent to a differential amplifier and fed back to the Peltier cooling element. The output from the differential amplifier maintained the central wavelength of the laser output at a fixed wavelength corresponding to the maximum slope point. Their results suggested that frequency fluctuation could be reduced below 10MHz [6].

A slightly modified version of the above scheme was proposed by Frave and Gaven, where the output from the differential amplifier was fed to the laser diode current driver instead of the Peltier [7]. The advantage of this scheme was its fast response compared to the system of Okoshi *et al*. Frave and Gaven reduced the long-term fluctuation to 8 MHz and the short term fluctuation to 1.5MHz.

However, the temperature dependence of the FP cavity will cause fluctuations in the wavelength reference. To overcome this, improved materials such as ultra-low expansion (ULE) glass has allowed the demonstration of sub Hz wavelength stability of a laser. Alnis *et al* [8] reported a frequency drift of 0.1Hz/s using ULE and a vertically mounted FP cavity. Kessler *et al* [9] proposed an FP cavity made from single-crystal silicon. The cavity configuration was insensitive to vibration, with superior stiffness of the silicon crystal. They reported frequency stability of $1x10^{-6}$ in the time scale of 0.1-1s and the stability remained at a low level of 10^{-6} for 10s. Hirata *et al* [10] showed an improved laser frequency stability, with frequency drift of 25 MHz/s.

2.2.2 **Atomic transitions**

Solids or gases emit light due to heat or electric discharge. This light contains spectral lines corresponding to definite wavelengths. These spectral lines from atomic transitions can be used as wavelength references for stabilising the laser diode wavelength [2]. This emission of light can be described by the quantum theory of radiation:

$$hv = E_{upper} - E_{lower} \qquad (2.10)$$

E_{upper} and E_{lower} represent the upper energy level and lower energy level respectively. h is the Plank constant and v is the frequency of the emitted photon.

Historically, atomic transitions have been used as wavelength references in the microwave region, in the so-called atomic clock [2]. The use of an atomic transition as a wavelength reference was first attempted by Arditi and Picque, using a microwave frequency standard technique [11]. They achieved absolute wavelength stability to within 2 parts in 10^{10} for a duration of 5minutes.

Yabusaki *et al* in 1981 carried out the first direct stabilisation of a laser diode's output wavelength using an atomic transition [12]. They stabilised the wavelength of a GaAlAs laser diode by using the Doppler free spectrum of the Cs-D_2 line at 0.8521μm.They achieved an estimated stability between $3x10^{-12}$ and $1x10^{-11}$ for the average time durations of 0.1s and 1000s respectively.

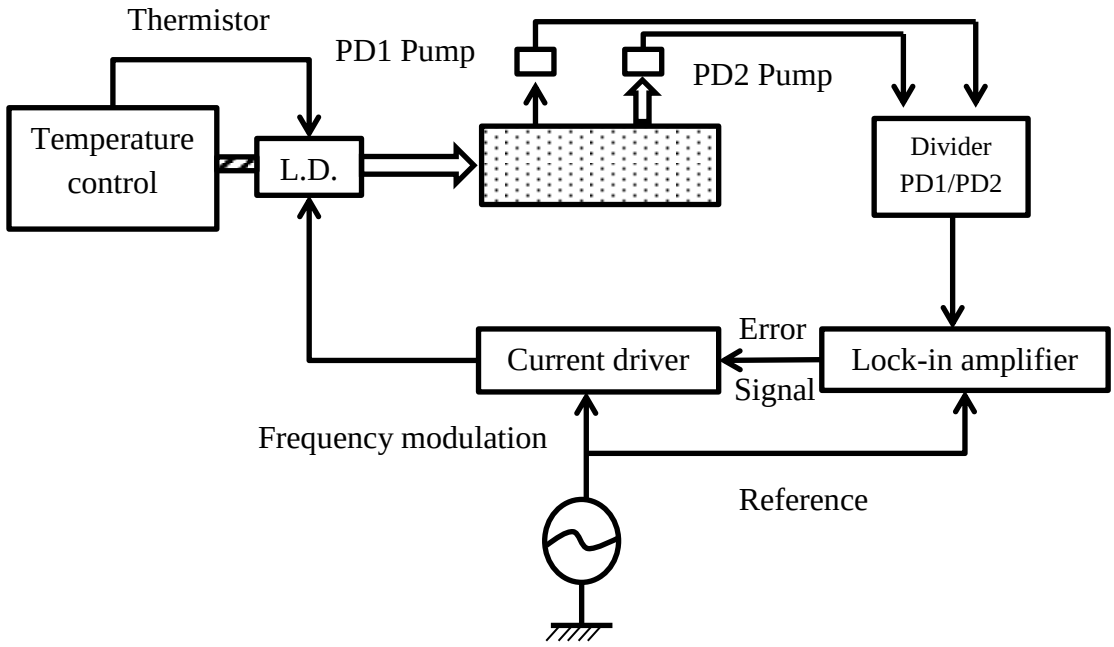

Figure 2.4 Experimental setup for the stabilization of laser wavelength using the Cs-D_2 line at 0.8521μm [12]

Figure 2.4 shows the block diagram of the experimental setup used in wavelength stabilisation of the laser diode. The wavelength of the laser diode was stabilised by stabilising temperature within $\pm 10^{-3}$ °C. They obtained an Allan variance between $3x10^{-12}$ and $1x10^{-11}$ for the average time ranges 0.1s to 1000s, respectively.

Tanaka *et al* [13] reported the wavelength stabilisation of a laser diode using a combination of a confocal Fabry-Perot (CFP) cavity and a Rb-D_2 line to simultaneously improve long and short term frequency stability. The CFP was used to achieve short term stability and, for long

term stability, the cavity length of CFP was controlled by the Rb-D_2 line. The authors achieved stabilities of $2x10^{-12}$ and $2x10^{-14}$ in the time ranges 0.1 and100s, respectively.

Crowin *et al* [14] achieved a frequency stability of 0.5MHz peak to peak over a period of 38 h. They locked to a Doppler broadened Rb line by employing a Zeeman shift (spectral lines are divided into closely spaced lines upon the application of magnetic field), generating an anti-symmetric resonance.

Zhao *et al* [15] reported the frequency stabilization of an external cavity laser using the sub Doppler spectrum of Cs atoms and achieved a stability of $5x10^{-11}$ over a duration of 200s.

2.2.3 **Optogalvanic effect**

When a flame or a discharge is illuminated by radiation which has a wavelength corresponding to an atomic or molecular transition, then the electrical properties of the radiation change due to the optogalvanic effect [2].

The optogalvanic effect can be observed in all types of discharges such as normal discharges, hollow cathode discharges, microwave discharges and even flames.

Green *et al* first reported the observation of a laser-induced change in the voltage of a gas discharge tube plasma and then used this voltage as a wavelength reference for a dye laser[16][17]. The apparatus used by Green *et al* is shown in the Figure 2.5.

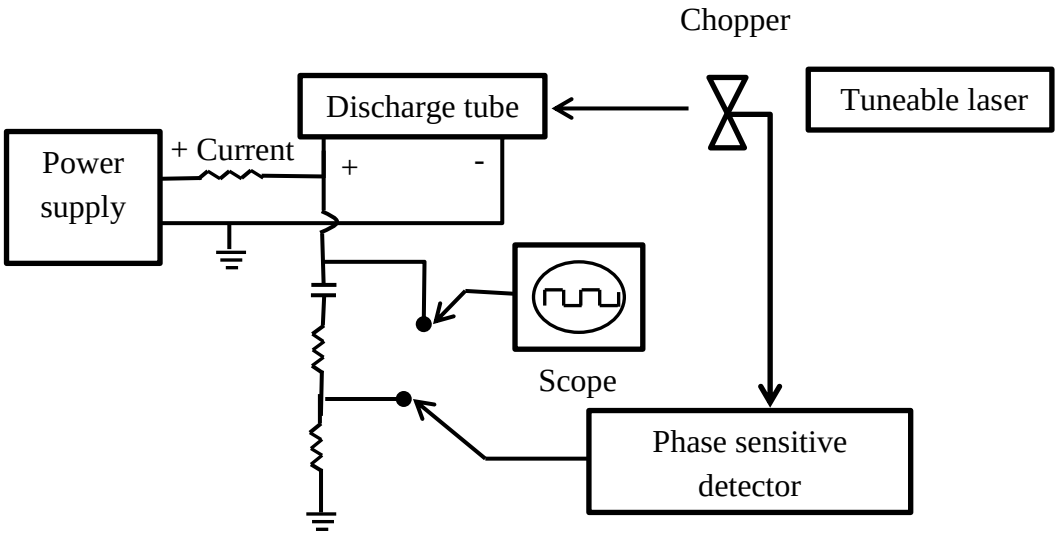

Figure 2.5 Block diagram of the experimental setup for laser wavelength stabilisation using the optogalvanic effect. Redrawn from [16]

The opto-galvanic error signal arises due to the variation in the discharge voltage of a plasma. When the optical radiation, having a wavelength corresponding to the atomic transition in the discharge, is passed through the plasma, optical absorption changes the ionization potential of atoms in the discharge. This change in ionization potential translates to a variation of the voltage of the gas discharge tube plasma. The voltage of the plasma decreases due to the increase in discharge current, as atoms are excited from a level with small ionization probability to a level that has a large probability of ionization.

The opto-galvanic effect was discovered by Green *et al* in 1976, but little attention was given to this method until the mid-1980 due to the requirement for a large optical power to induce a large change in the voltage of the gas discharge. In 1988, Cheung *et al* succeeded in producing an opto-galvanic signal at a relatively low power (0.5mW) using a DFB laser diode. They used argon (Ar) at 1.3μm and krypton (Kr) at 1.5 μm for a wavelength reference [18][19]. Cheung *et al* reported a reduction in wavelength fluctuation of their laser system from 25MHz to 1.2MHz [18][19].

2.2.4 **Gas molecule absorption**

The absorption lines of gas molecules can be used as wavelength references for stabilizing the emission wavelength of laser diodes, as shown in Figure 2.6. These absorption lines correspond to electronic and vibrational - rotational transitions of the gas molecules. Most of the electronic transitions for the gas molecules (except for iodine) are in the ultraviolet region, which cannot be used as reference for laser diode wavelength stability [2]. Thus, vibrational – rotational transition with wavelengths in the range of 0.5μm-10μm are used as wavelength references.

Shimoda in 1968, for the first time, developed a scheme for stabilizing the wavelength of a laser diode [20]. Shimoda used the absorption line of the CH_4 v_3 transition as a wavelength reference.

The choice of the molecular absorption line as a wavelength reference was based on the following advantages [2]:

- The probability of finding a molecular transition that will match the laser transition is very high
- Molecular absorption lines have narrow linewidths due to their long radiative life times, making them good candidate for wavelength referencing
- Absorption can be obtained from thermally populated states and when such absorption takes place from the ground states, perturbing effects like discharge can eliminated

It has been reported that the vibrational- rotational absorption lines of methane are the best candidates for use in laser wavelength stabilisation schemes [2]. In addition, the absorption lines of the iodine molecule (499nm-909.1nm) were found to be another good wavelength reference. The following block diagram shows a wavelength stability scheme using a gas molecular absorption line.

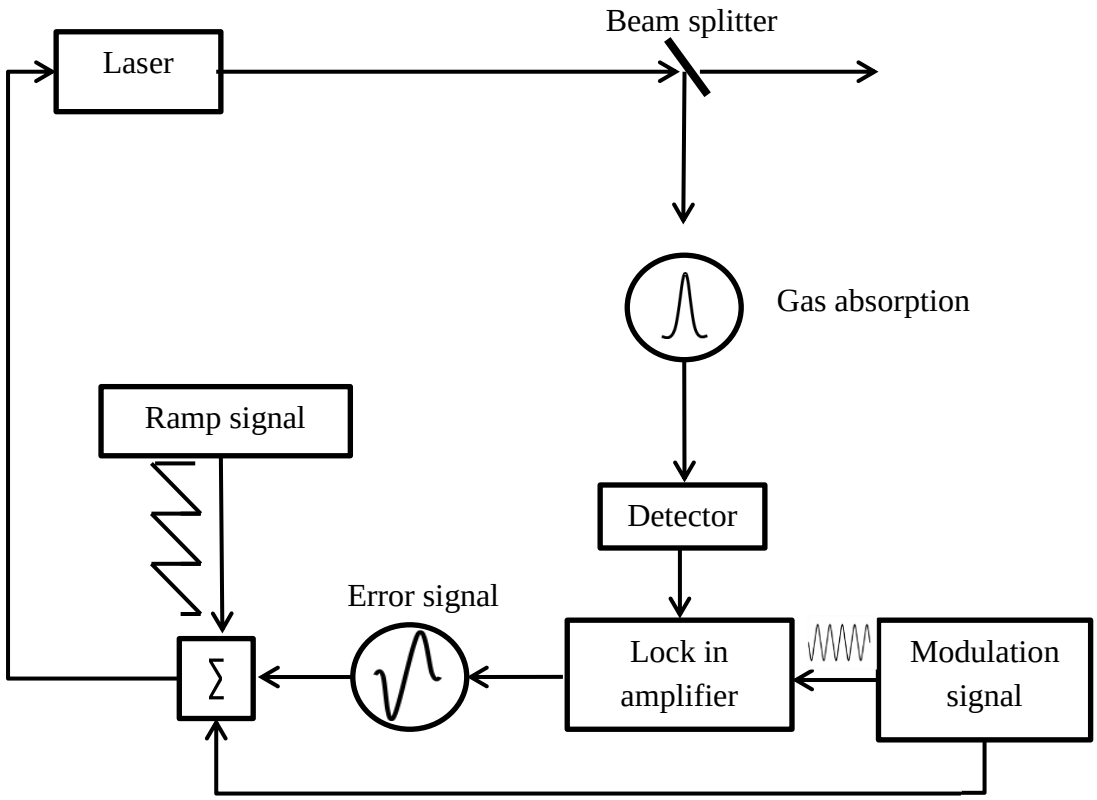

Figure 2.6 Molecular absorption line typical arrangement used for laser frequency stabilisation

Table 2.2 lists the frequency stability achieved using different molecular gas absorption lines.

Table 2.2 Frequency stability achieved using molecular absorption line as a wavelength reference

Molecular absorption line	Wavelength range (μm)	Frequency stability (Allan variance)	Time duration	Reference
CH_4	7.7	4.3 x10-11 (1.6 kHz)	15s	[21]
NH_3	1.5	8 x10-11(16 kHz)	1s	[2]
C_2H_2	1.5	2 $x10^{-10}$ (40 kHz)	$1 \leq \tau \leq 100$s	[2]
HF	1.3	7.9 $x10^{-11}$ (18 kHz)	240s	[22]
H_2O	0.8	1.1 $x10^{-11}$(4 kHz)	100s	[23]

More recently, Ryu *et al* [24] reported on the frequency stabilisation of a widely tuneable external cavity laser using an optical frequency comb. This optical frequency comb was

generated using a seed laser stabilised by an acetylene absorption lines. They reported a frequency stability of 1.1 x10^{-12} (220Hz) for an averaging time of 1s.

2.3 Optical absorption spectroscopy

This section starts with the underlying principle behind absorption spectroscopy, with emphasis on methane gas detection, which is the target gas in this project. The choice of methane gas for this project is due to its will characterised spectrum and narrow line width. A detailed discussion on the gas absorption molecule spectrum and line shape is provided, which is relevant in understanding wavelength modulation spectroscopy

2.3.1 Basic principles of optical absorption spectroscopy

Absorption spectroscopy is described by the Beer-Lambert law, as shown in Figure 2.7 [25], where an electromagnetic wave with intensity I_o and frequency v is transmitted through an absorption medium. The concentration of the gas is measured from the attenuation of the incident light. The length of the absorption medium is L with a gas concentration C .The absorption medium has a frequency dependent absorptivity k cm^{-1} atm^{-1}. The intensity of the transmitted electromagnetic waves decays exponentially with length on interaction with the absorption medium. The exponential decay of the transmitted intensity is described in the following equation (2.11) [25].

$$I_{(v)} = I_o(v)\exp(-k(v)LC) \tag{2.11}$$

I (v) represents the transmitted intensity.

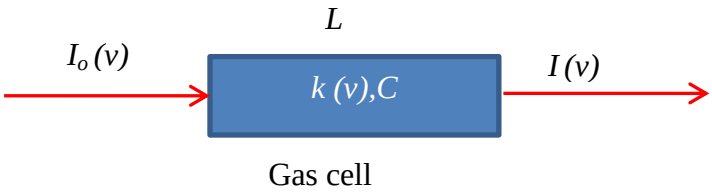

Figure 2.7 Principle of Beer Lambert Law

The proportion of transmitted light can be represented by its transmittance, T, given below in equation (2.12)

$$T = \frac{I(v)}{I_o(v)} = \exp(-k(v)LC) \cong 1 - k(v)LC \tag{2.12}$$

Equation (2.12) can be written in linear form for low gas concentrations, to give a measure of absorbance or optical density A by the probes species.

$$A \approx \ln\left(\frac{1}{T}\right) = k(v)LC \qquad (2.13)$$

Equation (2.13) shows that the absorbance (A) is directly proportional to the concentration C of the target gas. Concentrations of unknown gases are measured in the gas mixture in terms of volume mixing ratio, expressed in parts per million by volume (ppmv). For an ideal gas, this represents a mole fraction of the gas molecule in a gas mixture [26].

Figure 2.8 represents the methane spectrum in the wavelength range 1610-1690nm. The spectrum was plotted for a path length of 10cm with 1atm pressure.

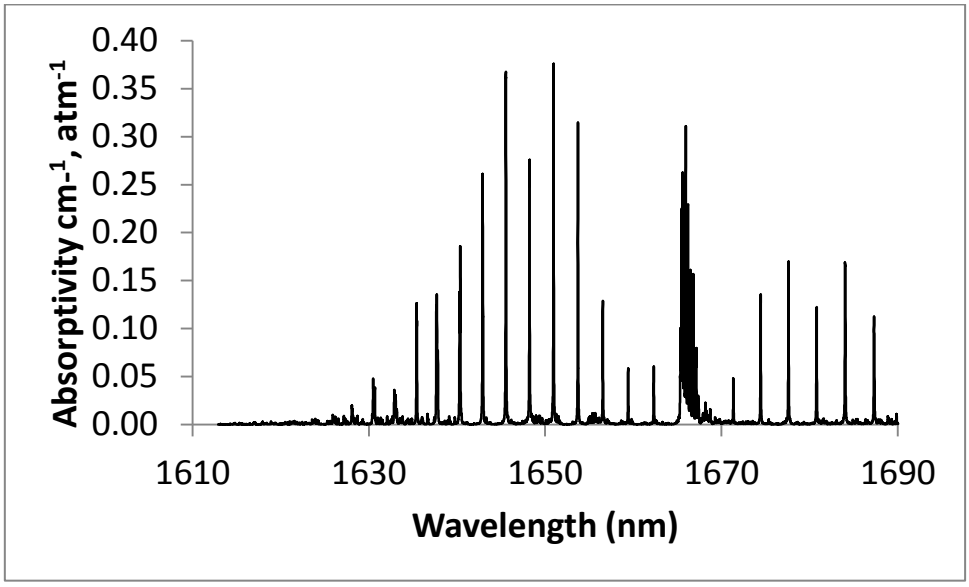

Figure 2.8 Methane spectrum in the wavelength range 1610-1690nm. Re plotted from [27]

This is the wavelength range targeted in this project for the absorption spectroscopy. The gas absorption lines are well isolated from neighbouring methane absorption lines (approximately 3nm) and other molecules such as water.

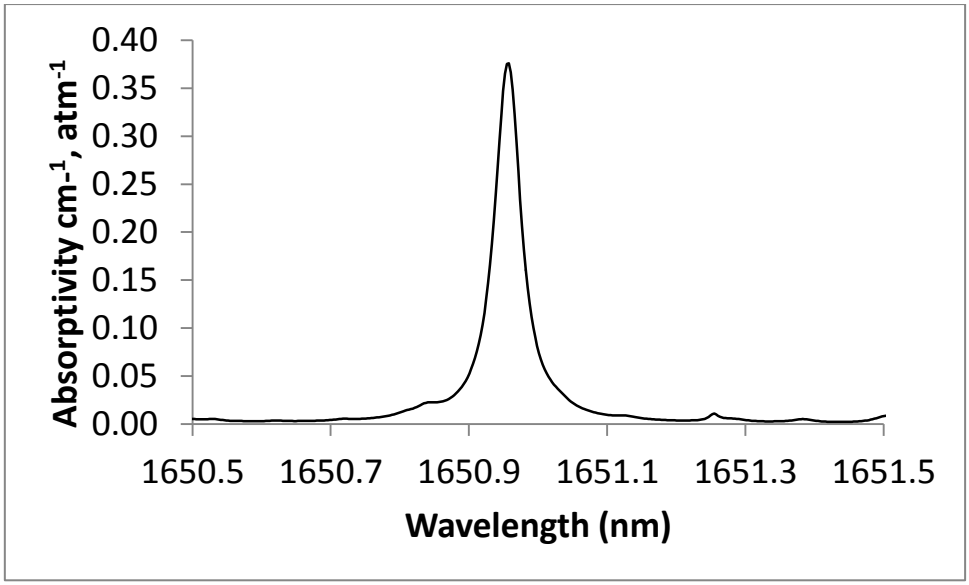

Figure 2.9 Methane absorption line at 1650.96 nm at 1atm pressure and 10 cm path length. Re plotted from [27]

The strongest absorption line is at a 1650.96 nm, as shown as shown in Figure 2.9. This is the target wavelength of the project due to its strength and isolation from neighbouring molecules. The path length for the plot in Figure 2.9 was 10cm, which is approximately the length of the gas cell used in this project (10cm length will reduce the effects of interference fringes as will be discussed in detail in section 2.4.5). The full width half maximum of this absorption line is 50pm.

2.3.2 **Origin of gas molecules absorption spectra**

Molecules are excited from their ground state to an excited state due to the absorption of a photon; this changes the rotational, vibrational or electronic energy of the gas molecule. The transition of energy states in the gas molecules can be interpreted in terms of spectral lines; molecule absorption spectroscopy is the study of these spectral lines. Each gas molecule has a unique absorption spectrum, as gas molecules will absorb frequencies (energies) resonant with their natural frequencies [28].

The absorbed wavelengths range from the microwave region to the vacuum ultraviolet (VUV) region of the electromagnetic spectrum. However, spectroscopic gas detection is often concerned with the infra-red region (1.5μm - 25μm) of the electromagnetic spectrum. In the middle infra-red region, the molecular absorption cross section (absorptivity/atomic number density) is $10^{-18}cm^2$ and absorption bands of many gasses of interest, such as methane, hydrogen sulphide and carbon mono oxide, are present in this region [29]. Therefore, in the

infra-red region, the detection sensitivity is high and the spectrum can be used as a fingerprint for identifying gas molecules in a gas mixture.

An infrared radiation corresponds to absorption energy in the range 8-40 kJ/mole (assuming it is an ideal gas). This energy range represents the bond frequencies corresponding to stretching and vibration in many covalently bonded molecules. When a molecule absorbs infrared radiation its vibrational energy increases. Not all molecules in a gas produce absorption spectra; only molecules with a dipole moment, which absorb energy due to the vibrational or rotational motion of the dipole, produce a vibrational or rotational spectra spectrum [28].

$$\overline{v} = 4.12\sqrt{K/\mu} \tag{2.14}$$

$$\mu = \frac{M_1 M_2}{M_1 + M_2} \tag{2.15}$$

$\overline{v}$ is the natural frequency of vibration of a bond, K is the force constant which varies from bond to bond e.g. a triple bond has higher force constant than does a double bond, and a double bond has higher force constant than single bond . μ is the reduced mass of the system, and M_1 and M_2 are the atomic weights [28].

By analysing equations (2.14) and (2.15), it can be concluded that stronger bonds have higher vibrational frequencies than weaker bonds and that bonds between lighter atoms vibrate at higher frequencies than the bonds between heavier atoms [28].

2.3.3 **Methane Gas line**

Methane is a tetrahedral molecule with four fundamental vibrational modes *v*1 (3.432μm), *v*2 (6.563μm), *v*3 (3.311 μm), and *v*4 (7.656 μm) as shown in Figure 2.10. *v*1 and *v*3 represents the bending modes, whereas *v*2 and *v*4 characterise the stretching bands. *v*3 and *v*4 are the two strong fundamental bands.

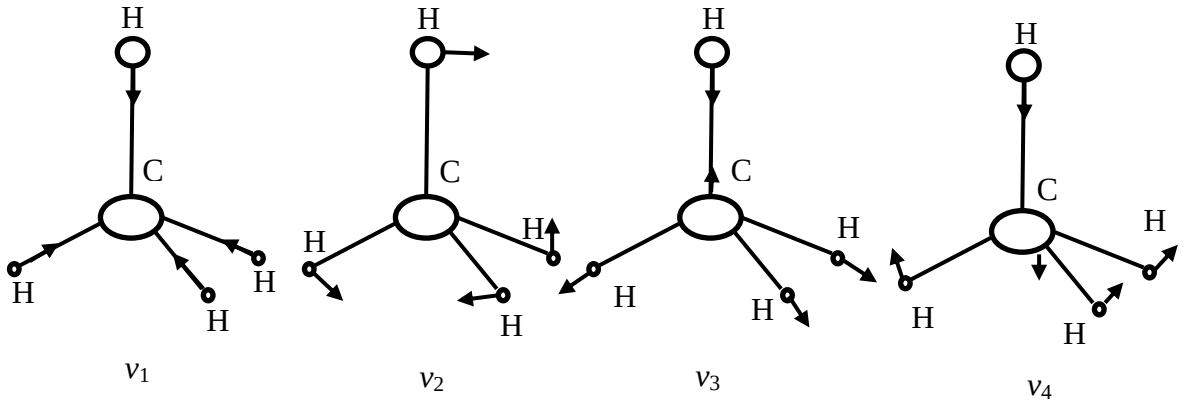

Figure 2.10 Fundamental vibration modes for CH_4 molecule. Redrawn from [2]

Tuneable lasers with wavelength lower than 2μm when operating at room temperature, in the near infrared region, which contains overtones and combination bands, are also used for the detection of methane measurement. The strength of overtones and combination bands in this region are 10-1000 times weaker than the fundamental bands, but commonly available lasers and detectors operate in this region. Therefore, TDLAS is carried out in near infrared region where the 2*v*3 band is the strongest absorption band with centre wavelength 1.665 μm.

Table 2.3 shows the overtone and bands for methane in the near infra-red region, which is the target region of this project.

Table 2.3 Overtones and combination of methane absorption bands in the near infrared region [2]

Band(μm)	***v* (GHz)**	**Classification**
1.135	263.8	v1+2v3
1.1620	25.8	3v3
1.1873	25.2	2v1+2v4
1.3305	22.5	v2+2v3
1.6645	18	2v3
1.7335	17.3	v1+v2+v4
1.7898	16.77	v1+2v4

2.3.4 **Absorption line shape**

Absorption spectroscopy quantifies concentration of gas analytes using the Beer-Lambert law. Absorption spectroscopy is also dependent on the width of the line, line strength and line shape of the probed gas species. Pressure and temperature can change the shape and width of

the absorption line. Under certain temperatures and pressures, gas lines for some gases are well defined and separated, allowing highly sensitive gas detection. However, at higher pressures these gas molecules can experience width broadening and cross interference from neighbouring gas lines.

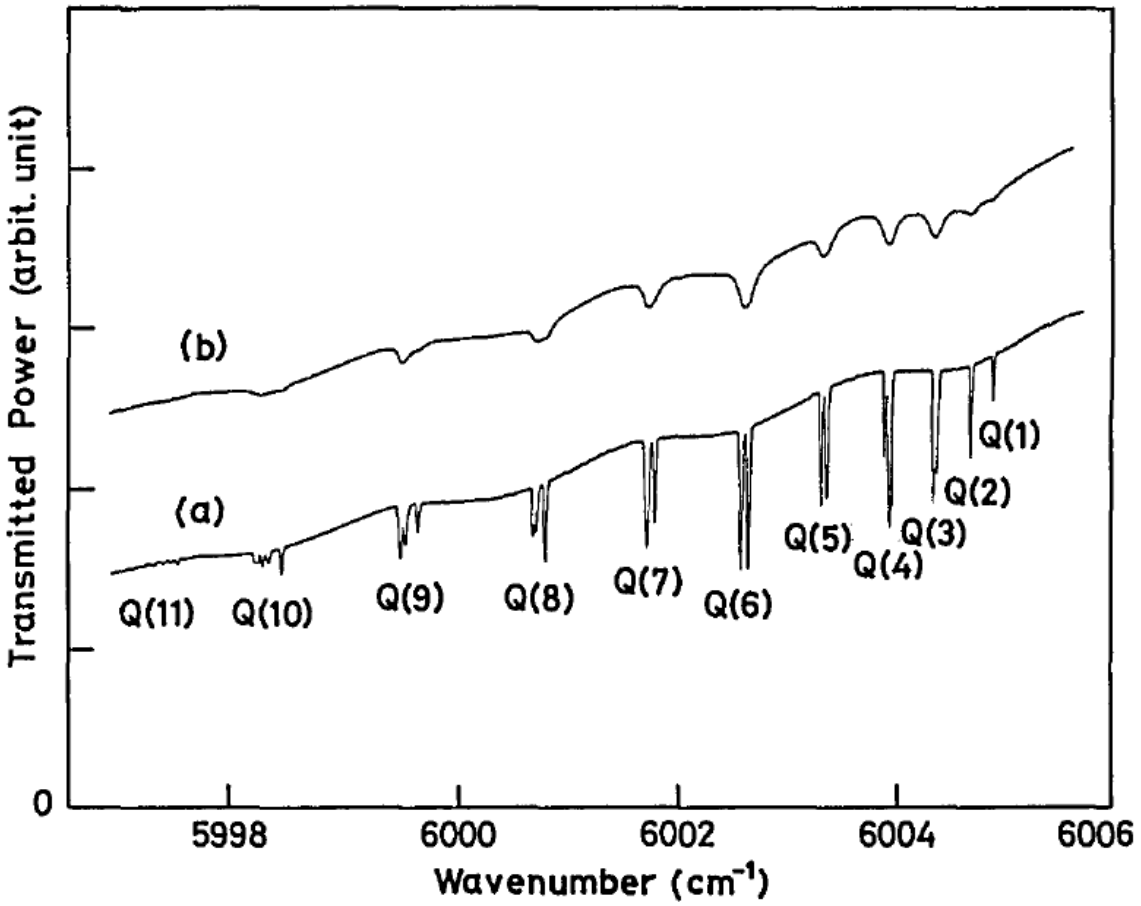

Figure 2.11 Absorption spectra of the of the 2*v*3, band of methane obtained by Uehara *et al* [30] (a) Doppler broadened absorption spectrum and (b) Pressure broadened methane absorption spectrum The methane partial pressure was 4 Torr in both traces, but 1-atm air is added in (b). The absorption cell length was 50 cm

Figure 2.11 shows the absorption spectrum of the Q branch of the 2*v*3 band of methane at different pressures. The widths of the methane absorption lines in Figure 2.11 (a) are very narrow and well defined at 4 Torr. While, on the other hand, where 1atm air has been to the 4 Torr methane pressure, these absorption lines are wide with less defined structure, translating to a low absorption coefficient [31]

Linewidths of gas spectral lines are modelled using spectral lineshape functions such as Lorentzian and Gaussian line shapes. Atmospheric gases measurement is affected by two broadening mechanism, collisional (pressure) broadening and Doppler broadening.

Collisional (pressure) broadening of gas spectral lines occurs due to the collision of different gas molecules contributing to gas line shape. In collisional broadening, the energies in the ground or excited states of the gas molecules are changed slightly by the collision [29]. Collisional broadening is dominant above a pressure of 100 Torr. The linewidth of a gas line increases linearly with pressure at a given temperature [29]

$$\Delta v_L = 2b_c p \tag{2.16}$$

Where Δv_L is the Lorentzian linewidth; p is gas pressure and b_c is the pressure broadening coefficient which is determined experimentally. The absorption cross section at a line centre v_o is given by

$$k(v_o) = \frac{2S}{(\pi \Delta v_L)} = {}^{2S}/_{\pi b_c} \tag{2.17}$$

Where S is the line strength and $k(v_o)$ is the absorption cross section [29]. At conditions where pressure broadening is dominant, the peak absorption cross section decreases linearly with increasing pressure and the line widths are typically around 0.1cm^{-1} at atmospheric pressure [31].

Doppler broadening is caused by the thermal excitation of gas molecules along the observation path. As the gas molecules are continuously moving with respect to the source or detector, the frequency of the gas molecules appears to be Doppler shifted, resulting in increased linewidth [32].

At pressure of less than 10 Torr, Doppler broadening defines lineshapes and linewidth of gas molecules. Doppler broadened linewidths are 1-2 orders of magnitude smaller than collisional broadened linewidths at atmospheric pressure.

A Doppler broadened lineshape is a Gaussian function, which depend on the linewidth. The Doppler broadened linewidth Δv_D can be described as [29]

$$\Delta v_D = 71.16 \times 10^{-7} \overline{v_o} \left(\frac{T}{M_m}\right)^{\frac{1}{2}} \quad (2.18)$$

$\overline{v_o}$ (in wavenumbers) is the frequency of the line centre; T ,the temperature in Kelvins; and M_m, is molecular mass in g mol-1.

For example, methane molecule (M_m=16) has a Doppler broadened line width of

9.53×10^{-3}cm^{-1} at a line centre of 3100cm^{-1} at 295K.

At a line centre, the peak absorption cross section σ_o can be represented as

$$\sigma_o = 0.94 \times \frac{S}{\Delta v_D} \quad (2.19)$$

In the Voigt regime, the line shape and width are described by the convolution of the Doppler and pressure broadening lineshapes. The Voigt regime applies to a pressure range of 10-100Torr or at altitudes between 10-40km [29].

The Voigt linewidth Δv_v is generally calculated numerically and by referring to look up tables. However, the Voigt line width can be approximated in terms of Δv_D and Δv_L

$$\Delta v_v^2 = (\Delta {v_L}^2 + \Delta {v_D}^2) \quad (2.20)$$

Typical line widths of atmospheric gas species lie in the range of 5×10^{-3} to 2×10^{-2} cm^{-1}. This linewidth range is smaller than the spacing of the rotational lines of many of the gas molecules of interest. Hence, this allows more sensitive and specific gas concentration measurement [29].

This project is targeting gas linewidths in the atmospheric pressure broadened regime and therefore gas detection will be carried out at atmospheric pressure

2.4 Wavelength Modulation Spectroscopy

Wavelength modulation spectroscopy (WMS) is a widely used trace gas detection technique with a high signal to noise ratio and immunity from low frequency laser noise [29]. WMS uses the technique of modulation of the injection current of a semiconductor laser diode at a frequency much smaller than the half width of the absorption peak of the gas species under investigation. The modulated signal is scanned through the absorption line. Interaction of the modulated signal with the absorption line produces signals that are at different harmonics of

the modulation frequency. These frequency harmonics are then detected with the help of a lock-in amplifier. WMS enables the detection of the modulation signal at higher frequencies, therefore avoiding excess laser noise which decrease with increasing frequencies as (>1kHz) $\frac{1}{f}$ [29][30].

Tang *et al* were the first to use WMS [31], whereas Pokrowsky *et al* used a GaAlAs semiconductor laser for sensitive detection in WMS [32]. Various techniques such as high frequency WMS, one tone and two tone FMS have been used for sensitive detection of trace gases.

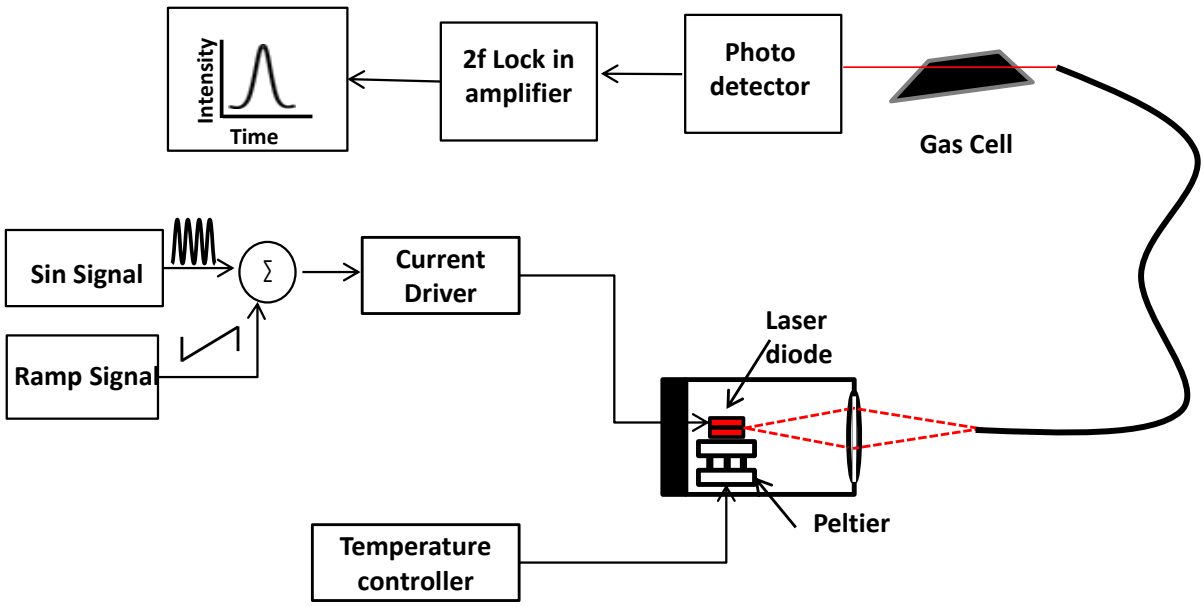

Figure 2.12 Basic Description of wavelength modulation spectroscopy

WMS is adversely affected by interference fringes resulting from etalons between reflecting or scattering optical surfaces and by residual amplitude modulation signal (RAM) resulting from the modulation of the intensity of the laser output [33].

This thesis will use WMS for gas detection. The following sections will describe WMS in detail. The aim of this project is to develop a wavelength length locking technique for laser diode used in WMS, which is described in chapter 6. Therefore, it is important to detail the WMS background theory and noise sources affecting its performance.

2.4.1 **WMS Background theory**

WMS involves modulating the laser diode current with a sinusoidal signal with a frequency lower than the half width of the absorption feature [34]. The following equation (2.21) describes the change in wavelength with time [34]

$$\lambda(t) = \lambda_c + \lambda_{mod} \sin(2\pi f_m t) \tag{2.21}$$

Where f_m is the modulation frequency, λ_c is the centre wavelength, and λ_{mod} is the wavelength modulation amplitude.

In WMS, a frequency of typically few kHz is used to modulate the injection current of the laser diode. This modulation process translates into the wavelength (frequency) modulation as well as intensity modulation, also called the residual amplitude modulation or RAM signal, of the output of the laser [34] [35] . Equation (2.21) can be written in frequency terms as:

$$v(t) = v_c + v_{mod} \sin(2\pi f_m t) \tag{2.22}$$

Here $v(t)$is the laser frequency, v_c is the laser frequency tuned to the absorption centre frequency and v_{mod} is the modulation amplitude of the signal [34]. The intensity of the output power is:

$$I(t) = I_o + \eta_i I_o (\sin 2\pi f_m t) \tag{2.23}$$

Where I_o is the laser intensity and η_i is the intensity modulation index [30]. The interaction of the instantaneous frequency of the laser source with the absorption feature is converted into an intensity modulation that is detected by the photo detector, as described in the following section.

2.4.2 **Time dependent absorption signal**

The modulated output of the light source is passed through a gas cell containing the probed gas species. The interaction of light with the gas species can be described by the Beer-Lambert law, as shown in equation (2.11).

The transmittance of the gas can be approximated, as was described by Reid and Labrie [36]

At a low level of absorption ($k(v)L \lesssim 0.0$), we have

$$I \simeq I_o(v)[1 - (k(v)LC)] \tag{2.24}$$

The Beer-Lambert law in equation (2.11) can be rewritten after taking into account the wavelength modulation of the light output as:

$$I(t) = I_o(1 + \eta_i \sin(2\pi))[1 - k(v_c + v_{mod} \sin(2\pi f_m t)\ LC)] \tag{2.25}$$

As the intensity modulation is small, equation (2.25) can be re-written by approximating $\eta_i \ll 1$ [33]

$$I(t) \simeq I_o(1 + \eta_i \sin(2\pi f_m t)) - k(v_c + v_{mod} \sin(2\pi f_m t)\ LC) \tag{2.26}$$

Neglecting the higher order terms obtained from the simplification of equation (2.26), the absorption coefficient, $k(v)$, describing features of the absorption line, can be written in terms of the line shape *F* and absorption line strength *S* as:

$$k(v) = SF(v - v_o) \quad \text{where } S = \int k(v)d(v) \tag{2.27}$$

Assuming that pressure broadening in the line shape of the absorption signal dominates, then the $k(v)$ can be described by a Lorentzian function

$$k(v) = \frac{k_o}{1 + \left(\frac{v - v_o}{\delta v}\right)^2} \tag{2.28}$$

Where, δv is the half-width of the absorption line and k_o is the absorption coefficient at the centre of absorption line. By substituting $k(v)$ in equation (2.26),

$$I(t) = I_o[(1 + \eta_i \sin 2\pi f_m t) - \frac{k_o(LC)}{1 + \left(\frac{v_c + v_{mod}\ \mathrm{SIN}(2\pi f_m t) - v_o}{\delta v}\right)^2} \tag{2.29}$$

At the central frequency of the absorption (i.e. $v_c = v_o$) equation (2.29) can be simplified as [34]:

$$I(t) = I_o[(1 + \eta_i \sin 2\pi f_m\ t)] - \frac{k_o(LC)}{1 + \left(\frac{v_{mod} \sin(2\pi f_m t)}{\delta v}\right)^2} \tag{2.30}$$

By substituting $x = \frac{v_{mod}}{\partial v}$ equation (2.30) can be simplified according to Jin *et al* [37].

$$I(t) = I_o[(1 + \eta_i \sin 2\pi f_m\, t)] - \frac{k_o(LC)}{1 + x^2 \sin^2(2\pi f_m t)} \qquad (2.31)$$

Where $I(t)$ can be written in terms of its Fourier series, with the magnitudes of the first and second harmonics represented as [37]:

$$I_1 = I_o \eta \qquad (2.32)$$

$$I_2 = -2U k_o I_o LC \qquad (2.33)$$

Where I_1 is magnitude of the first harmonic, where as I_2 is the magnitude of the second harmonic, and U can be expressed as a function of modulation index x

$$U = \frac{2[2 + x^2 - 2(1 + x^2)^{\frac{1}{2}}]}{x^2(1 + x^2)^{\frac{1}{2}}} \qquad (2.34)$$

A maximum second harmonic signal can be obtained by optimising the value of modulation index *x*. The maximum second harmonic signal is obtained for *x* = 2.2 as shown in Figure 2.13.

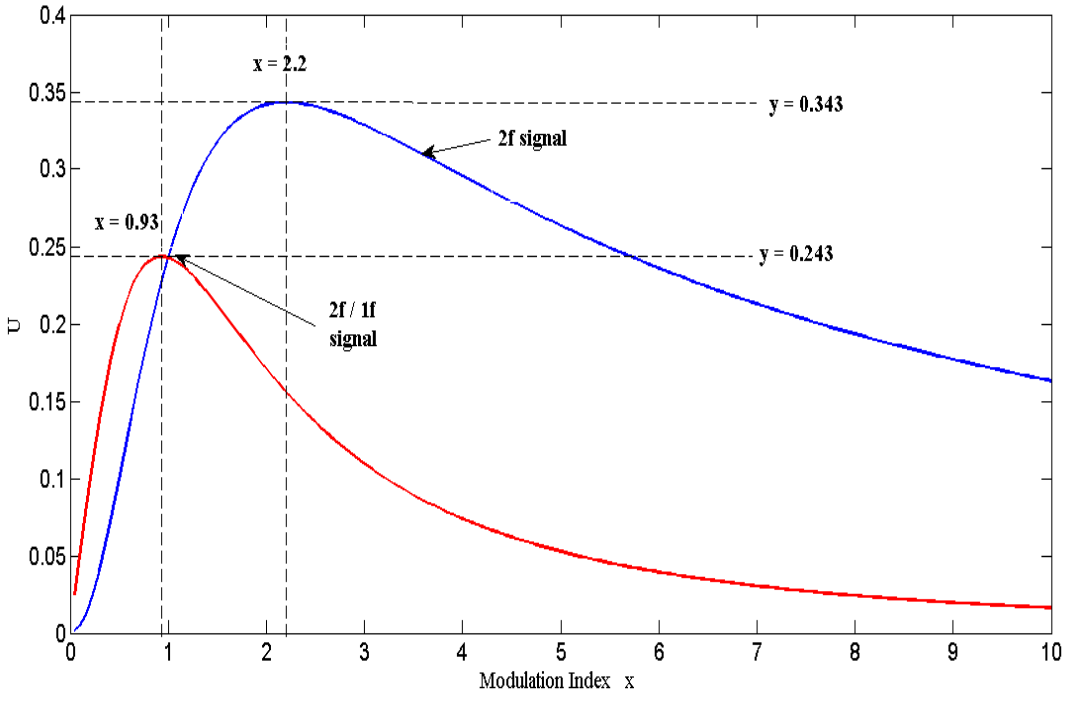

Figure 2.13 Modulation index U vs x showing that x=0.93 and x=2.2 for optimum 2f/1f and 2f signal respectively

The intensity fluctuation in the output of the laser diode can be overcome by adopting the ratio detection method [37] expressed as

$$\frac{I_2}{I_1} = -\frac{2Uk_oLC}{\eta_i} \tag{2.35}$$

The optimal value of *x* is 0.93 in ratio detection method, with *U* corresponding to 0.243 as shown in Figure 2.13 [37][337][39].

2.4.3 **Harmonic detection**

The consequences of the previous analysis are as follows. The output light after scanning the peak of the absorption line is detected with a lock- in amplifier at the modulation frequency or its harmonics. Demodulation of the output light is at the same frequency as the modulation frequency, it is termed 1f *detection*, whereas detection at twice the frequency is termed *second harmonic (2f) detection* [34], as shown in Figure 2.14 . The nonlinear changes in the output power of the laser with applied current create a substantial zero offset in the 1f signal. Therefore, the magnitude of the 1f signal will fluctuate with the fluctuation in the intensity of the laser diode. A 2f detected signal is therefore used in WMS. The line shape produced at the output of the detector is proportional to the 2nd derivative of the original line shape when the modulation amplitude is very small in relation to the line width. The maximum signal is obtained when the modulation index is 2.2 times the half width at half maximum of the absorption line. 2f detection reduces the $\frac{1}{\mathrm{f}}$ noise of the laser and the sensitivity to thermal fluctuations. Moreover, WMS has an absorption sensitivity of 10^{-4} to 10^{-5}(absorbance) at 2f [34][36]. However, 2f detection is sensitive to the curvature and the sharp absorption feature of the probed gas, therefore heavier atomic mass molecules cannot be detected with this technique in the absence of well resolved ro-vibrational absorption bands (due to overlap between fundamental and overtone vibrations or their combination) [40].

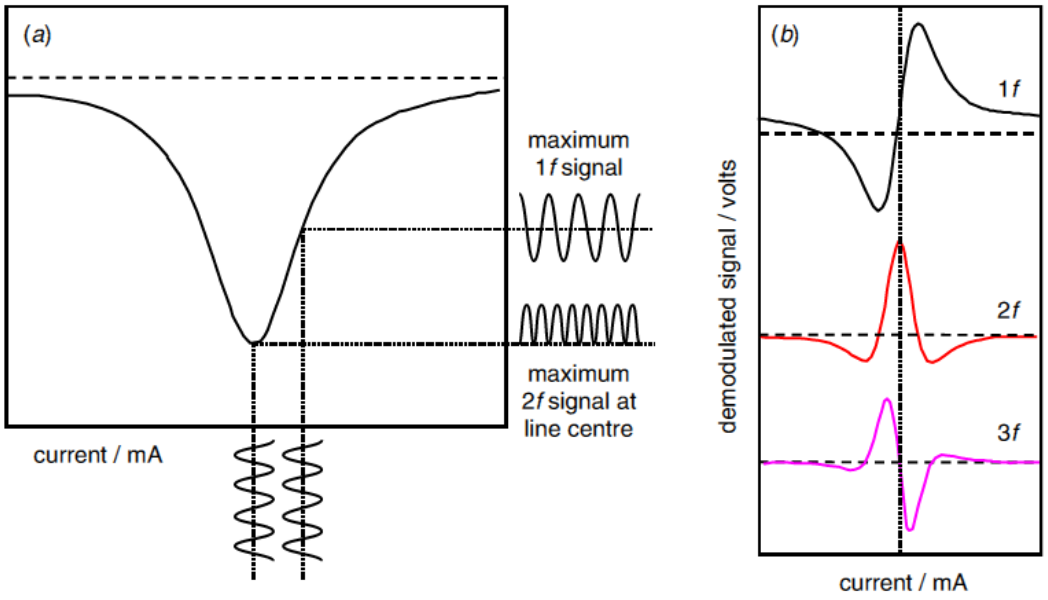

Figure 2.14 Description of Lorentzian profile of 1f and 2f detection in WMS for Lorentzian absorption line. Taken from [41]

Figure 2.14 (a) demonstrates 1f and 2f detection. Figure 2.14 (b) is the comparison of 1f, 2f and 3f Lorentzian line shapes. The 1f harmonic line shape is asymmetric with respect to the line centre of the absorption line and has a zero crossing at the line centre but with a DC offset. Therefore, 1f modulation can be used for line locking to establish the line centre if the DC offset is constant and accurately known. The amplitude of the 1f signal is bigger than the 2f signal, but due to high base line signals and asymmetry, the 1f signal is not generally used for the detection of gases. The 2f harmonic is symmetric with respect to the absorption line with two zero crossings and with a peak signal at the absorption line centre. The 2f signal however does not give the absolute concentration measurement of the gas (requiring calibration with known concentration). However, RAM and $\frac{1}{f}$ of the laser used in WMS is low; allowing the measurement of small changes in the absorption lines of the probed species [29]. The 3f signal, unlike the 1f signal, has a zero DC offset at the gas absorption line centre and therefore can also be used for wavelength locking.

2.4.4 **Residual amplitude modulation**

The injection current of the laser diode is modulated in WMS, which modulates both the frequency and intensity of the emitted light of the laser diode. The intensity modulation (IM) and frequency modulation (FM) of the laser diode are out of phase by an amount that depends on the structure of the laser diode and modulation frequency [30]. Typical values of the phase

shift between IM and FM ranges from 0 at low frequencies to π at high frequencies [34]. In WMS the detection of the absorption line is dependent on the FM of the light, whereas IM is termed as residual amplitude modulation (RAM) and considered as an unwanted signal. IM introduces asymmetry in all the harmonics and a DC offset in the 1f signal, which increases with modulation frequency [29][30][42].

The AM signal-induced background is lower at higher derivatives of the absorption line. Therefore, in WMS, the 2f signal is used for the detection of absorption species. However, even detection at twice the modulation frequency does not overcome the problem of RAM-induced distortion, limiting the sensitivity of the system [43]. In addition, 2f detection does not give the absolute concentration of the probed gas, but the concentration measurement is carried out by comparing the 2f signal with a calibration curve under known conditions. Recently, the Hanson group proposed a calibration free measurement in WMS, where the normalisation of 2f signal by 1f signal and the use of laser specific tuning characteristics avoid the need for calibration [44]. Overcoming the RAM allows calibration free absolute measurement of the gas lines and detection at 1f signal with low baseline [45].

2.4.5 **Interference fringes in wavelength modulation spectroscopy**

Detection sensitivity in WMS is often limited by interference fringes in the gas detection system. The effect of interference fringes in WMS is described in Figure 2.15. Interference fringes appear due to Fabry-Perot etalons between reflecting optical surfaces such as mirrors, detectors and laser head windows, optical fibre ends, semiconductor surfaces and components of multi pass cells [29][46].These etalons are dependent on the reflectivity of the surfaces, the distance between the structures, the angle of incidence, the centre frequency around which the laser injection current is modulated, the modulation index, amplitude of the modulation and the mode of detection. The free spectral ranges of these etalons are in the range 150MHz – 30GHz [46][47][48].

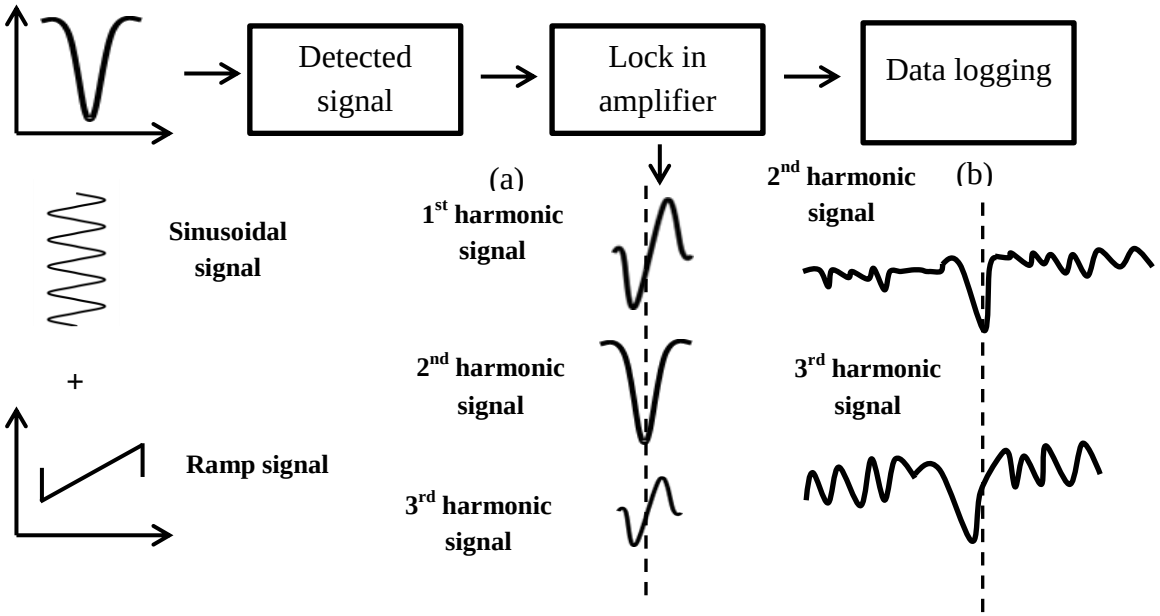

Figure 2.15 Description of WMS system and the resultant signals with interference fringes on (a) WMS harmonic signals in absence of interference fringes (b) WMS harmonic signals in the presence of interference fringes. Re drawn from Masiyano [49]

The influence of interference fringes can be reduced by reducing the etalon effect using anti reflection optics (where possible), avoiding parallel surfaces, avoiding sharp focus, and by mode selection of the laser diode and of the modulation waveform and amplitude. Several techniques have been implemented to reduce the effect of interference noise, including signal averaging, mechanical vibration and balanced detection. However, interference fringes cannot be eliminated completely but the level of noise due to interference fringes can sometimes be minimised below other limiting noise factors affecting the detection of the absorption signal [46][47][48] .

2.5 Summary

Table 2.4 summarises the wavelength references and methods that have been reported in the literature for stabilising laser wavelengths.

Table 2.4 Laser frequency stabilisation techniques

Method	Advantages	Disadvantage
Fabry-Perot interferometer	• A common and convenient method • Wide tuning range	• Temperature dependence of resonant wavelength of the etalon
Atomic transition	• Narrow line width • Rich spectra • Absolute reference	• Slow response
Optogalvanic effect	• Rich spectra • Absolute reference	• Requires high power to generate optogalavanic signal • Discharge effect
Molecular absorption	• Narrow line width • Rich molecular spectra for laser transitions • Absence of discharge effect	• Complicated setup

The above motioned methods have their advantages and disadvantages as well as their suitability for laser wavelength locking in WMS.

All the wavelength reference techniques reported in this chapter have excellent wavelength stability but for short times only. In addition, many of are only suited to laboratory experiments. Interferometers and molecular lines are often used for long term stability.

WMS has been chosen for this project is due to its widespread application in methane detection and its high selectivity and sensitivity.

In WMS, the wavelength of the laser output light is modulated and detected with lock-in amplifiers. 1f and 2f signals are used to measure the probed gas species. The 2f signal is preferred over the 1f signal for gas measurement due to instabilities in the DC offset, a

sloping background and higher laser excess noise in the 1f signal. However, 2f signal based WMS does not provide absolute gas measurement without some form of calibration. In addition, 2f signal based WMS sensitivity is limited by interference noise due to the etalon effect, wavelength stability and residual amplitude modulation (RAM).

Wavelength stability is an important parameter, as the target gas has a very narrow line width and due to the laser wavelength drift, the detection measurement will have poor SNR.WMS requires laser wavelength stability of better than 10% of the absorption line width of the target gas species

In WMS, the linewidth of the laser diode is often stabilised using a gas absorption line 3f signal. In WMS based methane gas detection, a methane reference cell can be used to lock the laser wavelength and wavelength stability of 500kHz has been reported by Sudo et al using an acetylene absorption line. However, this technique requires careful and tedious alignment. The aim of this project is to develop a laser wavelength locking technique that can reduce the long term and short term wavelength drift of the laser diode in WMS and could keep laser wavelength stable when operated in variable ambient temperature.

2.6 References

[1] W. Koechner, Solid-State Laser Engineering, New York: Springer, 1996.

[2] T. Ikegami, S.Sudo and Y.Saki, Frequency Stabilization of Semiconductor Laser Diodes, Boston: Artech House, 1995.

[3] W. Demtroder, Laser Spectroscopy volume 1 Basic Principles, Berlin: Springer, 2008.

[4] D. G. Peterson and A. Yariv, "Interferometry and Laser Control with Solid Fabry–Perot Etalons," *Applied Optics,* vol. 5, no. 6, pp. 985-991, 1966.

[5] J. Picqué and S. Roizen, "Frequency-controlled cw tunable GaAs laser," *Applied Physics Letters* , vol. 27, no. 6, pp. 340-342, 1975.

[6] T. Okoshi and K. Kikuchi, "Frequency stabilisation of semiconductor lasers for heterodyne-type optical communication systems," *Electronics Letters,* vol. 16, no. 5, p. 179 – 181, 1980.

[7] F. Favre and D. l. Guen, "High frequency stability of laser diode for heterodyne communication systems," *Electronics Letters,* vol. 16, no. 18, pp. 709-710, 1980.

[8] J. Alnis, A. Matveev, N. Kolachevsky, T. Wilken, T. Udem and T. Hänsch, "Sub-Hz line width diode lasers by stabilization to vibrationally and thermally compensated ULE FabryPerot cavities," Physical Review A 77, p. 053809, 2008.

[9] T. Kessler, C. Hagemann, C. Grebing, T. Legero, U. Sterr and F. Riehle, "A sub-40 mHz linewidth laser based on a silicon single-crystal optical cavity," Nature Photonics, vol. 6, no. 10, pp. 687 - 692, 2012.

[10] S. Hirata and T. Akatsuka, "Sub-hertz-linewidth diode laser stabilized to an ultralow-drift high-finesse optical cavity," *Applied Physics Express* , vol. 7, no. 2, p. 022705, 2014.

[11] M. Arditi and J. Picqué, "Application of the light-shift effect to laser frequency stabilization with reference to a microwave frequency standard," *Optics Communications,* vol. 15, no. 2, p. 317–322, 1975.

[12] T. Yabuzaki, A. Ibaragi, H. Hori, M. Kitano and T. Ogawa, "Frequency- Locking of a

GaAlAs Laser to a Doppler-Free Spectrum of the Cs-D2 Line," Japaneses journal of applied Physics, vol. 20, pp. 451-454, 1981.

[13] U. Tanaka and T. Yabuzaki, "Frequency stabilization of diode laser using external cavity and doppler- free atomic spectra," Japanese Journal of Applied Physics, vol. 33, no. Part 1, Number 3B, pp. 1614 - 1622, 1994.

[14] K. L. Corwin, Z. T. Lu, C. F. Hand, R. J. Epstein and C. E. Wieman, "Frequency-stabilized diode laser with the Zeeman shift in an atomic vapor," Applied Optics, vol. 37, no. 15, pp. 3295 - 3298, 1998.

[15] Y. T. Zhao, T. H. J. M. Zhao, L. T. Xiao and S. T. Jia, "Frequency stabilization of an external-cavity diode laser with a thin Cs vapour cell," Journal of Physics D: Applied Physics, vol. 37, pp. 1316 - 1318, 2004

[16] R. B. Green, R. A. Keller, G. G. Luther, P. K. Schenck and J. C. Travis, "Galvanic detection of optical absorptions in a gas discharge," Applied Physics Letters, vol. 29, no. 11, pp. 727-729, 1976.

[17] R. B. G. Keller, A. Richard, G. G. Luther, K. P. Schenck and J. Travis, "Use of an opto-galvanic effect to frequency-lock a continuous wave dye laser," Quantum Electronics, vol. 13, no. 2, pp. 63-64, 1977

[18] Y. C. Chung and R. W. Tkach, "Frequency stabilisation of a 1.3 μm DFB laser to an argon line using optogalvanic effect," Electronics Letters , vol. 24, no. 13, pp. 804-805, 1988.

[19] Y. C. Chung and C. B. Roxio, "Frequency-locking of a 1.5 μm DFB laser to an atomic krypton line using optogalvanic effect," electronics letters, vol. 24, pp. 869-876, 1990.

[20] K. Shimoda, "Absolute frequency stabilization of the 3.39-μm laser on a CH4 line," Instrumentation and Measureme , vol. 17, no. 4, pp. 343-346, 1968.

[21] M. Ohi, "Frequency Stabilization of a PbSnTe Laser on a Methane Line in the v4 Band," Japanese Journal of Applied Physics , vol. 19, no. 9, pp. 541-543, 1980.

[22] S. Yamaguchi and M. Suzuki, "Frequency locking of an InGaAsP semiconductor laser to the first overtone vibration-rotation lines of hydrogen fluoride," Applied Physics Letters , vol. 41, no. 11, pp. 1034-1036, 1982.

[23] H. Tsuchida and M. O. T.Tako, “Frequency Stabilization of AlGaAs Semiconductor Laser to the Absorption Line of Water Vapor,” Japanese Journal of Applied Physics, vol. 21, pp. 1-3, 1982.

[24] H. Y. Ryu, S. H. Lee and H. S. Suh, “Widely tunable external cavity laser diode Injection locked to an optical frequency comb,” IEEE Photonics Technology letters, vol. 22, no. 14, pp. 1066 - 1068, 2010.

[25] W. Demtroder, Laser Spectroscopy volume 2 Experimental techniques, Berlin: Springer, 2008.

[26] C. Dyroff, “Tunable diode laser absorption spectroscopy for trace gas measurement with high sensitivity and low drift,” PhD thesis, University of Karlsruhe, 2009.

[27] L.S. Rothman *et al*. “The HITRAN 2008 molecular spectroscopic database,” *Journal of Quantitative Spectroscopy and Radiative Transfer,* vol. 110, no. 9 - 10, pp. 533 - 572, 2009.

[28] D. L. Pavia, G. M. Lampan and G. S. Kriz, Introduction to Spectroscopy, Stamford: Thomson Learning, 2001.

[29] M. W. Srigrist, Air Monitoring by Spectroscopic Techniques, vol. 127, New York: John Wiley & Sons, 1994.

[30] S. Schilt, L. Thévenaz and P. Robert, “Wavelength modulation spectroscopy: Combined frequency and intensity laser modulation,” Applied Optics, vol. 42, no. 33, pp. 6728-6738, 2003.

[31] C. L. Tang and J. M. Telle, “Laser modulation spectroscopy of solids,” *Journal of Applied Physics,* vol. 45, no. 10, 4503, 1974.

[32] P. Pokrowsky, W. zapka, F. Chu and G. C. Bjorklund, “High ferquency wavelength modulation spectroscopy with diode lasers,” Optics communications, vol. 44, no. 3, pp. 175 - 179, 1983.

[33] C. Jia-nian, W. Zhuo, Z. Ke-ke, Y. Rui and Wang Yong, “Etalon effects analysis in tunable diode laser absorption spectroscopy gas concentration detection system based on wavelength modulation spectroscopy,” in Photonics and Optoelectronic, Chengdu, 2010

[34] D. Rojas, P. Ljung and O. Axner, “An investigation of the 2f - Wavelength modulation

technique for detection of atoms under optically thin as well as thick conditions," Spectrochimica Acta - Part B Atomic Spectroscopy, vol. 52, no. 11, pp. 1663-1686, 1997.

[35] M. Fehar and P. A. Martin, "Tunable diode laser monitoring of atmospheric trace gas constituents," Spectrochimica Acta Part A: Molecular Spectroscopy, vol. 51, no. 10, pp. 1579-1599, 1995.

[36] J. Reid and D.Labrie, "Second-harmonic detection with tunable diode lasers — Comparison of experiment and theory," Applied Physics, vol. 26, no. 3, pp. 203-210, 1981.

[37] W. Jin, Y. Z. Xu, M. S. Demokan and G. Stewart, "Investigation of interferometric noise in fiber-optic gas sensors with use of wavelength modulation spectroscopy," Applied Optics, vol. 36, no. 28, pp. 7239-7246, 1999.

[38] K.Yamamoto, M.Uchida, S. Osawa and K.Uehara, "Long-distance simultaneous detection of methane and acetylene by using diode lasers coupled with optical fibers," Photonics Technology Letters, IEEE, vol. 4, no. 7, pp. 804 - 807, 1992.

[39] T.Iseki, "Calculation of the ratio between the second and first harmonic signals in wavelength-modulation spectroscopy for absorption measurement," Optical Review, vol. 10, no. 1, pp. 24-30, 2003.

[40] K. L. McNesby, R. T. Wainner and A. W. Miziolek, "High-sensitivity laser absorption measurements of broadband absorbers in the near-infrared spectral region," Applied Optics, vol. 39, no. 27, pp. 5006 - 5011, 2000

[41] J. Hodgkinson and R. P. Tatam, "Optical gas sensing: a review," Measurement Science and Technology , vol. 24, no. 1, 012004, 2013

[42] P. Kluczynski and O.Axner, "Theoretical description based on Fourier analysis of wavelength-modulation spectrometry in terms of analytical and background signals," Applied Optics, vol. 38, no. 27, pp. 5803-5815, 1999

[43] L. Philippe and R. Hanson, "Laser diode wavelength-modulation spectroscopy for simultaneous measurement of temperature, pressure, and velocity in shock-heated oxygen flows," Applied Optics, vol. 32, no. 30, pp. 6090-6103, 1993.

[44] L. Persson, F. Andersson, M. Andersson and S. Svanberg, "Approach to optical

interference fringes reduction in diode laser absorption spectroscopy," Applied Physics B, vol. 87, no. 3, pp. 523-530, 2007.

[45] W. Johnstone, K. Duffin, A. McGettrick, G.Stewart, A.Cheung and D. Moodie, "Tunable diode laser spectroscopy over optical fibres for gas measurements in harsh industrial environments," in *SPIE*, 2005.

[46] S. Martellucci, A. N. Chester and A. G. Mignan, Optical Sensors and Microsystems: New Concepts, Materials, Technologies, Kluwer Academic Publishers, 2002.

[47] P. Kluczynski, Å. Lindberg and O. Axner, "Characterization of Background Signals in Wavelength-Modulation Spectrometry in Terms of a Fourier Based Theoretical Formalism," Applied Optics, vol. 40, no. 6, pp. 770-782, 2001

[48] C.Nian, W. Zhuo, Z. Ke-ke, Y. Rui and W. Yong, "Etalon Effects Analysis in Tunable Diode Laser Absorption Spectroscopy Gas Concentration Detection System Based on Wavelength Modulation Spectroscopy," in Photonics and Optoelectronic, 2010

[49] D.Masiyano, "Use of Diffuse Reflections in Tunable diode Laser Spectroscopy", PhD thesis, Cranfield University, 2008.

3 Laser Diode Temperature Control and Series Resistance

The wavelength stability of a laser diode is vital in TDLAS. In TDLAS the target gas absorption line has narrow linewidth and therefore the detection technique requires excellent wavelength stability (10% better than the linewidth of the absorption line). The emission wavelength and output power of the laser diode are dependent on its operating temperature and injection current. Therefore, it is important to characterise the effects of temperature on laser diodes in order to operate them with a stable output power and emission wavelength.

In a conventional laser diode temperature controller, a thermistor sensor-based peltier thermo-electric cooler is used to stabilise the temperature of the laser diode. However, due to the laser diode package design, the thermistor is placed at a distance from the gain chip and does not sense the actual temperature of the laser gain chip. Therefore, the laser diode may drift with change in the ambient temperature. As the laser diode wavelength has large temperature gradient, the laser diode emission wavelength will vary with the change in temperature. Therefore, an alternative method is required to measure the actual temperature of the laser gain chip and to improve the stability of the emission wavelength of the laser diode.

Several techniques, such as the forward voltage method, the power averaged wavelength method and the null method, will be reviewed and compared for measuring the junction temperature (temperature of the gain chip) of the laser diode.

Moreover, the effects of temperature on the laser diode series resistance will also be discussed. The laser diode series resistance is calculated from the voltage drop across the laser diode. Different methods of calculating the laser diode series resistance from the voltage drop across the laser diode will also be reviewed in this chapter.

3.1 Temperature effects on laser diode

The wavelength of the laser diode increases with increasing temperature. This is an important parameter that needs to be taken into consideration in wavelength dependent applications such as TDLS, which have stability requirements of less than 0.2- 0.3 nm. The temperature of a laser diode e is a function of ambient temperature, junction heating and thermal design of

the laser diode package. Laser diodes' and LEDs' performances and reliabilities are temperature dependent. Changes in these parameters may lead to a change in their behaviour. In addition, the junction temperature of the laser diode is a function of the injection current and ambient temperature. At constant ambient temperature, an increase in the injection current will increase the junction temperature operating temperature. Therefore, the temperature change caused by the injection current will affect the output characteristics of the laser diode and thus should be taken into consideration [1]. A change in temperature affects the slope efficiency of the laser diode. The current density and noise of the laser diode increase with increasing temperature, and therefore decrease the efficiency of the laser diode. In general, the performance of the laser diode degrades with increasing temperature.

3.1.1 **Laser slope efficiency**

A laser diode is characterised by its slope efficiency η, which is a plot of the rate of change of output power P against the injection current, I_f , as shown in Figure 3.1 [2]

$$\eta = \frac{dP}{dI_f} \tag{3.1}$$

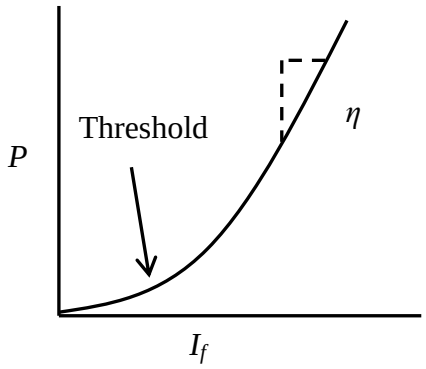

Figure 3.1 Diagram of the relation P vs If

The temperature dependence of the laser diode slope efficiency can be described by the following equation

$$\Delta\eta(T) = \eta ex\,p - \left(\frac{T - T_{ref}}{T_0}\right) \tag{3.2}$$

Where $\Delta\eta$ is the change in slope efficiency with temperature, T_{ref} is the reference temperature and T_0 is the characteristic temperature [3].

The slope efficiency has units of W/A and a better laser diode will have a higher slope efficiency. The slope efficiency of a laser diode generally depends on the internal quantum efficiency (the efficiency of the laser diode in converting injection current into light with in the laser structure), the reflectivity of the front and back facets, and absorption within the semiconductor material [4].

3.1.2 **Threshold Current vs. Temperature**

Laser diode threshold increases exponentially with higher operating temperature as compared to lower operating temperature. A laser diode's spontaneous and lasing emissions both suffer from lower external quantum efficiency (slope efficiency) due to increasing operation temperature.

Figure 3.2 shows the temperature dependence of a bulk laser and a strained quantum well laser in the 1300nm wavelength range. The laser diode output power and slope efficiency degrade with increasing temperature for both types of lasers [5][6].

.

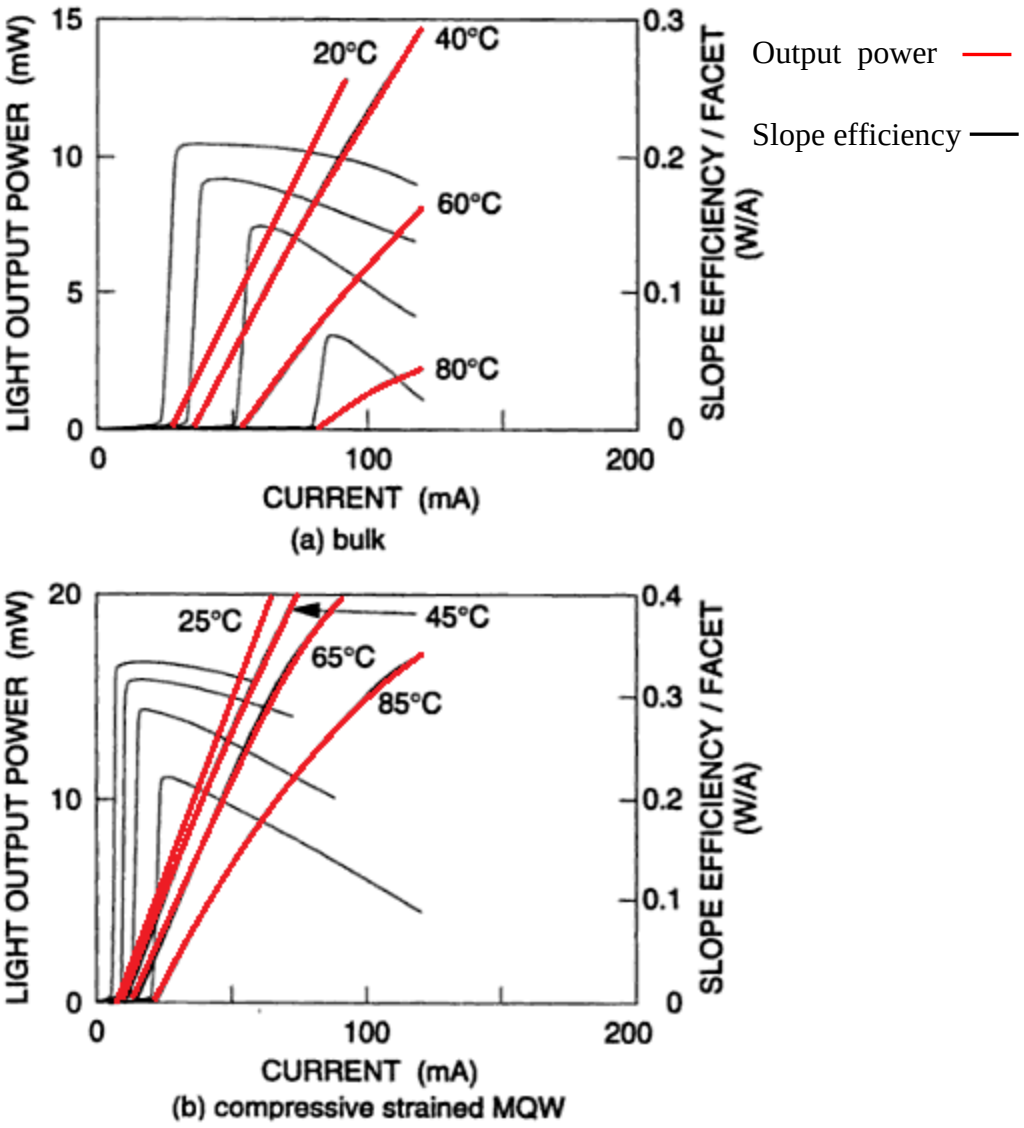

Figure 3.2 slope efficiency (black line)and light out power (red line) dependence on the operating temperature for 1300nm band (a) bulk type laser (b) strained quantum well InGaAsP/InP laser diode. Taken from M.Fukuda [7]

There are several factors that contribute to laser diode heating which are given below.

1) Heat generation in the diode laser. A fraction of input electric power is converted to heat via non-radiative effects i.e. the internal quantum efficiency is less than unity.
2) Heat generation due to radiative reabsorption processes i.e. the external quantum efficiency is less than unity and only a small proportion of light generated is emitted by the laser diode.
3) Joule heating due to ohmic contacts and series resistance [6][7].

Pilkuhn *et al* examined experimentally the effect of diode heating under stimulated emission using a GaAs laser diode operated in CW mode [8]. They reported that the rise in junction temperature was linear with direct injection current when the product of series resistance (bulk resistance + contact resistance) and current was smaller than the band gap voltage. However, when the product of direct current and series resistance was larger than the band gap voltage, then the rise in junction temperature is quadratic with current. The relationship between temperature and threshold current is given below [9]

$$I_{th} = I_0 \exp\left(\frac{T_J}{T_0}\right) \tag{3.3}$$

I_{th} is the threshold current, I_0 is the operation current, T_J is the junction temperature and T_0 is the characteristic temperature, which represents the dependence of the threshold current on temperature. T_0 increases with decreasing junction temperature. When a laser diode has a large characteristic temperature (T_0), the operating temperature will have a small effect on the lasing characteristics (such as slope efficiency and emission spectrum) of the laser diode [7].

Thermal runaway (increase in the junction temperature of the laser due to current) may limit the maximum output power of a laser at ambient temperature. To compensate the effect of thermal runaway, increased injection current is required, which further increases the junction temperature of the laser [10].

The laser diode characteristic temperature is dependent on the following physical mechanisms;

- Overflow of injected carriers from wells to barrier, optical confinement and cladding layers due to the increase in threshold current caused by a temperature increase of the active region.
- Free carrier absorption in the active and cladding area.
- Auger recombination (non radiative recombination which contributes to device degradation).
- Intervalance band recombination (a photon emitted during the recombination process is absorbed in the valence band during lasing) [11].

Figure 3.3 shows the temperature dependence of various laser diodes' threshold currents. The characteristic temperature for AlGaAs / GaAs laser diodes is around 100K-200K, caused primarily by the over flow of injected carriers.

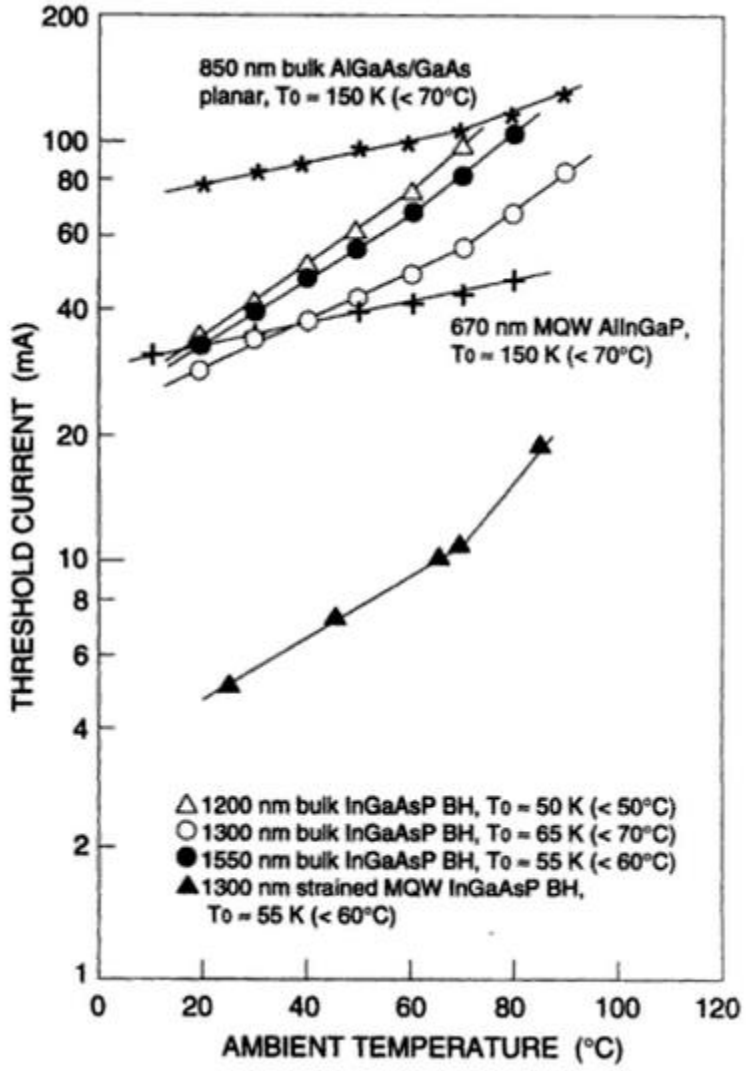

Figure 3.3 Threshold temperature dependence of different laser diodes. Taken from [7]

The Augar recombination rate and carrier overflow are constant above the threshold due to constant carrier density while above lasing. Therefore, free carrier absorption and intervalence band absorption in the active and cladding layers of the semiconductor device are the main factors that affect the temperature characteristics of laser diodes [7].

Quantum well and strained quantum well laser have better temperature characteristics than bulk laser diodes. This improved temperature characteristic is due to the reduction in threshold current density and carrier overflow as well as optical confinement layers. Strained quantum well InGaAsP / InP laser diodes have maximum lasing operating temperatures of

more than 100˚C , whereas InGaAsP/InP lasers with bulk active layers have operating temperatures of usually less than 100˚C [7][12].

3.1.3 **Wavelength vs. Temperature**

The emission wavelength of a laser diode is temperature dependent. The refractive index and band gap energy determines the laser diode wavelength, both of which vary with temperature. An increase in temperature usually increases the emission wavelength of the laser diode [1][13].

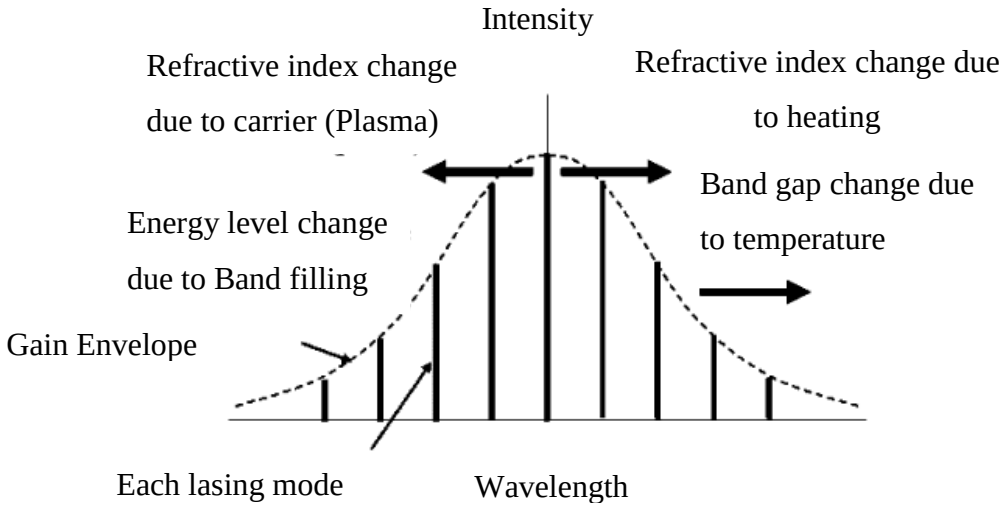

Figure 3.4 Laser wavelength variation. Taken from M.Fakuda *et al* [14]

The arrows in Figure 3.4 show the laser diode wavelength variation due to band gap energy and refractive index .The laser diode gain curve and longitudinal modes are both temperature dependent. The laser diode gain curve shifts to shorter wavelength with increasing injection when operated below the threshold. This shortening in the wavelength of the gain curve is caused by the band filling effect [15]. This effect can be express below as:

$$\lambda_p \approx \frac{1.24}{[E_g + (E_{FC} - E_C) + (E_V\_E_{F_V})]} \tag{3.4}$$

λ_p and E_g are the peak lasing wavelength and band gap energy and E_{FC}, E_{FV} are the quasi Fermi level of the conduction band E_c and valence band E_V.

Laser diode longitudinal modes also shift with changes in refractive index and cavity length. The longitudinal mode shift with injection current is described by equation (3.5)

$$\delta\lambda_m(N) = \left(\frac{\lambda_p}{n_r}\right)\left(\frac{dn}{dN}\right)\Delta N \tag{3.5}$$

$\delta\lambda_m$ is the size of wavelength shift of a laser diode, n, ΔN and λ_p are the refractive index, change in carrier density, and peak wavelength respectively. Table 3.1 shows the refractive index change with injection current for different gain materials.

Table 3.1 The change in refractive index as function of current density [7]

Gain material	$\boldsymbol{\frac{dn}{dN}}$
AlGaAs /GaAs (850nm)	-1.3 x10^{-21} cm^3
InGaAsP/InP (1300nm)	-4 x10^{-21} cm^3
InGaAsP/InP (1550nm)	-6 x10^{-21} cm^3

The central wavelength of the laser diode (above the threshold current) increases with increase in injection current due to Joule heating. The size of the wavelength shift for each longitudinal mode as a function of junction temperature T_j can be described by the following equation [7]

$$\delta\lambda_m(n) = \left(\frac{\lambda_0}{n}\right)\left(\frac{dn}{dT_j}\right)\Delta T_j \tag{3.6}$$

For the laser diodes in the infra-red region the value of $\frac{dn}{dT_j}$ is between 2 x10^{-4} and 5 x10^{-4} K^{-1} [5]. As a result laser longitudinal modes shift to longer wavelengths with increasing temperature [7].

Table 3.2 shows the effect of temperature on the longitudinal mode as a function of temperature for different gain materials. The temperature dependent longitudinal mode wavelength shift increases with increasing emission wavelength.

Table 3.2 Longitudinal mode shift with temperature [7]

Gain material	Longitudinal mode shift
AlGaAs /GaAs (850nm)	0.008 nm/ °C
InGaAsP/InP (1300nm)	0.1 nm/ °C
InGaAsP/InP (1550nm)	0.12 nm/ °C

The temperature dependence of the laser diode peak wavelength gain curve can be described as:

$$\frac{d\lambda_g}{dT_j} = -\left(\frac{hc}{E_g^2}\right)\left(\frac{dE_g}{dT_j}\right) = -\frac{1.24}{E_g^2}\left(\frac{dE_g}{dT_j}\right) \tag{3.7}$$

Where E_g is the band gap energy of the laser diode. At low temperatures, the band gap energy changes with the square of the temperature, however at room temperature E_g decreases with increasing temperature. Therefore, $\frac{\mathrm{dE_g}}{\mathrm{dT_j}}$ at temperatures near to room temperature, can be roughly approximated to [7]:

$$\frac{dE_g}{dT_j} = -\alpha_a \tag{3.8}$$

Where α_a is the temperature coefficient ($\frac{\mathrm{eV}}{\mathrm{k}}$) of the band gap energy. Combining equation (3.8) with equation (3.7) gives [7]

$$\frac{d\lambda_g}{dT_j} = \frac{1.24}{E_g^2}(\alpha_a) \tag{3.9}$$

The wavelength variation due to the change of operation temperature increases with the decrease in the band gap of the active layer material [7]. The wavelength shift due to the band gap energy as a function of temperature is given in the Table 3.3.

Table 3.3 Gain curve wavelength shift as a function of temperature [7]

Gain material	wavelength shift
AlGaAs /GaAs 850nm	0.25 nm/ °C
InGaAsP/InP 1300nm	0.4 nm/ °C
InGaAsP/InP 1550nm	0.6 nm/ °C

The laser diode wavelength varies with temperature largely due to the change in bad gap energy as a function of temperature. In a Fabry-Perot laser, the emission wavelength follows the dependence of the band gap energy on the temperature, whereas a DFB laser has improved temperature stability due to the optical losses introduced by the grating to select a wavelength [16]. In a DFB laser, the emission wavelength shift is due largely to the variation of refractive index with temperature. Therefore, a DFB laser has greater wavelength stability with temperature compared to a Fabry-Perot laser [13]. In this thesis, the wavelength stability under constant and variable ambient temperature of a DFB laser (IngaAsP/InP) at central wavelength of 1651nm was investigated for use in WMS.

3.1.4 **Light intensity vs Temperature**

A laser diode's output power decreases with increasing temperature. As the injection current is increased, the resultant Joule heating and increased operating temperature (ambient and heat sink) cause the output power to saturate. A laser diode's threshold current increases with increase in temperature due to the reduction of gain at a constant current. This reduction of the laser diode gain is due to the carriers occupying higher energy states [17][18]. Due to the increase in the laser diode threshold current, the efficiency of injection also decreases, which in turn decreases the slope efficiency, as shown in Figure 3.3. Moreover, the laser diode slope efficiency curve exhibits non-linearity with increasing operating temperature [1].

3.1.5 **Laser diode packaging**

Laser diode packaging is designed by taking into consideration the material, optical, mechanical and thermal engineering aspects of the laser. A laser diode can be packaged either actively cooled or uncooled. In an actively cooled packaged laser diode, no external cooling is required and the laser diode is mounted on a heat sink with a dual in-line packaging [19].

A cooled laser diode makes use of a thermoelectric cooler (TEC) and thermistor devices to keep its operating temperature stable. The laser diode is bonded to a ceramic subcarrier using eutectic bonding. The laser diode subcarrier is mounted on a TEC. In addition, a thermistor is attached to the laser diode's subcarriers, as shown in Figure 3.5, and is mounted to the TEC to monitor the temperature of the laser diode [20]. Figure 3.5 shows a schematic of basic laser diode elements [19]

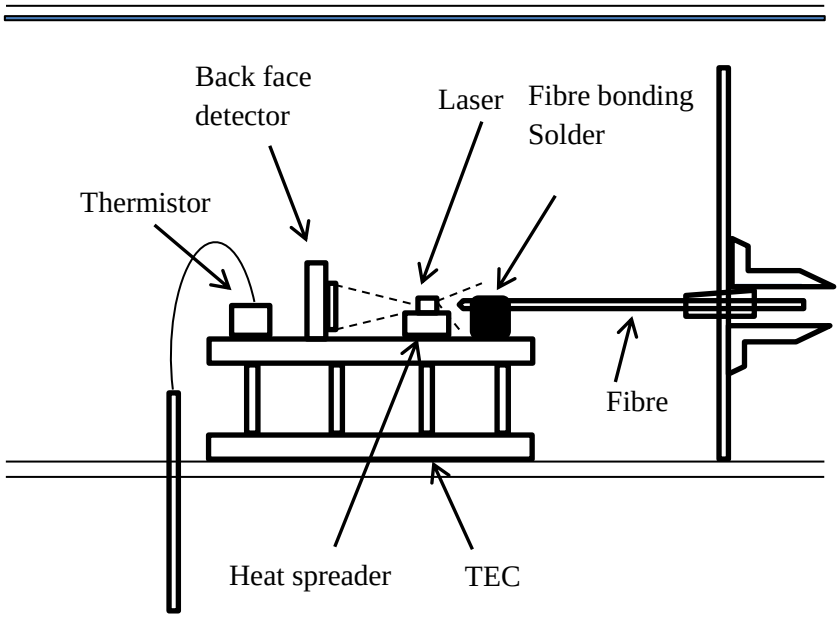

Figure 3.5 Schematic of basic laser diode elements. Redrawn from [19]

3.2 Techniques to measure junction temperature of laser diodes

Semiconductor devices such as laser diodes and light emitting diodes are sensitive to their operating temperatures and their performance and reliability are affected by temperature. A Laser diode's characteristics, such as peak wavelength, output power and voltage drop, are temperature dependent.

The junction temperature of a laser diode is a function of both ambient temperature and injection current [1]. The junction temperature measures the temperature of the active region.

However, the junction temperature is difficult to measure as laser diodes are very small. The laser diode junction temperature can be determined by methods such as measuring the wavelength of the laser diode, measuring the variation in the output power of the laser diode, and by measuring the threshold and variations in the threshold current and voltage drop across the laser diode in CW and pulsed modes due to the change in temperature.

3.2.1 **Forward voltage method**

The junction temperature of a laser diode has been determined by measuring the voltage drop across the laser diode [21]. This method consisted of two sets of experiments, where, firstly the laser diode was biased with a short pulse current of 1μs and duty cycle of 0.1%. It was assumed that no heat was generated when the laser diode was pulsed. Then, the voltage across laser diode was measured at different temperatures and pulse currents. The voltages measured at these short pulses were used to calibrate the laser diode. In the second part of the experiment, the laser diode was injected with a DC current, and the junction temperature was measured by comparing voltages measured under pulsed and DC currents [22]. The relationship between forward voltage and junction temperature is reported by Xi *et al* [23] and is given by equation (3.10).

$$\frac{dV_f}{dT_j} = \frac{eV_f - E_g}{eT_j} + \frac{1}{e}\frac{dE_g}{dT_j} - \frac{3k}{e} \tag{3.10}$$

Where V_f and T_j are forward voltage and junction temperature respectively. E_g is the band gap energy and k represent Boltzmann's constant. As the laser diode has a series resistance of a few ohms (series resistance is of a laser diode is of the order of 5-10 Ω. A detailed discussion on the effect of temperature on laser diode series resistance is undertaken in section 3.4) [24], the equation (3.10) can be further expanded by including the voltage drop due to series resistance, which is thermally activated.

$$\frac{dV_f}{dT_j} = \left[\frac{eV_f - E_g}{eT_j} + \frac{1}{e}\frac{dE_g}{dT_j} - \frac{3K}{e}\right] - \left[\frac{1}{2}\frac{E_a + 2S_T kT_j}{kT_j{}^2} IR_s\right] \tag{3.11}$$

Where E_a is the dopant activation energy of the series resistor R_s and S_T represent the temperature dependence of the carrier mobility.

The forward voltage technique has been used for measuring the junction temperature of GaN based laser diodes. Ryu *et al* suggested that forward voltage technique can be used for laser diodes with large forward voltages [25]. Therefore, in general, this method has not been used

for laser diodes with a gain material of InP or GaAs, which have small forward voltages. However, Jeong *et al* reported measurement of the junction temperature using the forward voltage method for high power InAs based quantum dot lasers [26].

An accuracy of ±3˚C has been reported for measuring junction temperature for LEDs [27]. However, this technique needs calibration for individual lasers. In addition, generating a very short current pulse signal and its interpretation is complex, requiring careful design and interpretation for the measurement of laser diode junction temperature.

3.2.2 **Peak Emission Wavelength**

The temperature dependence of the bandgap energy (and therefore peak wavelength) can be used to measure the junction temperature of semiconductor devices. This method also requires calibration, where the peak energy (the wavelength at which the emitted energy is the greatest) is measured at different short pulse currents with low duty cycle, in a similar manner to the forward voltage method. The calibration method establishes the relationship between peak energy and junction temperature at different currents. Semiconductor devices (such as LEDs and laser diodes) are then injected with different DC currents and the peak emission energy is measured at a constant temperature, as shown in Figure 3.6. The junction temperature for each current is then determined from the calibration data [24]

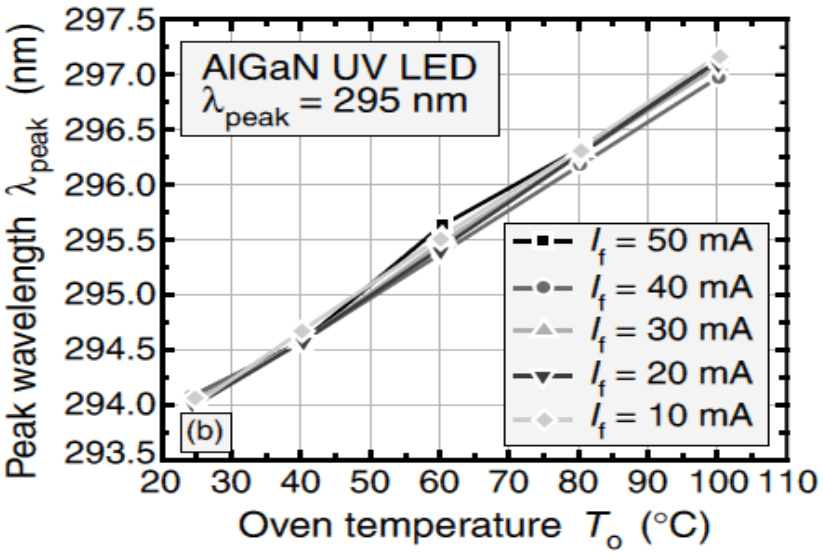

Figure 3.6 LED peak wavelength at different oven temperature and pulsed injection current. Taken from Xi *et al* [24]

The peak energy for band- to-band recombination from bulk semiconductor optical emission is given by equation (3.12) [28]:

$$hv_{peak} = E_g + \frac{1}{2}kT \tag{3.12}$$

Where v_{peak} is the peak frequency. As $\frac{dE_g}{dT} > \frac{1}{2}\frac{d}{dT}kT$, the peak energy as a function of temperature can be derived from Varshni equation which is given below [22]:

$$E_g = E_g|_{0K} - \frac{\alpha T^2}{\beta + T\beta} \tag{3.13}$$

Where α and β are the Varshni parameters. Therefore, the junction temperature of LEDS and laser diodes can be estimated from the peak position of the emission spectrum [21][28].

This method requires calibration of individual devices and the accuracy of the junction temperature measurement is limited by the lack of accuracy (error bar of the peak wavelength is 5-10% of the FWHM of the luminescence line) in determining the position of the peak wavelength [22].

3.2.3 **Null measurement method**

This method was put forward by Paoli where, the modal wavelength (lasing longitudinal mode) was used to measure the junction temperature of the laser diode [29]. The refractive index of the laser waveguide is a function of temperature, which has been exploited in this technique for measuring temperature. This method makes use of a null measurement where the laser diode wavelength in CW mode at constant current is measured. Then the laser diode is pulsed with a short current pulse and a very low duty cycle. The drop in the heat sink temperature (ΔT_{hs}) (while pulsing the laser diode) required to maintain the wavelength in CW mode is measured. The temperature drop (ΔT_{hs}) can be considered to be the temperature rise (ΔT) in the laser cavity when the laser diode is operated in CW mode while maintaining the same wavelength. The laser diode thermal impedance R_{th} is related to ΔT

$$\Delta T = R_{th}P_j \tag{3.14}$$

Where

$$P_j = I_f V_f - P_o \tag{3.15}$$

Where P_j is the power dissipated when the laser is operated in CW mode. I_f ,V_f are the injection current and voltage drop across the laser diode and P_o is the output. The junction temperature T_j is given by:

$$T_j = T_{hs} + \Delta T \tag{3.16}$$

Where T_{hs} is the heat sink temperature.

This method does not require calibration and very small temperature differences (0.2 $^{\circ}$C) can be measured[29]. However, this method requires an extrapolation to the CW condition, making it less reliable. In addition, the need for short current pulses (ns) with duty low cycle (0.1%) makes it difficult to implement [29].

3.2.4 **Power averaged wavelength method**

The measurement of the laser diode junction temperature can be carried out by measuring the laser diode output power and the power averaged wavelength in CW mode [30]. This is a modified version of the null method described in section 3.2.3.

The laser diode wavelength, voltage drop and output power are measured at different currents and temperatures. The laser diode waste thermal power, P_j , is calculated using equation (3.15) at these currents and temperatures and is plotted against the wavelength. The power averaged wavelength is defined as the zero power intercept of this plot, i.e. the point at which $P_j = 0$ and $P_o = IV$. At the zero power intercept $T_j = T_o$. This power averaged wavelength is then plotted against the thermistor based Peltier temperature and the junction temperature is determined from this plot [30].

The power averaged wavelength method does not require short current pulses, which can be difficult to generate and interpret due to pulse distortion.

3.2.5 **Method of Fabry-Perot mode**

This is a modified version of Null method section 3.2.4 for measuring junction temperature from the FP modes of the laser diode, where, instead of a short pulse injection current with varying duty cycle, the laser diode is modulated with a high frequency (500 MHz) square wave [31]. This high frequency square wave modulation results in a double peak FP mode, as shown in Figure 3.7.

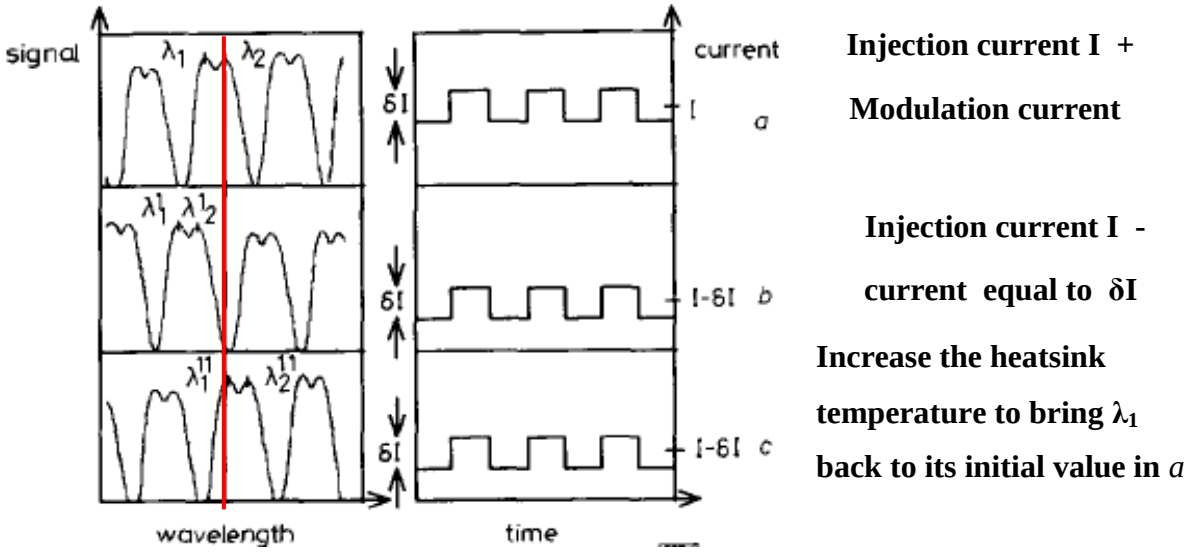

Figure 3.7 Results of Fabry-Perot mode tracking for thermal impedance measurement. Taken from Bhumbra *et al* [31]

A current equivalent to the modulation amplitude (δI) is subtracted from the average current I, while still modulating the laser diode with a square wave of amplitude δI. This reduction in injection current reduces the carrier density in the laser waveguide, hence shifting the Fabry-Perot modes to longer wavelengths. In addition, the junction temperature is also reduced, which shifts the modes to shorter wavelength. The shift to shorter wavelengths due to reduced junction temperature is dominant and therefore the net shift is towards shorter wavelengths, as shown in Figure 3.7b. The mode at wavelength λ_2 moves to λ_1, with this reduction of injection current by δI. The junction temperature of the laser diode is brought back to its original value by increasing the heat sink temperature. Therefore the Fabry-Perot mode at wavelength λ_1 is brought back to its initial value, as shown in Figure 3.7c.

The shorter and longer FP modes are due to carrier concentration when the laser diode square modulation is in “on” and “off” mode causing a variation in refractive index in the laser diode waveguide. The average temperature over the “on” and “off” periods is the same, due to the slow dissipation of heat compared to the period of modulation, and is dependent on the DC injection current. Therefore, the separation of FP mode peaks is due to carrier concentration only. Thus junction temperature of the laser diode can be correctly measured from the carrier density dependent wavelength shifts.

This method overcomes the problem of heating effects when the laser diode is pulsed.

3.3 Laser diode Series Resistance

Laser diode forward voltage is the sum of the junction voltage and voltage drop across its series resistance. Both junction voltage and series resistance are temperature dependent. Junction voltage decreases with increase in temperature and series resistance increases with increasing temperature. Therefore, to stabilise the laser diode temperature using the voltage drop across the laser diode (where this concept is explored in chapter 5 and 6), the temperature dependent properties of the series resistance needed to be taken into consideration.

Theoretical I-V characteristics of a diode can be described by the Shockley equation. The injection current I applied to a diode is related to its voltage V_f by the following Shockley equation

$$I = I_s \left[exp\left(\frac{eV_f}{\eta_{ideal} kT} \right) \right] \tag{3.17}$$

Where e is the electronic charge, k is Boltzmann's constant and T is temperature. I_s is the saturation current and η_{ideal} is the ideality factor, with a value of 1 for an ideal diode. For arsenide and phosphide diodes, the ideality factor can be as high as 2. For GaN/ GaInN an ideality factor of 6 has been reported [22].

Diodes are made of a semiconductor material, which does not behave as an ideal conductor when operated with a forward bias, and does not behave as a perfect insulator with a reverse bias [32].

Figure 3.8 shows the effect of series and parallel (shunt resistance) resistance on the I-V characteristic of the pn junction diode.

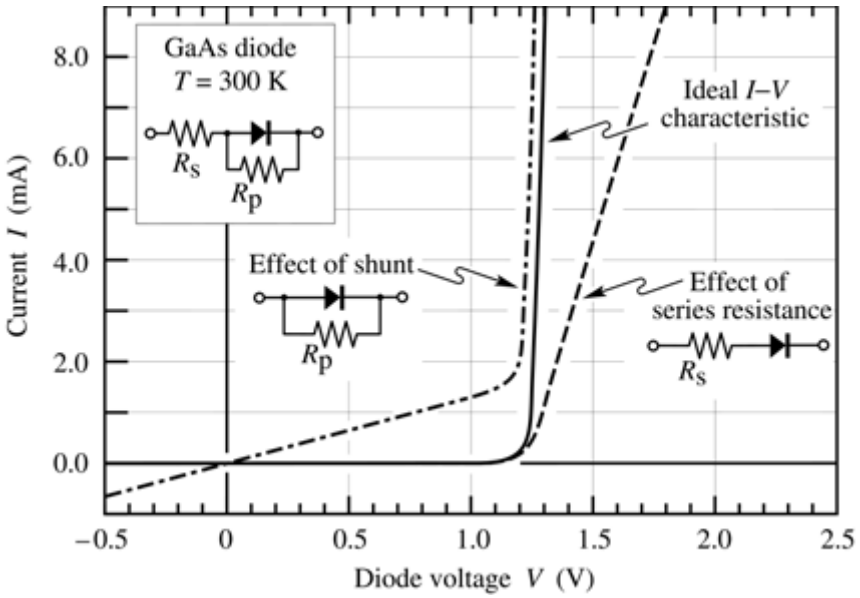

Figure 3.8 Effect of series and parallel (shunt) resistance on the I-V characteristic of a GaAs diode. Inset shows the equivalent circuit of the diode. Taken from [22]

The series resistance (R_s) of the diode is caused by the ohmic contact and the resistance of the diode's neutral region. A parallel resistance (R_p) is caused by a channel bypassing of the pn junction. To include these parasitic resistances, the Shockley diode equation (3.17) is modified to become:

$$I_f - \frac{(V_f - I_f R_s)}{R_p} = I_s\left[exp\left(\frac{e(V_f - I_f R_s}{\eta_{ideal} kT}\right)\right] \tag{3.18}$$

When $R_p \to \infty$ and $R_s = 0$ equation (3.19) reduces to the Shockley equation.

There are two types of resistances in a pn junction diode when operated with forward bias:

1. Static resistance: This is the resistance that applies when the laser diode is operated in DC mode. This is simply the ratio of DC voltage across the junction of the diode and the DC injection current, $\frac{V_f}{I_f}$
2. Dynamic resistance: This diode resistance is described by the diode junction opposition to the AC current riding on a DC current[32], $\frac{\delta V_f}{\delta I_f}$

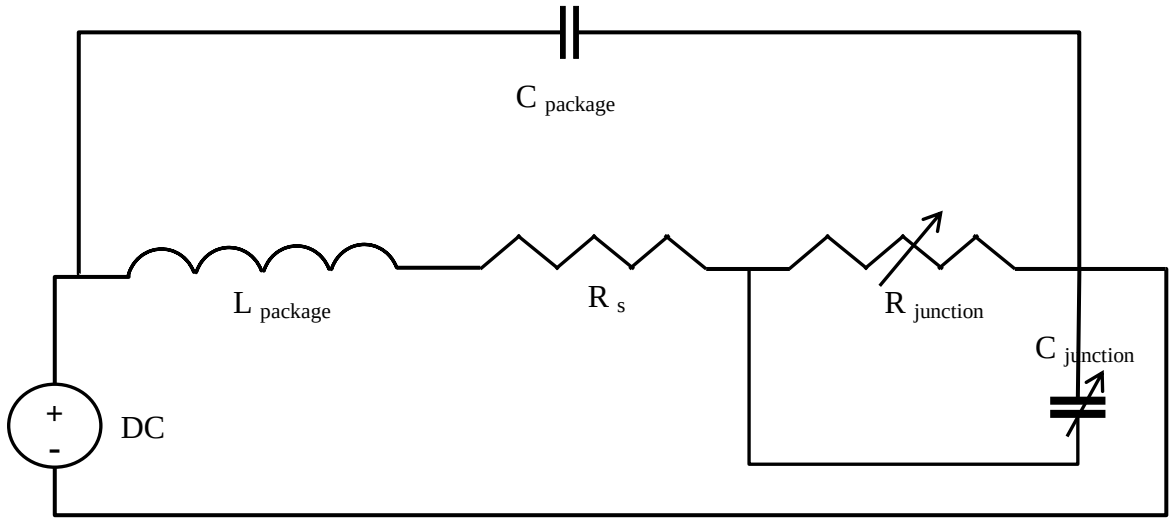

Figure 3.9 Small signal model of a diode [33]

Figure 3.9 shows the small signal model of a diode.

3.3.1 **Evaluation of laser diode resistance**

The resistance of a laser diode can be measured in the following two regions of the I-V curve:

1. Near the origin, where $V_f \ll \eta kT/e$, the pn junction parallel resistance is given by the following equation

$$R_p = \frac{dV_f}{dI_f}, \qquad V_f \ll \eta kT/e \tag{3.19}$$

The resistance measured near the origin is the parallel resistance. It is a very large resistance and the series resistance of the diode can therefore be ignored when evaluating the parallel resistance

2. At high voltage $V_f \gg \eta kT/e$, the resistance of the diode is series resistance and the I-V characteristics of the laser diode become linear

$$R_s = \frac{dV_f}{dI_f}, \qquad V_f \gg \eta kT/e \tag{3.20}$$

To evaluate the laser diode series resistance, it is recommended not to operate the laser diode at high applied bias, to avoid device heating.

For $R_p \to \infty$, the I-V characteristic for the diode can be written as

$$I_f = I_s\left[exp\left(\frac{e(V_f - I_f R_s)}{\eta_{ideal} kT}\right)\right] \tag{3.21}$$

Solving equation (3.21) for V with respect to injection current I

$$\frac{dV_f}{dI_f} = R_s + \frac{\eta_{ideal} kT}{e}\frac{1}{I_f} \tag{3.22}$$

The second term on the right hand side of the above equation (3.22) represents the junction resistance R_j , as shown in Figure (3.9). A plot of $\frac{dV_f}{dI_f}$ vs $\frac{1}{I_f}$ can be used to calculate the series resistance of a diode.

3.4 Diode resistance measurement methods

There are several methods that can be used to measure the resistance of a diode based on the manipulation of equation (3.22). Detailed work on Schottky diode series resistance modelling and measurement has been reported in the literature [36][37][38][39]. However, literature on the laser diode series resistance modelling and measurement is scarce. Barnes and Paoli reported on the electrical characterisation of a double heterostructure junction laser for calculating the series resistance and laser threshold current [33]. The effect of the series resistance on the output power of a strained layer multiple quantum well ridge waveguide InGaAsP laser was reported by Elenkrig *et al* [34] . They investigated the effect of temperature on the laser diode series resistance and the reduction of output power of the laser diode due to the presence of series resistance. Xiangming undertook detailed modelling and measurements of the differential resistance and ideality factor of heterostructure LEDs and laser diodes in his doctoral thesis [35].

The following section covers several methods for measuring the series resistance of a Schottky diode. These methods were then adapted to measure the series resistance of the DFB laser diode, covered in chapter 5 of this thesis.

3.4.1 **Norde Method**

Norde proposed the calculation of the series resistance of an ideal Schottky diode using an auxiliary function [36]

$$F(V) = \frac{V_f}{2} - \frac{1}{\beta_N} \ln\left(\frac{I}{A^* AT^2}\right) \tag{3.23}$$

Where V_f and A_d are the voltage and area of the diode. A^* is Richardson's constant and $\beta_N = \frac{e}{kT}$

For a diode with series resistance, the Schottky diode equation can be written as

$$I_f = I_s exp[\beta_N (V_f - IR_s)] \tag{3.24}$$

Where $I_s = A^* A_d T^2 exp(-\Phi_B)$ (Φ_B is the barrier height of the diode junction). By substituting equation (3.24) in equation (3.23)

$$F(V) = -\frac{V_f}{2} + I_f R_s + \Phi_B \tag{3.25}$$

By differentiating equation (3.25) with respect to voltage

$$\frac{dF(V)}{dV_f} = R_s \left(\frac{dI_f}{dV_f}\right) - \frac{1}{2} \tag{3.26}$$

By differentiating the ideal Schottky diode equation

$$\frac{dI_f}{dV_f} = \frac{d}{dV}[I_s exp[\beta_N (V)] = \beta_N I_f \tag{3.27}$$

Substituting equation (3.25) in equation (3.24)

$$\frac{dF}{dV} = \frac{\beta R_s I}{1 + \beta R_s I} - \frac{1}{2} \tag{3.28}$$

By plotting $F(V)$ vs V_f, and V_f vs I_f, the minimum points F (V_o , I_o) can be calculated. From the value of F (V_o , I_o) and its minimum current I_0 will give the measure of series resistance

$$R_s = \frac{kT}{eI_0} \tag{3.29}$$

In the Norde method of calculating series resistance, the ideality factor for the diode was considered to be 1, which is not typically the case for the real diode (lies in the range 1-2). Moreover, a single minimum point (V_o , I_o) was used to calculate the barrier height and series resistance, which is not representative of the full range of the diode behaviour [37].

3.4.2 **Cheung and Cheung Method**

The Cheung and Cheung method uses the forward I-V data of given Schottky diode to calculate the series resistance of the diode [38]. By manipulating the Schottky diode equation (3.24) can be obtained

$$\frac{dV_f}{dln(I_f)} = R_s I_f + \left(\frac{\eta kT}{eI_f}\right) \quad \textbf{(}3.30\textbf{)}$$

A plot of $\frac{dV_f}{dlnI_f}$ vs I_f will result in a straight line, with a gradient at large I_f that gives the series resistance for the diode [38]. The advantage of this method is that it is simpler than the Norde method and only the V-I data is required to calculate the series resistance of the diode. Use in the high current range is emphasised in the Cheung and Cheung method due to the use of linear current as the abscissa; this may result in unreliable resistance measurements in high resistance diodes [37].

3.4.3 **Werner Method**

Werner proposed three plots using the diode Shockley equation [39]. One of the plots was similar to that used in the Cheung and Cheung method for calculating series resistance of a diode. Using the diode equation (3.24) under forward conditions with $V - R_s I_f \gg \frac{kT}{e}$,

$$\frac{1}{I_f}\frac{dI_f}{dV_f} = \frac{\beta_N}{\eta}\left(1 - \frac{dI_f}{dV_f}R_s\right) \quad \textbf{(}3.31\textbf{)}$$

Equation **(**3.31) shows that a plot between $\frac{1}{I_f}\frac{dI_f}{dV_f}$ and $\frac{dI_f}{dV_f}$ will result in a straight line with negative gradient whose x-axis intercept gives the measure of series resistance [39]. In the I-V data, small voltage steps are used to obtain more accurate values of $\frac{dI_f}{dV_f}$. The data in the intermediate voltages in the I-V characteristics are emphasised in this method, limiting the effect of the data in the low and high voltage regions. Therefore the effect of minority current (a leakage current which is generated due to thermally generated carriers at the diffusion

length of the junction) is reduced in the calculation of series resistance using this method [37].

3.5 Summary

The effect of temperature on laser diode threshold current and emission wavelength has been discussed in this chapter. Laser diode output characteristics such as output power and wavelength degrade with increases in operating temperature. The laser diode junction temperature increases because of heat generation due to non-radiative processes, heat generation because of less than unity quantum efficiency, and Joule heating. The laser's characteristic temperature determines the effect of operating temperature on laser diode behaviour. High characteristic temperature laser diodes have lasing characteristics that are less sensitive to the temperature. Thermal resistance is the measure of increase in junction temperature caused by external factors (ambient temperature and TEC temperature) is indicated by its thermal resistance. A low thermal resistance reduces the level of degradation of the diode's performance at high temperature.

There are several techniques which are used to measure the junction temperature of LEDs and laser diodes which are summarised it in the Table 3.4 below.

Table 3.4 Comparison of techniques for measuring junction temperature

Technique	Advantages	Disadvantages
Forward voltage [23]	An accurate technique widely used for LEDs and Laser diode (GaN, and quantum dot laser). It can be implemented in TDLS	Need calibration for each device. Requires extremely short pulse current which is difficult to produce and susceptible to distortion.
Peak emission wavelength [23]	The accuracy of this technique is similar to that of forward voltage	This technique requires calibration. It lacks accuracy due to difficulty in determining the peak wavelength.

Technique	Advantages	Disadvantages
Null measurement [29]	This technique does not require calibration. It is an accurate technique for measuring small variation in junction temperature.	Requires an extrapolation to CW condition making it less reliable. Requires short current pulses and low duty cycle where the heat during the pulse is ignored underestimating junction temperature.
Power Averaged wavelength method [30]	It is a CW technique	Only proven to be accurate for high power laser diodes. This method cannot be implemented in TDLS.

With the exception of the forward voltage method, the techniques summarised in Table 3.4 cannot be implemented in controlling the emission wavelength of the laser diode. The voltage drop across the laser could be used in a feedback loop to stabilise the temperature and eventually the wavelength of the laser diode used in TDLS.

Laser diode series resistance has also been discussed in this chapter, with a focus on its effect on the performance of the laser diode. As the injection current to the laser diode is increased, Joule heating increases in the active area and the ohmic resistance (due to the neutral region of the semiconductor and contacts) becomes larger. The laser diode output power saturates due to this increase in the active region temperature and resistance.

The measurement of diode series resistance was first proposed by Norde, who developed an auxiliary function to calculate this series resistance. However, this method is limited to measurement at a single data point to calculate series resistance and may result in erroneous series resistance calculation.

Cheung and Chung provided an alternative method which took into consideration several data points over the linear region of the I-V plot to calculate series resistance. The Cheung and Cheung method required an I-V plot with small steps to accurately calculate the series resistance.

Werner proposed three different plots for calculating the series resistance, with one plot similar to that of the Cheung and Cheung method. Using a plot of $\frac{1}{I_f}\frac{dI_f}{dV_f}$ vs $\frac{dI_f}{dV_f}$ gave the best result by reducing the effect of minority carries in the calculation of series resistance

In the next chapter these methods for measuring the series resistance of a diode will be extended to the laser diode used in this thesis. The Cheung and Cheung method will be used to measure the series resistance of the laser diode.

The effect of temperature on the laser diode series resistance and its contribution to the forward voltage will be investigated and integrated in the forward voltage based control feedback method to stabilise the laser diode wavelength.

3.6 References

[1] H. Zappe, Laser Diode Microsystems, New York: springer, 2003.

[2] C. H. Cox III, Analog Optical Links: Theory and Practice, Cambridge: Cambridge University Press, 2006.

[3] H. Liu, X. Liu, L. Xiong and W. Zhao, Packaging of High Power Semiconductor Lasers, New York: Springer, 2014.

[4] T. Numai, Laser Diodes and Their Applications to Communications and Information Processing,New Jersey: John Wiley & Sons, Inc, 2010.

[5] O. Madelung, Physics of III-V Compounds, New York: John Wiley & Sons, 1964.

[6] W. Susaki, "Current dependence of junction temperature in C-W Operated GaAs laser diodes," Japanese Journal of Applied Physics, vol. 6, no. 8, 1967

[7] M. Fukuda, Optical Semiconductor Devices, New York: John Wiley & Sons, 1999.

[8] M. H. Pilkuhn and H. Rupprecht, "Optical and electrical properties of epitaxial and diffused GaAs injection lasers," Applied Physics, vol. 38, no. 1, pp. 5-10, 1967.

[9] S.W. Park and J. H. Han, "Effect of temperature and injection current on characteristics of TO-CAN packaged Fabry-Perot laser diode," Current Applied Physics, vol. 7, no. 1, pp. 6-9, 2007.

[11] G. Morthier and P. Vankwikelberge, Handbook of Distributed Feedback Laser Diodes, Norwood: Artech House, 2013.

[12] C. E. Zah, M. C. Wang, R. Bhat, T. P. Lee, S. Chuang, Z. Wang, D. Derby, D. Flanders and a. J. J. Hsieh, "High-temperature modulation dynamics of 1.3 μm $Al_xGa_yIn_{1-x-y}As$/InP compressive-strained multiple-quantum-well lasers," in Semiconductor Laser Conference, 1994., 14th IEEE International , vol., no., pp.215-216, 19-23 Sep 1994.

[13] R. G. Hunsperger, Integrated Optics Theory and Technology, New York: Springer, 2009.

[14] M.Fakuda, T.Mishima, N.Nakayama and T.Masuda, “Temperature and current coefficients of lasing wavelength in tunable diode laser spectroscopy,” Applied Physics B, vol. 100, no. 2, pp. 377-382, 2010.

[15] T. Numai, Fundamentals of Semiconductor Lasers, Japan: Springer Science & Business Media, 2004.

[16] G. Morthier, P. Vankwikelberge Handbook of Distributed Feedback Laser Diodes, Artech House, 2013.

[17] E.Kapon, Semiconductor Lasers: Materials and structures, London: Academic Press, 1999.

[18] W. G. Scheibenzube, GaN-Based Laser Diodes: Towards Longer Wavelengths and Short Pulses, Springer-Verlag, 2012.

[19] S.C.Gupta, Textbook on Optical Fiber Communication And Its Applications, New Delhi: PHI Learning Pvt. Ltd, 2004.

[20] P. H. Holloway and G. E. McGuire, Handbook Of Compound Semiconductors Growth, Processing, Characterization and Devices, Noyes Pulications, 1995.

[21] E.F.Schubert and Y.Xi, “Junction-temperature measurement in GaN ultraviolet light-emitting diodes using diode forward voltage method,” Applied Physics letters, vol. 85, no. 12, pp. 2163-2165, 2004.

[22] E.F.Shubert, Light-Emitting Diodes, Cambridge: Cambridge University Press, 2006.

[23] Y. Xi, T. Gessmann, J. Xi, J. K. Kim, J. M. Shah, E. F. Schubert, A. J. Fischer, M. H. Crawford, K. H. A. Bogart and A. A. Allerman “Junction temperature in Ultraviolet Light-Emitting diodes,” Japanese Journal of Applied Physics, vol. 44, no. 10, pp. 7260-7266, 2005.

[24] K Petermann, Laser Diode Modulation and Noise, Springer Science & Business Media, 1991.

[25] H. Ryu, K. H. Ha, J. H. Chae, O. H. Nam and Y. J. Park, “Measurement of junction temperature in GaN-based laser diodes using voltage-temperature characteristics,” Applied Physics letters, vol. 87, no. 9, 093506, 2005.

[26] J. H. Jeong, K. C. Kim, J. I. Lee, H. J. Kim and I.K.Han, " Junction temperature measurement of InAs Quantum-Dot laser diodes by utilizing voltage-temperature method," IEEE Photonics Letters, vol. 20, no. 16, pp. 1354-1356, 2008.

[27] Y. Xi, J-Qun. Xi,T. Gessmann, J. M. Shah, J. K. Kim, E. F. Schubert, A. J. Fischer, M. H. Crawford, K. H. A. Bogarz and A. A. Allerman, " Junction and carrier temperature measurement in deep-ultraviolet light-emitting diodes using three different method," Applied Physics Letters, vol. 86, no. 3, 031907, 2005.

[28] S. Chhajed , Y. Xi , T. Gessmann , J-Qun. Xi , J. M. Shah , J. K. Kim , E. F. Schubert, "Junction temperature in light-emitting diodes assesed by different methods," in SPIE, vol. 5739, 2005.

[29] T. L. Paoli, "A new technique for measuring the thermal impedance of junction lasers," Quantum Electronics, vol. 11, no. 7, pp. 498-503, 1977.

[30] L. A.Johnson, A.Teh, " Measuring high power laser diode junction temperature and package thermal impedance," [Online]. Available: www.ilxlightwave.com. [Accessed 2012].

[31] B. S. Bhumbra, G. H. B.Thompson and A. P. Wright, "Thermal impedance measurement of semiconductor lasers," Electronics Letters, vol. 30, no. 10, pp. 793-794, 1994.

[32] R. K. Garg, A. Dixit and P. Yada, Basic Electronics, NewDelhi, Laxmi Publications, 2008.

[33] P. A. Barnes and T. L. Paoli, "Derivative measurements of the current-voltage characteristics of double-heterostructure injection lasers," Quantum Electronics, vol. 12, no. 10, pp. 633-639, 1976.

[34] B. B. Elenkrig, S. Smetona and J. G. Simmons, "Series resistance and its effect on the maximum output power of a 1.5um strained-layer multiple-quantum well ridge waveguide InGaAsP lasers," Applied Physics, vol. 87, no. 1, pp. 1-4,2000.

[35] L. Xiangming, "Modeling and Measurement of the Differential Resistanc and Ideality Factors in Heterostructure Light Emitting Diodes", PhD thesis, North Carolina state univeristy, 2008.

[36] H. Norde, “A modified forward I-V plot for Shottky diode with high series resistance,” Applied Physics, vol. 50, no. 7, pp. 5052-5053, 1979.

[37] V. Auby and F. Meyer, “Schottky diodes with high series resistance: Limitation of forward I-V method,” Applied Physics, vol. 76, no. 12, pp. 7973-7984, 1994.

[38] S. K. Cheung and N. W. Cheung, “Extraction of Schottky diode parameters from forward current voltage characteristics,” Applied Physics, vol. 49, no. 2, pp. 85-87, 1986.

[39] J. H. Werner, “Schottky barrier and pn junction I/V plots- small signal evaluation,” Applied Physics A, vol.47 no. 3, pp. 291-300, 1988.

4 Laser Diode Junction Temperature Measurement

Junction temperature measurement of the laser diode is carried out by experientially evaluating forward voltage and power averaged wavelength method reviewed in chapter 3. The junction and thermal impedances of three different types of light sources i.e. two distributed feedback laser diodes (DFB), a vertical cavity surface emitting laser diode (VCSEL) and an ultra violet (UV) light emitting diode (LED) is calculated and compared. The forward voltage method in this chapter does not take into account contribution of the voltage drop across the laser diode series resistance to the forward voltage, which will be the topic of chapter 5

In the first section of the chapter, the difference between voltage controlled current pulse and current controlled pulses, and their effects on the accuracy of laser diode junction temperature measurement are discussed. This section is followed by an investigation of laser diode junction temperature measurement techniques, such as forward voltage and power average wavelength techniques. The experimental work on these two techniques will suggest whether the junction temperature of the above mentioned light sources could be measured accurately. Then the junction temperature measurement results from these two techniques will be compared. The effect of ambient temperature on laser diode characteristics are explored in the final section of the chapter.

4.1 Forward Voltage theory

The injection current and laser diode junction voltage can be represented by the Shockley equation [1] as reported in section 3.3

$$I_f = I_s exp\left(\frac{eV_f}{\eta kT}\right) \tag{4.1}$$

Where I_f and I_s are forward and saturation current of the laser diode respectively. V_f is the forward voltage of the laser diode, e is the electronic charge, k is the Boltzmann's constant, and T is the thermodynamic temperature. η is the ideality factor and is approximately equal to 1 for an ideal laser diode operated above the threshold.

The voltage of the laser diode can be derived from equation (4.1)

$$V_f = \frac{\eta kT}{e}\ ln\frac{I_f}{I_s} \tag{4.2}$$

When $\frac{\eta kT}{e}$ « V_f , which is also called the thermal voltage then

$$\frac{dV_f}{d_T} = \frac{d}{dT}\left[\frac{\eta kT}{e} ln\frac{I_f}{I_s}\right] \tag{4.3}$$

Where saturation current I_s,

$$I_s = \left[T^3 exp\left(\frac{-E_g}{kT}\right)\right] T^{\frac{\gamma}{2}} \tag{4.4}$$

E_g is the band gap energy measured in volts and γ is a constant [2]. The $T^{\frac{\gamma}{2}}$ term is close to unity, and the saturation current can be approximated as

$$I_s = T^3 exp\left(\frac{-E_g}{kT}\right) C \tag{4.5}$$

Substituting equation (4.5) in (4.3) equation

$$\frac{dV_f}{dT} = \frac{d}{dT}\left[\frac{\eta kT}{e} \ln\left(\frac{I_f}{C}\right) - \frac{3lnT\,\eta kT}{e} + \eta E_g\right] \tag{4.6}$$

The above relationship in equation (4.6) gives the temperature dependence of the laser diode forward voltage when the laser diode is operated above the threshold with $V_f >> \frac{\eta kT}{e}$. This forward voltage V_f temperature dependence is used to calculated the junction temperature of the laser diode. Equation (4.6) is the compact version of equation (3.6), where in equation (3.6) the current is further defined in terms of its intrinsic carrier concentration. Equation (4.6) shows the temperature dependence of the laser diode forward voltage.

4.2 Equipment

The equipment used for the measurement of the laser diode temperature using the forward voltage is described in the following sections, starting (in section 4.2.1) with the source used to bias the laser diode. Three different light sources were used to investigate the performance of the forward voltage method in measuring the diode's temperature. The descriptions of these light sources are given in section 4.2.2, followed by a discussion of the instruments used in the experiment in section 4.2.3

4.2.1 **High speed constant current pulse source**

A constant current pulse source was designed and built to drive the laser diode. The circuit diagram for the pulse source is provided in Appendix A. This circuit makes use of a voltage controlled pulse source (BNC model 555), and a high voltage and current power supply (Thurlby Thandar model PL320). A voltage source provides current based on the resistance according V=IR. As the laser diode resistance is dynamic, the current to the source will also be dynamic. The design of the current pulse generator ensures that a constant current was continuously supplied to the laser diode, irrespective of transient variations in laser diode impedance due to rapid changes in operating temperatures and currents. In addition, the designed current pulse generator prevented transient current generation and minimised pulse distortion.

4.2.2 **Light sources**

Two distributed feedback (DFB) laser diodes were used (Laser components HHI and NEL NLK1U5EAAA). The first was packaged in miniature thermo electric (MTE) T08 can, while the latter was butterfly packaged. Both lasers were single mode at 1650nm. Both include a Peltier TEC element with thermistor sensor resistance of 10kΩ at 25 ^{0}C.

A vertical cavity surface emitting laser (VCSEL) can packaged (Vertilas VL-1651-1-SQ-TS) at 1651nm was also investigated for junction temperature measurement using the laser diode forward voltage.

An ultra violet (UV) LED TO18 can package (Sensor Electronic Technology UVTOP335) with ball lens and no Peltier packaging was also used.

4.2.3 **Measurement Instruments and temperature controller**

The laser diode thermistor temperature was controlled by a temperature controller (ThorLab TED200) with accuracy of ±0.1 ºC. The laser diode forward voltage was measured with a high frequency (1GHz) oscilloscope (Agilent MSO6104A). A high precision digital multimeter (Keithly 195A) was used to measure the DC forward voltage.

4.3 Setup and Measurements

The laser diode thermistor temperature was controlled with the temperature controller as shown in section 4.2.3. The laser diode pulse current was provided by the custom-built current pulse generator.

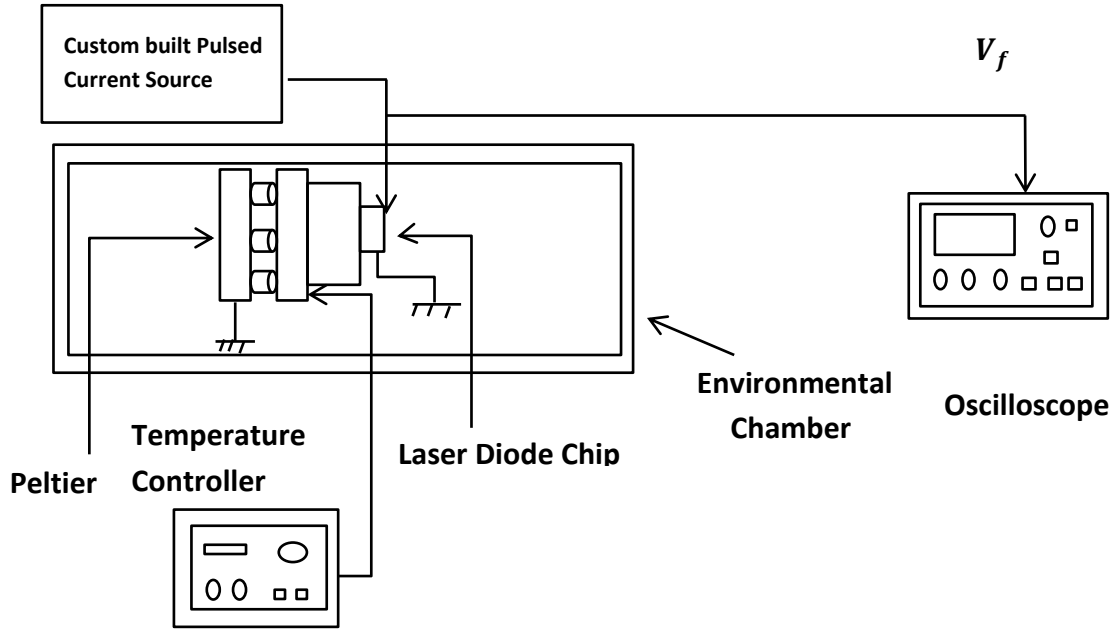

Figure 4.1 Basic setup for the forward voltage method

Figure 4.1 shows the basic setup for the forward voltage method. A high-wattage, low-inductance 5Ω resistor was used to calculate a known pulse current in order to bias the laser diode. The current pulse was injected into the laser diode and the voltage drop across the laser diode was measured at different temperatures and currents, using an oscilloscope.

4.3.1 **Pulse parameters**

Laser diode P-I-V characteristics are temperature dependent and variation in temperature can vary the forward voltage, output power and emission wavelength. In order to minimise internal junction heating when calibrating laser diode temperature, a short pulse of duration1-10μs was applied to the laser diode while keeping the duty cycle in the range 0.01-0.1%. Therefore, the laser diode average power dissipation (heat) was negligible [3]. The sum of the rise and fall time of the current pulse delivered to the laser diode was less than 30% of the total pulse width, in order to preserve the pulse width of the current pulse [3].

4.3.2 **Impedance matching and pulse delivery**

When an electromagnetic signal passes between different materials or impedances, reflections and coupling losses occur, resulting in potential signal distortion and in the output signal exceeding the desired level. When a laser diode is pulsed at high speed and there is mismatch in impedance between the transmission cable and laser diode, output power losses occur which manifest themselves as a standing waveform resulting in ringing effect on the

pulse. This pulse distortion can translate to erroneous results and can even damage the laser diode [3].

The impedance of a typical laser diode is 3-4Ω and the impedance of a typical transmission cable is 50 Ω. To overcome this impedance mismatch between laser diode and cable, a series resistance of 46 Ω can be placed between the cable and laser diode.

However, this technique has a serious disadvantage as the pulse source has to provide voltage equal to the resistance in series times the desired current, resulting in a high voltage drop; which can be a safety hazard and can damage the device.

The distance of the pulse source from the load also affects signal quality to the laser diode. An electrical pulse suffers from pulse lengthening or pulse dispersion. In the event of any signal being reflected from the end of the transmission line, the signal travels back up the line and is either reflected or absorbed by the drive source. The settling time of the pulse can greatly increase due to the reflection of the pulse signal back and forth s. Therefore, to reduce the pulse signal settling time, the length of the cable between the laser diode and the pulse source must be kept to a minimum. In this project, the distance between the pulse source and the load (laser diode) was < 5cm [4][5].

4.3.3 **Current source**

A laser diode is inherently current dependent and its resistance is both dynamic and temperature dependent. Therefore, when a laser diode is injected with current, the resistance of the laser diode decreases, and when a laser diode is pulsed with a voltage source then the resistance of the laser diode will change, making it complicated to deliver a known constant current to the laser diode [4].

Moreover, the diode current is exponentially dependent on voltage, so when a voltage pulse source is used to supply a current pulse, then a small change in voltage source can result in a large change in the current pulse to the laser diode.

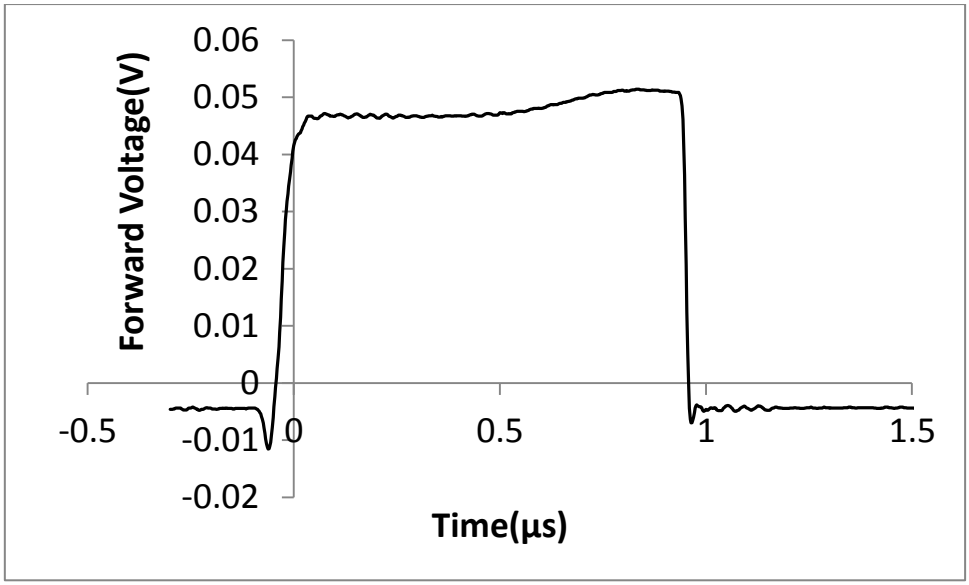

Figure 4.2 Pulse signal delivered to the LED using voltage controlled current source

Figure 4.2 represents the current pulse sent to the LED using the voltage controlled pulse source (BNC 555). The current sent to the LED was calculated by measuring the voltage drop across a low inductance 5Ω resistor. The pulse shape was deformed when a voltage controlled pulse source was used. This deformation of the pulse could result in erroneous measurement of the current sent to the LED.

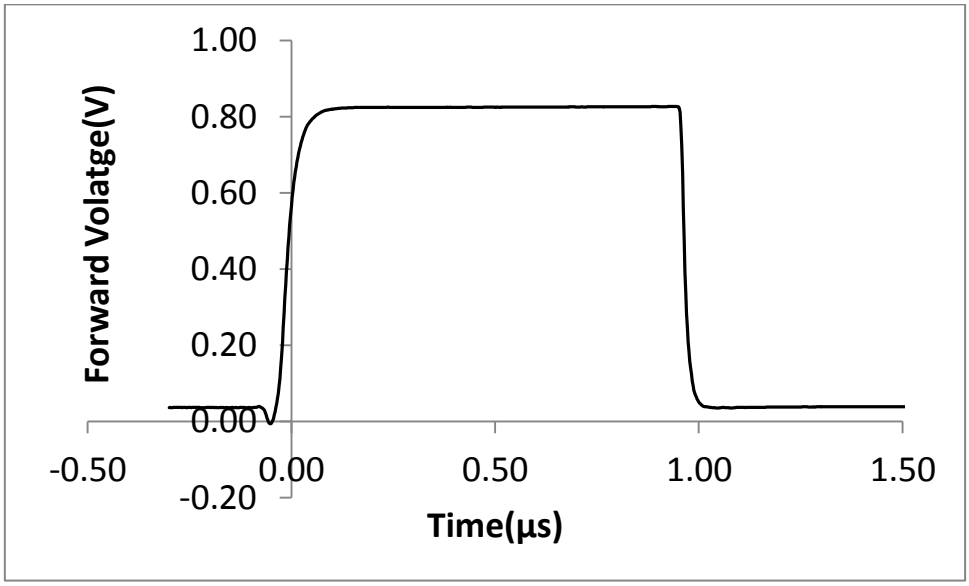

Figure 4.3 Voltage drop across LED using Voltage controlled pulse

Figure 4.3 shows the voltage drop across the LED using the voltage controlled current source (VCCS). The forward voltage drop measured using VCCS was 0.83 V.

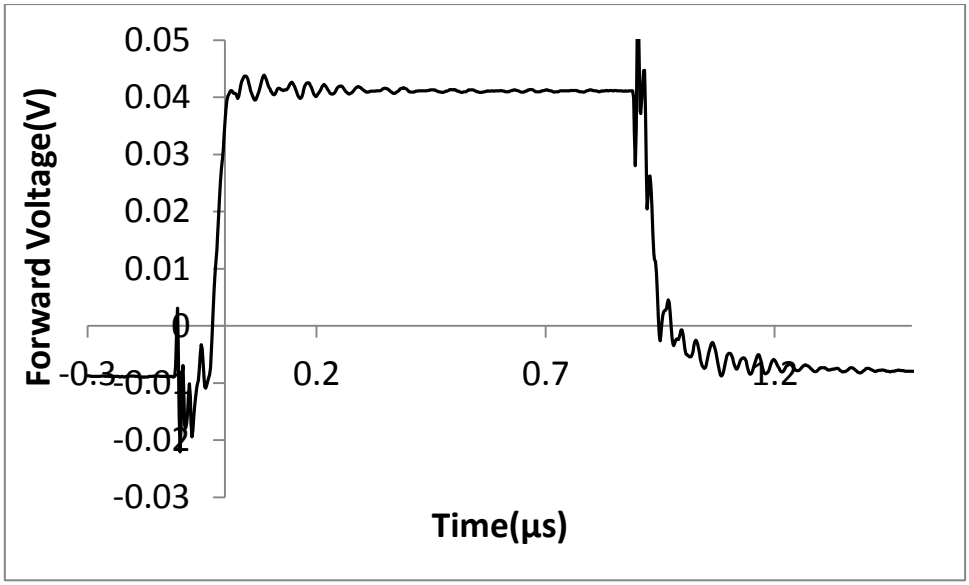

Figure 4.4 Pulse signal delivered to the LED using current controlled current source

Figure 4.4 represents the current pulse sent to the LED using custom built current source. The current sent to the LED was calculated by measuring voltage drop across a low inductance 5Ω resistor.

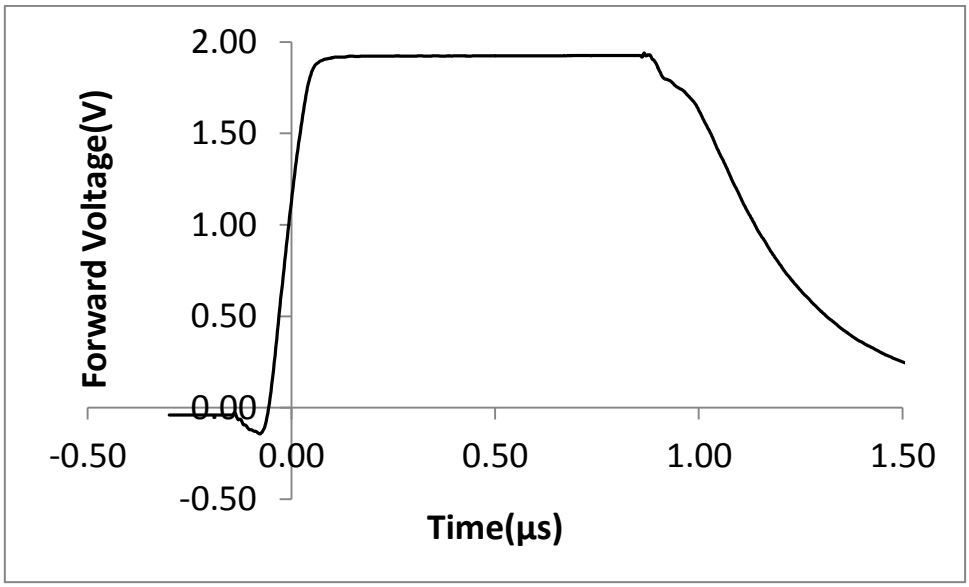

Figure 4.5 Voltage drop across LED using Current controlled pulse

Figure 4.5 shows a voltage drop across a LED using current controlled current source (CCS). The voltage drop across the LED using constant current pulse source measured a voltage drop of 1.92V at 10mA injection current. The voltage drop measured (peak voltage) with VCCS in Figure 4.3 was less than half the forward voltage measured in Figure 4.5 using CCS, despite sending the same pulse current of 10mA.

The decaying behaviour of the pulse measured across LED was due to the capacitance of the LED.

Figure 4.5 suggests that the CCS pulse provided a constant current to the LED despite the LED dynamic resistance, which was a function of current and temperature, whereas in Figure 4.3 the current to the LED changed with the change in the dynamic resistance, resulting in wrong measurement.

In addition, the voltage source suffers from greater instantaneous current capabilities and can contribute to a transient current to the load, increasing the risk of damaging the laser diode [4][5]. Moreover, temperature changes cause changes in the resistance of the laser diode and thus a voltage source will not be able to maintain a constant current, complicating further the measurement of known current and the laser P-I-V characteristics.

To maintain a constant current to a laser diode with dynamic resistance, a current controlled current source should be used, which is independent of laser diode dynamic impedance. A known current can be supplied to the laser diode when characterising the laser diode at different currents and temperatures. In addition, an ideal current source has infinite impedance (in ideal case). Therefore, the laser diode can be protected from the dangers of transient current.

In the following section, the forward voltage of all the light sources were calculated a constant current pulse source.

4.3.4 **Forward Voltage Method**

The laser diode junction temperature was calculated in two steps; the calibration step and then using the calibration parameters to calculate the junction temperature of the laser diode.

The laser diode pulsed forward voltage $V_{pulse,f}$ has a linear relationship with thermistor temperature and can be fitted to the following equation

$$V_{pulse,f} = A + BT_0 \tag{4.7}$$

Where A and B are the fitting parameters. T_0 is the thermistor temperature (It is the set temperature of the laser temperature controller) of the laser diode.

Using equation (4.7), the calibration of the laser diode was carried out as the 1st step in measuring the junction temperature. The laser diode was pulsed with a short pulse of duration

1µs and with low duty cycle of 0.01%. The laser diode thermistor temperature was considered to be approximately equal to the junction temperature of the laser diode. It is assumed that negligible heat is generated in the active region of the laser diode when biased with a short pulse current at low duty cycle

The fitting parameters in equation (4.7) were used to calibrate the laser diode junction temperature by plotting the pulsed forward voltage $V_{pulse,f}$ against the thermistor temperature. After the calibration process, the laser diode DC forward voltage was measured. Then the fitting parameters calculated in the calibration process were used to calculate the junction temperature T_j of the laser diode at any direct current (DC) and temperature using equation (4.8).

$$T_j = \frac{V_{DC,f} - A}{B} \tag{4.8}$$

The ability of the laser diode to efficiently remove the heat generated during operation is defined by the measure of the thermal impedance.

$$\Delta T = T_j - T_0 \tag{4.9}$$

Where ΔT is the temperature rise in the active region. Thermal impedance R_{th} can be described as:

$$R_{th} = \frac{\Delta T}{I_f V_{DC,f}} \tag{4.10}$$

Where I_f is the DC injection current and $V_{DC,f}$ is the DC forward voltage.

4.4 Results

The results section is divided into 4 subsections, presenting and discussing results for a MTE module DFB laser having T08 can package, for a DFB laser in a butterfly package, for a VCSEL, and for an LED. The result sections will cover junction temperature measurements, the effect of injection current on the junction temperature and of operating temperature on thermal impedance.

4.4.1 MTE Module DFB laser

Figure 4.6 shows the relationship between the measured forward voltage drop of the laser diode and thermistor temperature in the pulse current range of 70mA-160mA. This current range is above the threshold while at a typical operating injection current of 160mA resulting in an emission wavelength of 1650nm used for methane gas sensing as covered in chapter 5 and 6. The laser diode thermistor temperature was changed using the temperature controller in a step of 5˚C in the range of 15-35 ˚C.

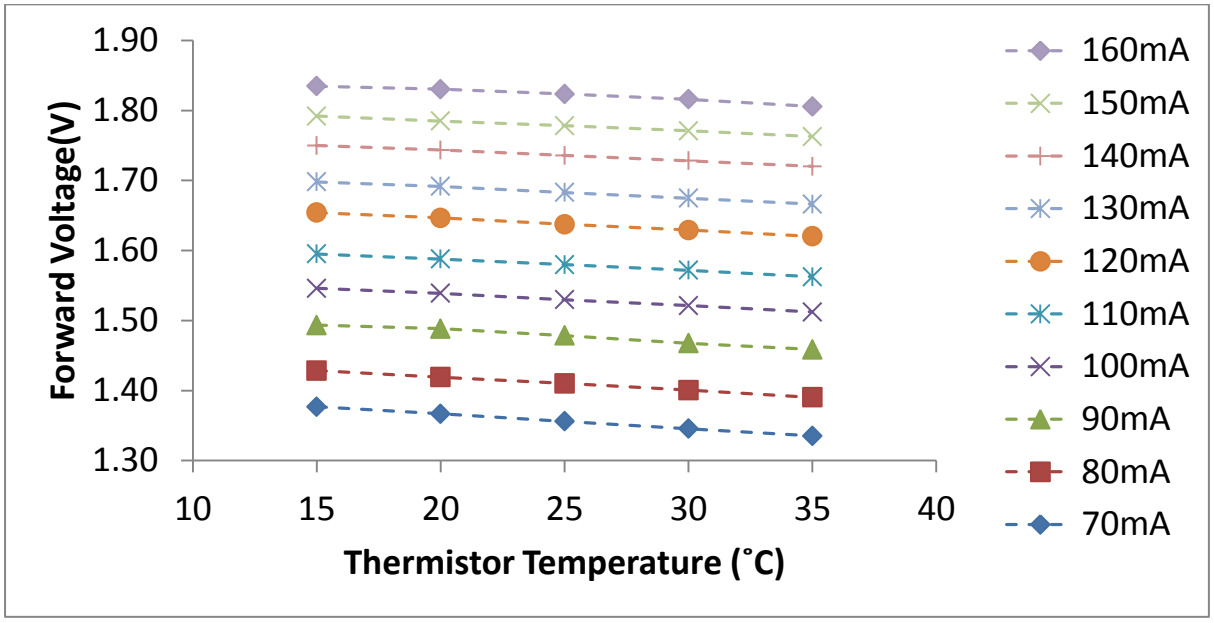

Figure 4.6 Relationship between laser diode forward voltage and Thermistor temperature in the current range 70-160mA

The relationship between the forward voltage drop and the thermistor temperature is approximately linear. Figure 4.6 shows the calibration curves for the laser diode, which were then used to calculate the junction temperature of the laser diode when operated in CW mode. Figure 4.7 shows the calibration plot for an injection current of 120 mA. The fitting parameters for this current were A(intercept) = 1.68V and B (gradient) =0.0017˚C/V.

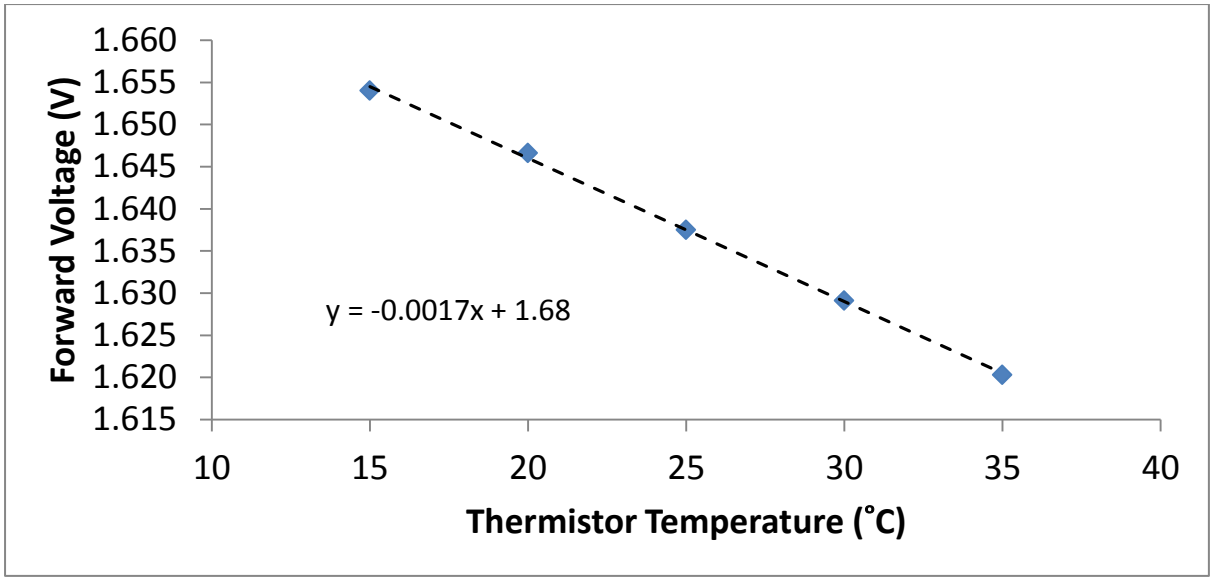

Figure 4.7 Calibration plot for pulse injection current of 120mA

Table 4.1 shows the fitting parameters for the MTE laser DFB laser, measured experimentally in the calibration process.

Table 4.1 Fitting parameters for MTE DFB laser at the temperature range 15-35 ºC

Injection current(mA)	Parameter A (V)	Parameter B (˚C/V)
70	1.4083	0.0021
80	1.4571	0.0019
90	1.5226	0.0018
100	1.5721	0.0017
110	1.6206	0.0016
120	1.68	0.0017
130	1.7227	0.0016
140	1.7728	0.0015
150	1.8139	0.0014
160	1.8581	0.0014

The fitting parameters in Table 4.1 were then used to calculate the junction temperature of the DFB laser at each thermistor temperature and injection current, using equation (4.8).

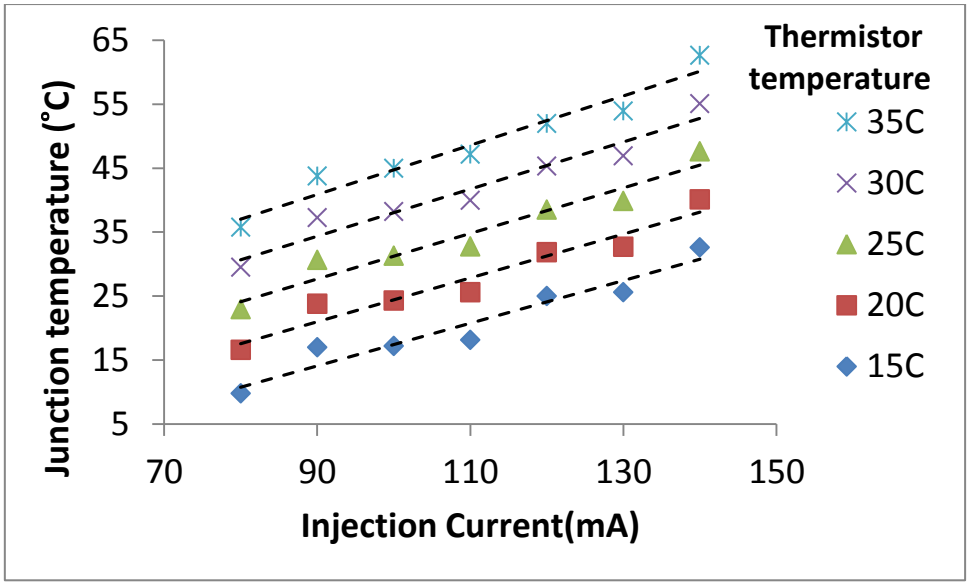

Figure 4.8 Junction temperature as a function DC injection current at different thermistor temperatures

Figure 4.8 shows the relationship between the DC injection current and the junction temperature of the laser diode. The laser diode junction temperature increased with the DC injection current. In addition, with increasing thermistor temperature from 15 °C to 35 °C at the same DC injection current, the laser diode junction temperature also increased. For example, at an injection current of 130mA and thermistor temperature of 30 ºC, the difference between the laser diode junction temperature (the temperature of the gain chip) and that as measured by the thermistor was estimated to be ΔT=16 ºC, as shown in Figure 4.8. This increase in junction temperature was due to the thermal gradient created between the laser diode chip, thermistor and the ambient temperature. Equation (4.6) shows temperature dependence of the laser diode forward voltage when operated above the threshold current. This equation (4.6) suggests that the forward voltage method can only be used to calculate the junction temperature of the laser diode when biased with a forward current above the threshold, and cannot be applied when the current is below the threshold.

Table 4.2 Average thermal impedance at various thermistor temperatures

Thermistor Temperature(˚C)	Average Thermal Impedance(˚C/W) Over the current range of 90-140mA
15	36.5
20	48.6
25	60.4
30	72.1
35	83.4

Table 4.2 shows the average thermal impedance in the current range of 90-140mA at different thermistor temperatures. This thermal impedance for the laser diode was calculated using equation (4.10). It can be seen in the table that with increasing thermistor temperature, the thermal impedance has doubled to 72 ˚C/W at thermistor temperature of 30˚C. This increased thermal impedance with thermistor temperature shows the inefficiency of the laser diode package heat sinking.

4.4.2 Butterfly packaged DFB laser

The junction temperature of a butterfly packaged DFB laser diode was calculated using the forward voltage method. The laser diode was operated well above threshold in the current range of 50-100mA at thermistor temperatures in the range15-35˚C.

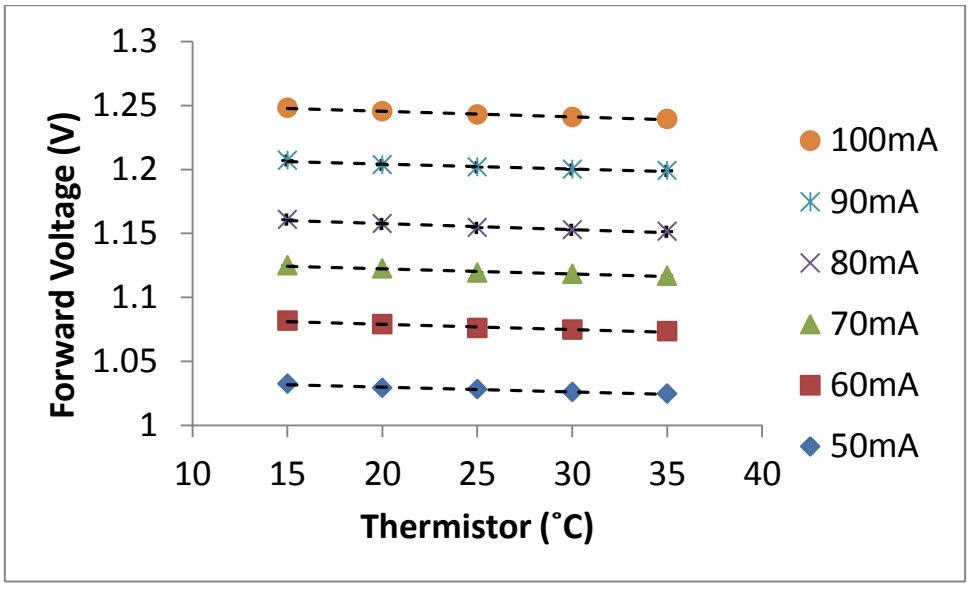

Figure 4.9 Laser diode forward voltage biased with pulsed current at thermistor temperature in the range 15-35˚C

Figure 4.9 shows the effect of thermistor temperature on the laser diode forward voltage when operated with a short duration pulse current of 1µs. The laser diode voltage decreased with increasing thermistor temperature and the relationship between the laser diode forward voltage and thermistor temperature was approximately linear, as shown by the dashed linear fit line in Figure 4.9.

Table 4.3 Calibration parameters for the butterfly package

Injection current(mA)	Parameter A (V)	Parameter B (˚C/V)
50	1.0373	-0.0004
60	1.0873	-0.0004
70	1.1306	-0.0004
80	1.1671	-0.0005
90	1.2121	-0.0004
100	1.2543	-0.0004

Table 4.3 shows the calibration parameters calculated for the butterfly package in the calibration process using equation (4.8).

The laser diode forward voltage under pulsed current condition should have been higher than the forward voltage measured under DC, due to negligible heat generated in the pulse operation. However, the forward voltage of the butterfly packaged DFB laser diode under DC current was higher than that of the pulsed current as shown in Figure 4.10.

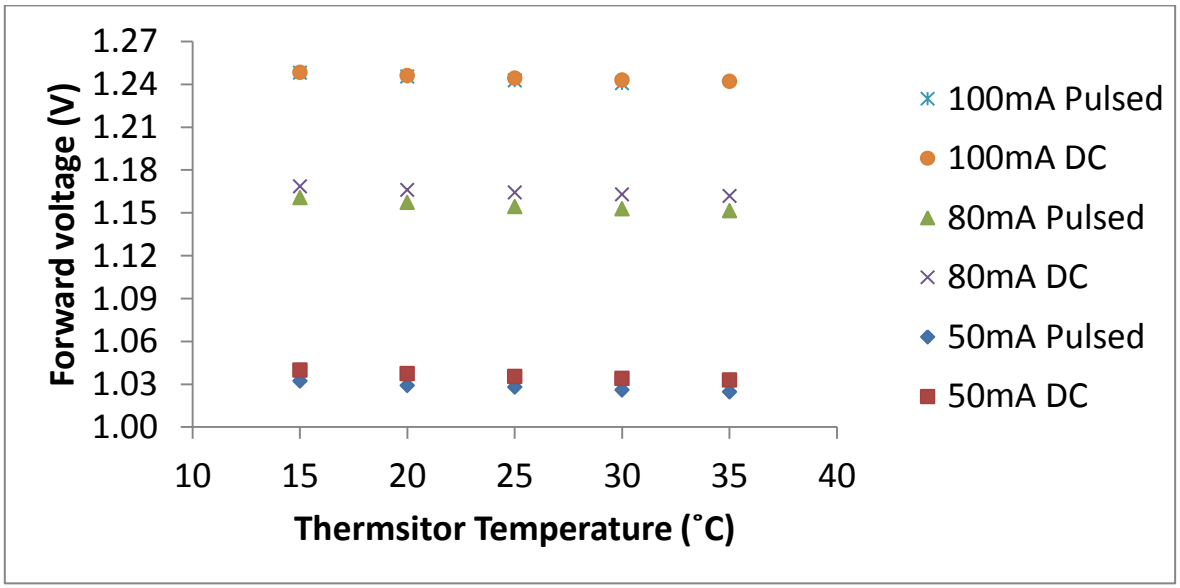

Figure 4.10 Laser diode forward voltage under Pulse and DC operation over the thermistor temperature range 15-35˚C

This lower pulsed voltage in Figure 4.10, suggests that the laser diode was not at the same temperature as the thermistor. The possible reasons behind the measurement of a lower forward voltage under pulsed conditions are 1) The laser diode chip is at higher temperature than that of the thermistor due to heat generation during pulsed operation and failure of the thermistor to detect heat during operation, 2) a thermal gradient between the laser diode chip and thermistor existed due to inefficient thermal design, 3) the combined effect of heating during pulse current and poor thermal design.

4.4.3 VCSEL Laser

The forward voltage method was used to calculate the junction temperature of the VCSEL laser in the current range 5-13mA (operating current range) at thermistor temperature 15-35 in a step of 5 ºC.

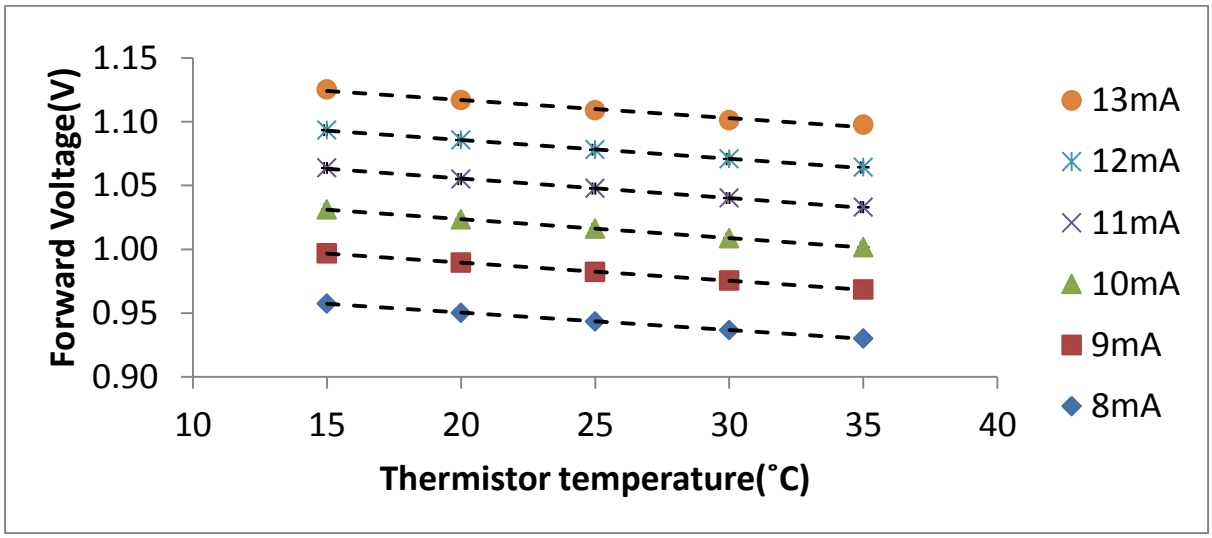

Figure 4.11 Laser diode forward voltage at various thermistor temperatures at pulse current 8-13mA

Figure 4.11 shows the effect of thermistor temperature on the forward voltage of the VCSEL. The relationship between the forward voltage and the thermistor temperature was linear. The laser diode forward voltage measured under pulse current was higher than the DC condition.

The threshold voltage for VCSEL laser was 0.5mA at 20ºC. However, when the VCSEL laser was operated well above the threshold in the current range 5-7mA, the laser diode forward voltage was lower than that of the VCSEL operated under DC operation. Figure 4.12 shows the comparison between measured forward voltages and pulsed forward voltages at various thermistor temperatures. At all the thermistor temperatures, the DC voltage was higher than

the pulsed voltage; however, the pulsed voltage was expected to be higher than the DC voltage

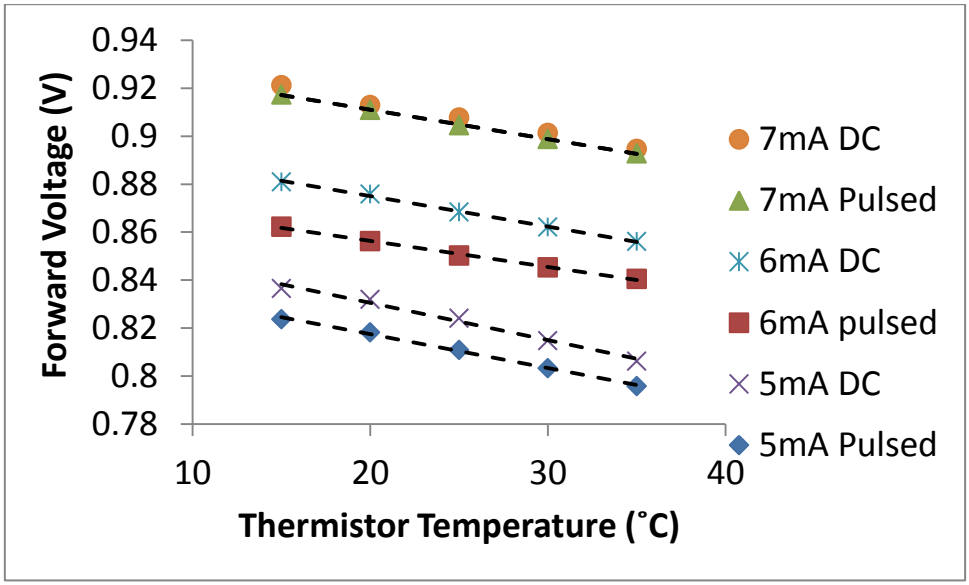

Figure 4.12 Comparison between pulsed forward voltage and DC forward voltage in the current range 5-7mA

The decreases in the forward voltage under pulsed current could be attributed to 1) heat generation during the pulse current and the inability of the thermistor to detect that heat during the course of the short duration pulse 2) poor thermal design and 3) the combined effect of 1) and 2).

Table 4.4 shows the fitting parameters calculated using equation (4.7). These parameters were then used to calculate the Junction temperature under DC conditions using equation (4.8).

Table 4.4 Fitting parameters for VCSEL laser

Injection current(mA)	Parameter A (V)	Parameter B (˚C/V)
5	0.8457	-0.0014
6	0.8782	-0.0011
7	0.9356	-0.0012
8	0.9776	-0.0014
9	1.018	-0.0014
10	1.0532	-0.0015
11	1.0862	-0.0015
12	1.1151	-0.0015
13	1.1454	-0.0014

The VCSEL junction temperature was calculated using the fitting parameter in Table 4.4 using equation (4.8)

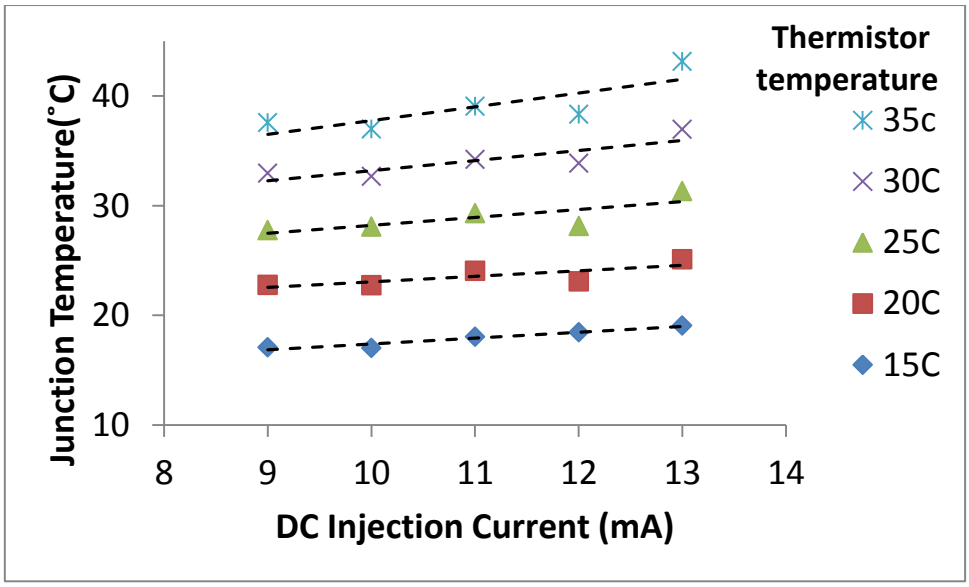

Figure 4.13 VCSEL junction temperature as a function of temperature in DC condition

Figure 4.13 shows that the laser diode junction temperature increased with increasing junction current. Therefore, laser diode chip temperature increased with increasing injection current. In addition, the laser diode junction temperature had also increased with increasing thermistor temperature due to the thermal gradient between the chip and laser diode package.

Table 4.5 Average thermal impedance measurement at various thermistor temperatures

Thermistor Temperature(˚C)	Average Thermal Impedance(˚C/W) Over a current range 7-13mA
15	0.25
20	0.3
25	0.33
30	0.35
35	0.7

Table 4.5 shows the average thermal impedance of the VCSEL laser at different thermistor temperatures calculated using equation (4.10). As the thermistor temperature was increased the thermal impedance also increased and at 35 ºC the thermal impedance increased to 0.7 ºC/W, almost a 3 fold increase in the thermal impedance from its value at 15 °C.

4.4.4 Light emitting diode

A light emitting diode (LED) was also tested for junction temperature calculation using forward voltage method. As the LED had no internal temperature controller, the LED was placed in a custom built environmental chamber with variable temperature in the range 10-40 ºC. The temperature of the environmental chamber was measured using three thermocouples placed at different points inside the environmental chamber employing a scanning thermometer (Kiethly 740) with a measured error of ± 0.5 ºC.

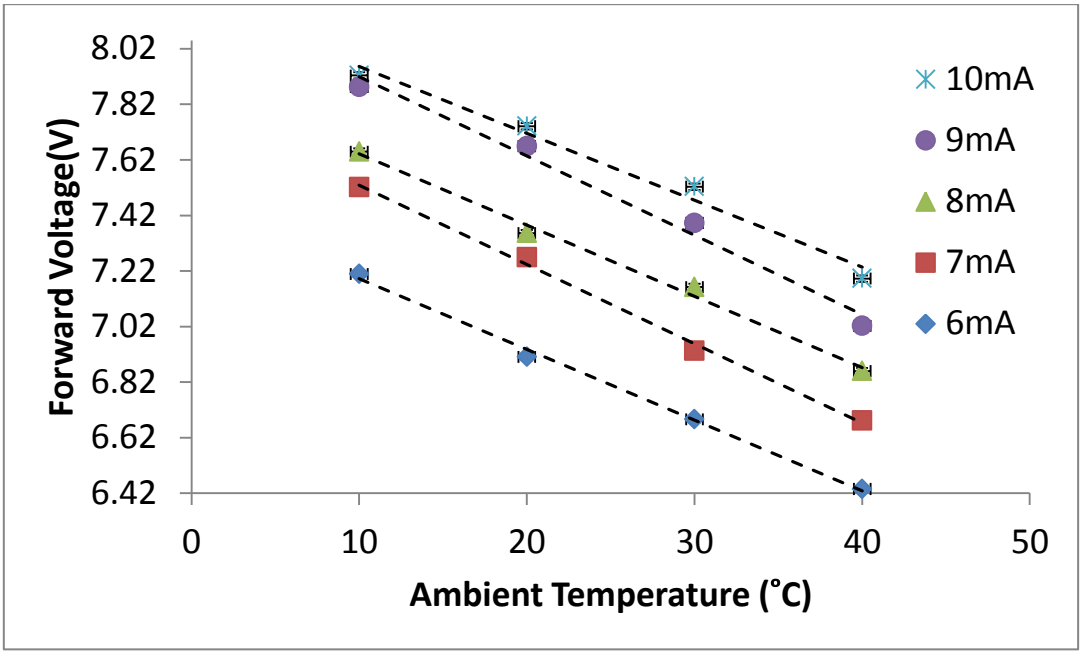

Figure 4.14 LED forward voltage as function of ambient temperature under pulse condition

Figure 4.14 shows the effect of varying ambient temperature on the LED forward voltage. The LED was pulsed in a current range 6-10mA at ambient temperature range 10-40ºC. The LED forward voltage had an approximately linear relationship with varying ambient temperature. The LED forward voltage was decreasing with increasing ambient temperature, showing similar behaviour to that of laser diodes discussed in the previous sections.

Table 4.6 Fitting parameter for LED

Injection current(mA)	Parameter A	Parameter B(˚C/V)
6	7.4471	-0.0255
7	7.8146	-0.0285
8	7.8978	-0.0256
9	8.2057	-0.0286
10	8.198	-0.0241

Table 4.6 gives the calibration parameters calculated for the LED calculated form the calibration process as described in section 4.3.4. These parameters are then used to calculate the junction temperature of the LED at a particulate current and temperature.

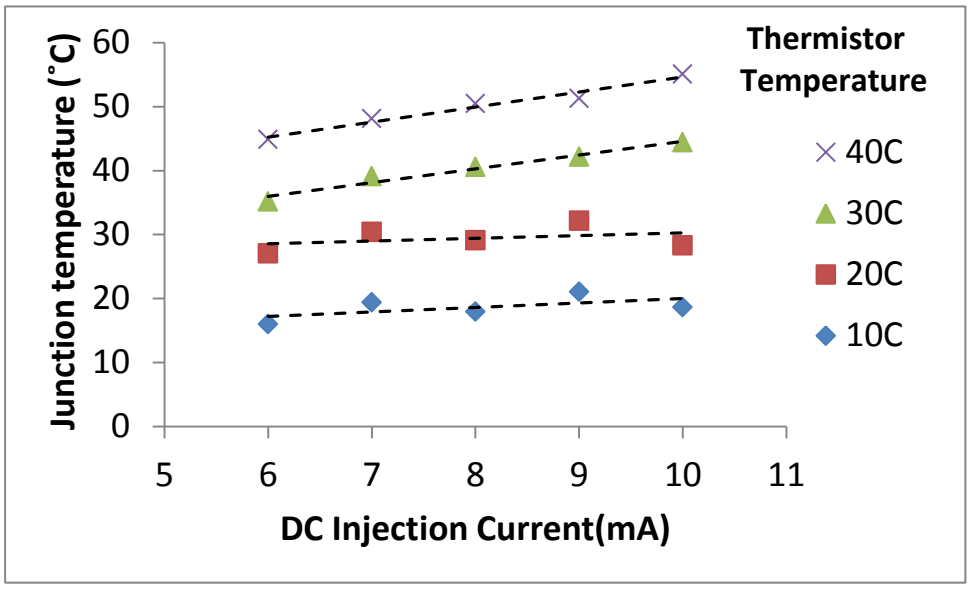

Figure 4.15 LED Junction temperature as a function of DC injection current

Figure 4.15 shows the LED junction temperature plotted as a function of DC injection currents. The laser diode junction temperature was calculated at different injection current and at various ambient temperatures using equation (4.8). The junction temperature of the LED increased with increasing junction current. In addition, the junction temperature of the LED also increased with increasing ambient temperature due to the thermal gradient between the LED active region, the package and the surrounding environment.

Table 4.7 Average thermal impedance of LED

Thermistor Temperature(˚C)	Thermal Impedance(˚C/W) Over a current 6-10mA
10	147
20	169
30	183
40	182

Table 4.7 shows the average thermal impedance of the LED while operated at different ambient temperature. The thermal impedance of the LED increased with increasing ambient temperature. The thermal impedance of the LED calculated using forward voltage was much higher than the thermal impedances for lasers as discussed in the previous sections. This high thermal impedance of the LED was due to the absence of an internal temperature controller.

4.5 Power averaged wavelength method

The so-called power averaged wavelength method is an alternative technique for calculating the junction temperature and thermal impedance of the laser diode and was described in section 3.2.4. In this technique the laser diode was operated under DC conditions and the P-I-V characteristics were exploited for the thermal characterisation of the laser diode [6]. This technique has been discussed in two sections. In the first section, the instruments and setup for the experiment has been described. The final section contains the results and discussion on the power averaged wavelength technique.

4.5.1 Measurement instruments

The laser diode was biased using a current controlled current driver (Thor Labs LDC 202) with precision of ±100µA and a temperature controller (Thor Labs TED200) with precision of ±0.1 ºC to control the laser diode temperature.

The distributed feedback (DFB) laser diode (NEL NLK1U5EAAA) used in section 4.4.2 was investigated for calculating junction temperature using power averaged method. The thermistor of the laser diode was 10kΩ at 25^0C.

The laser diode output wavelength was measured with an optical spectrum analyser (Yokogawa AQ6370D).The resolution of the spectrum analyser was 20pm. The output power of the laser diode was measured with an optical power meter (Ando AQ 2105). The DC forward voltage of the laser diode was measured with a digital multimeter (Keithly 195A).

4.5.2 System Setup

The laser diode was biased with a DC injection current above the threshold in the range of 50-100mA. The thermistor temperature was controlled by the temperature controller in the range of 15-35˚C. The injection current to the laser diode was varied in a steps of 10 mA and the laser diode emission wavelength, forward voltage drop and output power were measured at various temperatures. Figure 4.16 shows the basic setup used in the power averaged method.

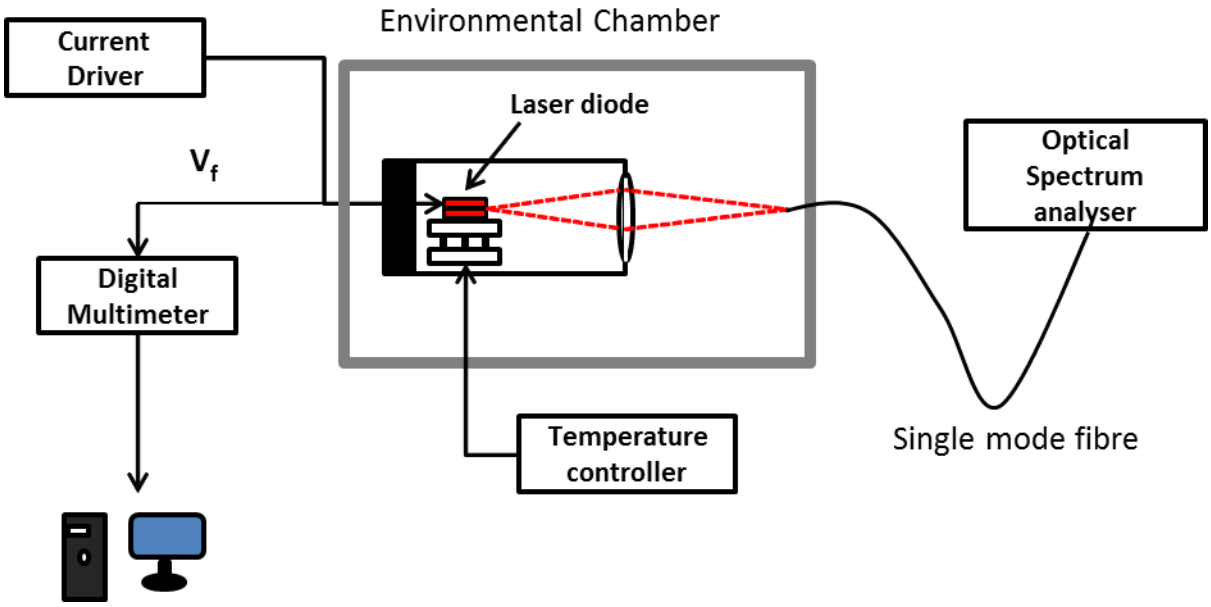

Figure 4.16 Basic setup for power averaged method

4.5.3 Method

The relationship between junction temperature T_j and thermistor temperature T_o is given in equation (4.11)

$$T_j = T_o + R_{th}P_j \tag{4.11}$$

The laser diode junction temperature is calculated from the relationship between waste thermal power P_j , input supplied power IV, and output optical power P_0 in equation (4.12)

$$P_j = IV - P_0 \tag{4.12}$$

In the first step of the experiment, the laser diode wavelength was established at zero waste thermal power. This was calculated by plotting the laser diode emission wavelength against the waste thermal power P_j for different injection currents.

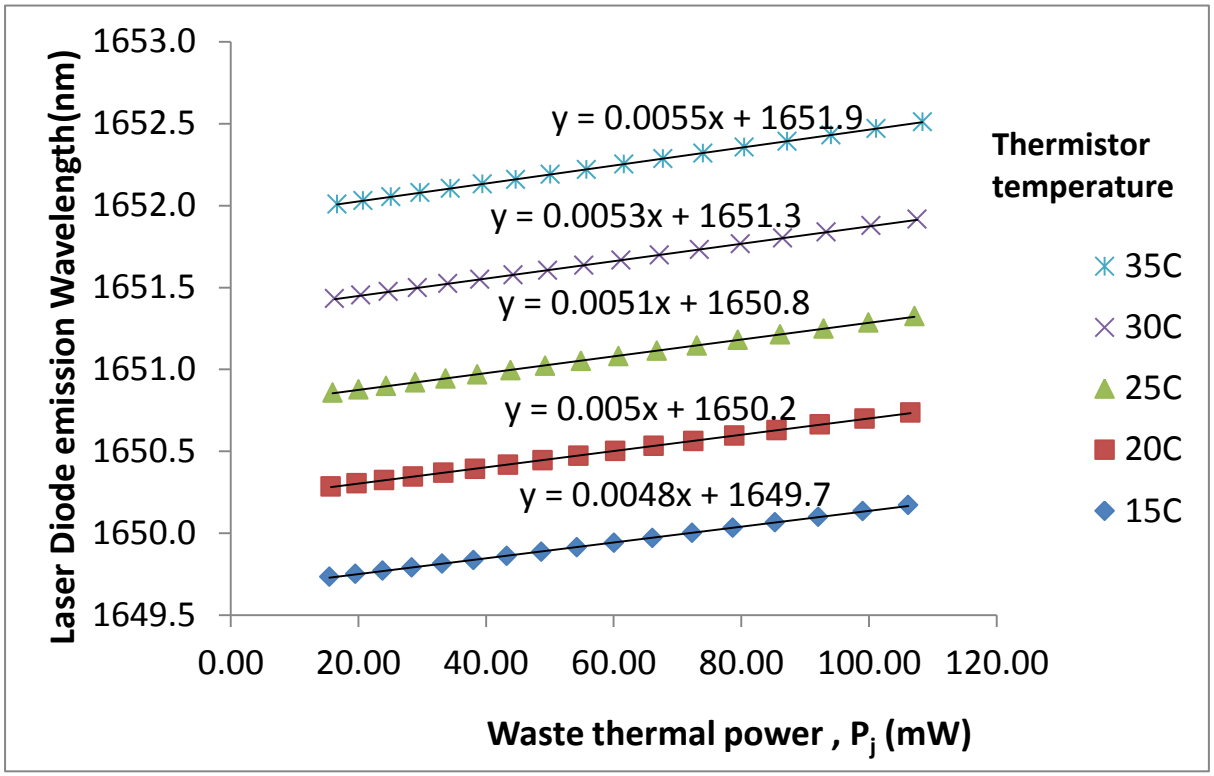

Figure 4.17 Laser diode peak wavelength as a function of. waste thermal power

Figure 4.17 shows the laser diode wavelength as a function of waste thermal power, calculated using equation (4.12). The laser diode thermistor temperature was varied in the range 15-35ºC. At $P_j = 0$ it is assumed that the thermistor temperature is equal to the junction temperature $T_j = T_o$.

The wavelength calculated at $P_j = 0$ was then plotted against T_o to determine the junction temperature from the temperature dependent wavelength shift at various injection currents and thermistor temperatures.

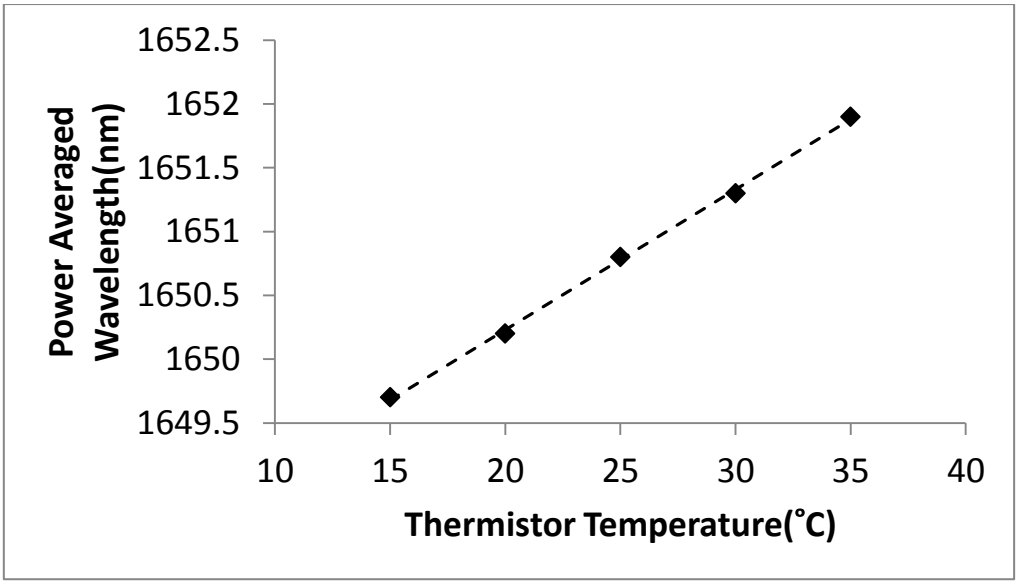

Figure 4.18 Laser diode power averaged wavelength variation with thermistor temperature (wavelength where$T_j = T_o$)

Figure 4.18 shows a linear relationship between power averaged wavelength (the y-axis intercept of Figure (4.17) wavelength) and thermistor temperature. The junction temperature T_j of the laser diode can be calculated using the above graph in Figure 4.18, using the following equation.

$$T_j = \frac{\lambda - \lambda_0}{m} \tag{4.13}$$

λ_0 is the wavelength at $P_j = 0$ calculated from Figure 4.18, m is the slope of the graph in Figure 4.19 , λ is the wavelength measured at DC current where waste thermal power $P_j \neq 0$.

Then junction temperature of the laser diode was calculated by substituting the wavelength λ calculated at different injection current and thermistor temperature. The value calculated for λ_0 was 1648nm and m=0.11nm / ºC over the thermistor temperature range 15-35 ºC.

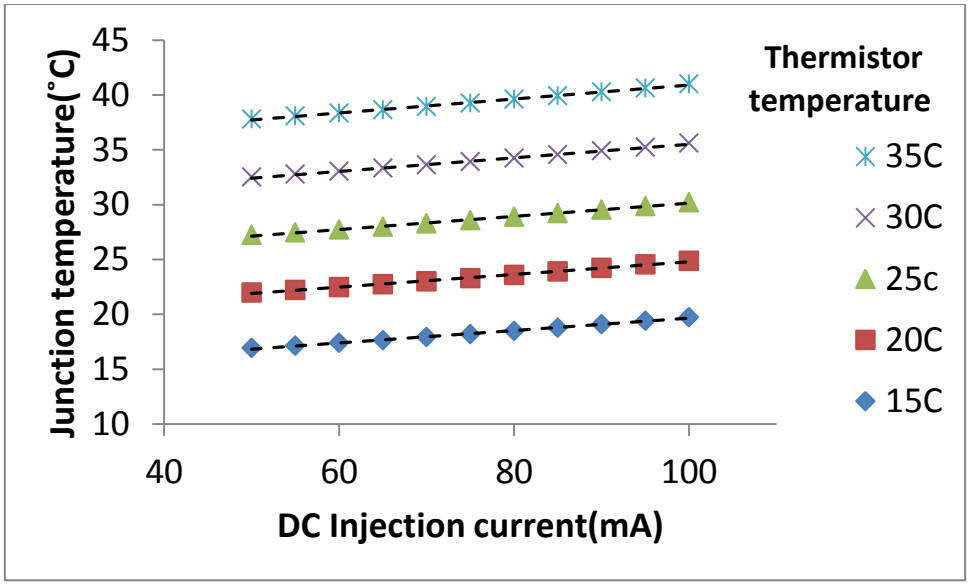

Figure 4.19 Laser diode Junction temperature as a function of injection current of butterfly packaged DFB laser using power averaged method

Figure 4.19 shows a linear relationship between the injection current and junction temperatures. The laser diode junction temperature increased with increasing injection current. In addition, the junction temperature had also increased with an increase in thermistor temperature due to increased thermal gradient between the chip and the laser diode package.

Table 4.8 Average thermal impedance of DFB laser at variable ambient temperatures using power averaged method

Thermistor Temperature ˚C	Average Thermal Impedance (˚C/W)
15	0.044
20	0.046
25	0.049
30	0.054
35	0.058

Table 4.8 shows the average thermal impedance calculated for the butterfly packed DFB laser. The thermal impedance of the DFB increased with increasing thermistor temperature.

The junction temperature calculated for the butterfly package laser diode using the power averaged wavelength method was higher than that calculated using forward voltage method in section 4.4.2. This higher junction temperature calculation using power averaged

wavelength method could be attributed to uncertainty in measuring laser diode emission wavelength using optical spectrum analyser and optical power

Table 4.9 Junction temperature for butterfly packaged DFB laser calculated with forward voltage method

Current(mA)	Thermistor Temperature				
	15 ˚C	**20 ˚C**	**25 ˚C**	**30 ˚C**	**35 ˚C**
80	-3.034	2.192	5.806	8.444	10.686
90	7.9225	13.68	18.2975	21.6625	23.9725
100	15.02	20.66	24.855	28.41	30.3875

Table 4.10 Junction temperature calculated with Power average wavelength method for butterfly packaged DFB laser

Current(mA)	Thermistor Temperature				
	15 ˚C	**20 ˚C**	**25 ˚C**	**30 ˚C**	**35 ˚C**
80	18.47818	23.6	28.89818	34.23364	39.59636
90	19.08636	24.21455	29.53182	34.89909	40.28
100	19.73364	24.88091	30.21545	35.60636	41.00545

Table 4.9 and Table 4.10 show the junction temperatures calculated using the forward voltage method and the power averaged method for the same butterfly packaged laser diode. In Table 4.9, the junction temperature calculated with the forward voltage was lower than the thermistor temperature. Whereas, in power averaged wavelength method in Table 4.10, the junction temperature was higher than the thermistor temperature and the junction temperature calculated with forward voltage method. This difference in junction temperature calculation using forward voltage and power average wavelength method could be due to

1) the inability of the thermistor to maintain the laser diode temperature at set temperature due to heat generation when the laser diode is pulsed with an injection current

2) uncertainty in measuring laser diode emission wavelength using an optical spectrum analyser due to its limited resolution of 20pm and uncertainty in measuring output power due to coupling efficiency

4.6 The effect of ambient temperature on the laser diode characteristics

The butterfly packaged DFB and VCSEL were investigated for the effect of ambient temperature on the laser diode forward voltage.

4.6.1 Method and Results

The laser diode was supplied with a constant current pulse having a width of 1μs and a duty cycle of 0.01%. The laser diode thermistor set point temperature was kept constant at 15 ˚C. An environmental chamber as shown in Figure 4.24 was used in the experiment, where the enclosed laser diodes temperature was varied in the range 10-40 ˚C.

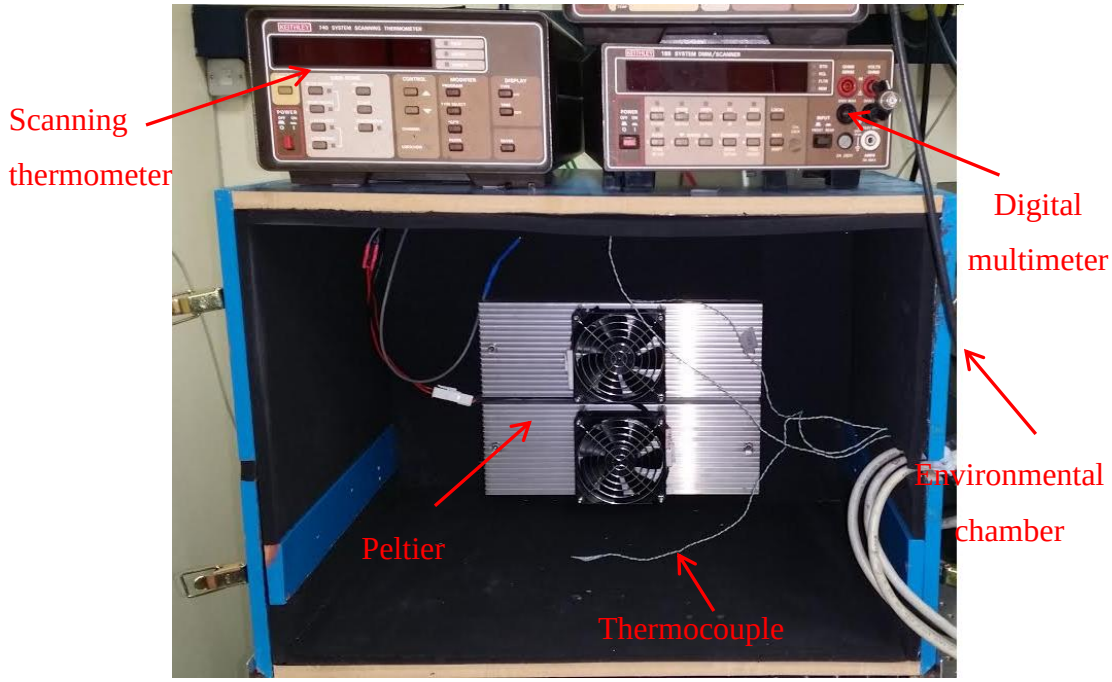

Figure 4.20 Homemade environmental chamber used investigating the effects of ambient temperature on light source

Two Peltier elements were used to vary the temperature of the environmental chamber. The environmental chamber had three thermocouple placed at three different locations to give measure of the environmental chamber temperature using a scanning thermometer. The environmental chamber had a temperature gradient of ±0.5ºC.

The laser diode forward voltages were measured with an oscilloscope (Agilent MSO6104A). The pulse was above the threshold current of 10mA for VCSEL and 100mA for the DFB laser.

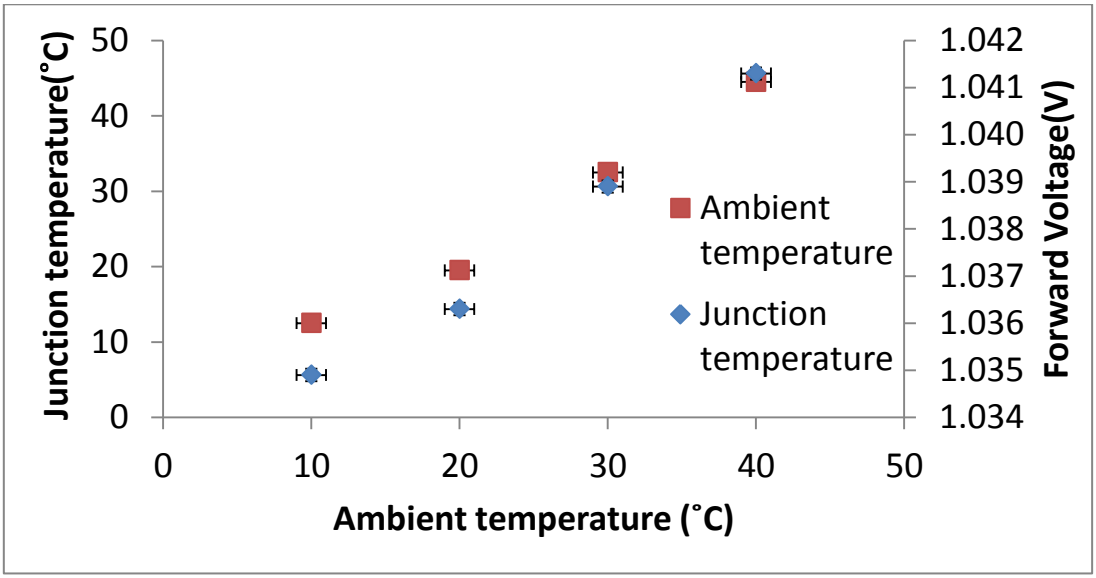

Figure 4.21 VCSEL Forward Voltage and junction temperature under pulsed current condition as function of ambient temperature at a constant thermistor temperature of 15°C

Figure 4.21 shows the effect of ambient temperature on the VCSEL forward voltage and junction temperature. The VCSEL laser had a constant thermistor temperature of 15 ºC and 10mA injection current in pulse mode. The forward voltage and junction temperature increased with increasing ambient temperature despite constant operating thermistor temperature.

This was an indication of thermal gradient between the VCSEL Laser chip, thermistor and the ambient temperature.

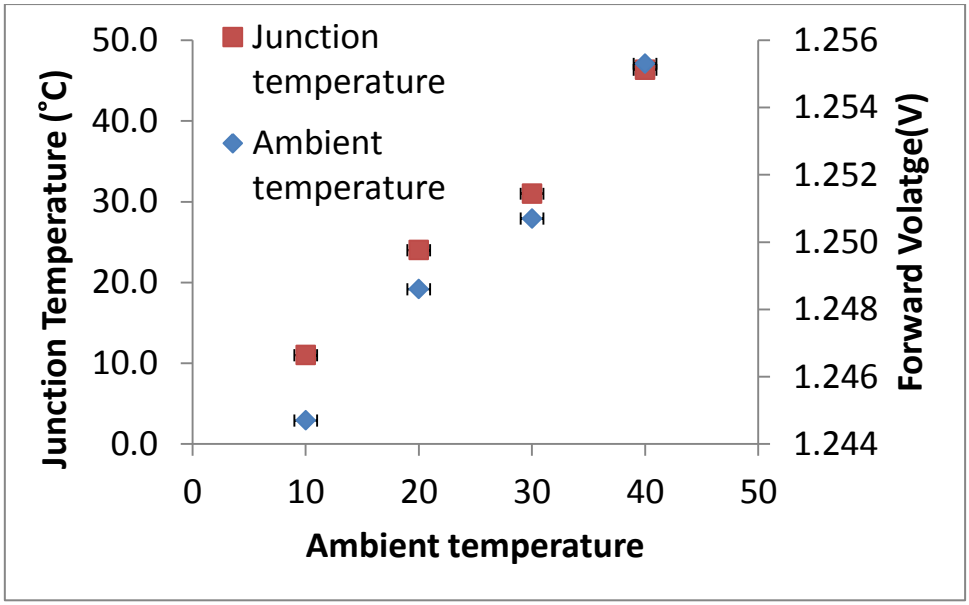

Figure 4.22 Butterfly packaged DFB forward Voltage and junction temperature under pulsed condition as a function of ambient temperature at a constant thermistor temperature of 15ºC

Figure 4.22 shows the effect of ambient temperature on the laser diode forward voltage and junction temperature at constant current pulse (100mA) and thermistor temperature (15˚C). In contrast to the results in Figure 4.10, the laser diode forward voltage increased with increasing temperature. In addition, the junction temperature of the laser diode also increased with increasing ambient temperature, despite using constant thermistor temperature.

These results suggested that

- There was a temperature gradient between thermistor and junction of the laser diode
- Ambient temperature affected the temperature gradient
- Thermistor control therefore forced the junction temperature to change when the ambient temperature was changed.

4.7 Summary

Laser diode P-I-V characteristics are functions of laser diode temperature. The laser diode temperature is a function of the ambient temperature and chip heating. The laser diode junction temperature can be calculated by several techniques. Two techniques, the diode forward voltage method and power averaged wavelength method were investigated to

calculate the junction temperature and thermal impedance of 3 different light sources i.e. DFB laser, VCSEL and LED.

In the first stage of the experiment a T08 can packaged DFB laser and a butterfly packaged laser were investigated using the forward voltage method. In the first step of calculating junction temperature, all the above mentioned light sources were calibrated using under pulsed current conditions as it was assumed that no heat will be generated during pulse current. The parameters calculated in the calibration process were then used to calculate the junction temperature under DC condition.

When the T08 can laser diode was operated under DC condition, the calculated junction temperature was higher than the thermistor temperature, indicating heat generation due to DC current and a thermal gradient between the thermistor and the laser gain chip. The thermal impedance calculated using forward voltage increased with increasing operating temperature.

For the butterfly packed DFB laser, the calculated junction temperature was not the same as the set thermistor temperature. The calculated junction temperature was on average lower than the thermistor temperature under DC condition.

The VCSEL laser junction temperature also increased with increasing injection current and temperature suggesting a thermal gradient between the thermistor and the gain The calculated thermal impedance for VCSEL was lower than that of the DFB laser due to the low operation current.

The junction temperature of the LED increased with increasing junction current. In addition, the junction temperature of the LED also increased with increasing ambient temperature due to the thermal gradient between the LED active region, the package and the surrounding environment. The average thermal impedance calculated for the LED was higher than those of the laser diodes, due to the absence of a Peltier cooling element within the device package.

The power averaged wavelength method was also investigated for measuring the junction temperature of the laser diode. The butterfly packaged DFB laser diode junction temperature was measured from the peak emission wavelength shift of the laser diode with temperature. There was a linear relationship between the laser diode peak wavelength at zero waste power and the operating thermistor temperature. The laser diode junction temperature was higher than the thermistor set point at higher currents. The junction temperature and thermal impedance increased with increasing operating thermistor temperature.

The effect of ambient temperature on the laser forward voltage was also investigated for the butterfly packaged laser diode and VCSEL laser. The ambient temperature was varied while maintaining the thermistor temperature and injection current constant. Results showed that the laser diode forward voltage increased with increasing ambient temperature rather than decreasing with temperature. The increase in the forward voltage can be attributed to the thermal gradient between the thermistor the laser diode chip, laser package and the ambient temperature.

The power averaged method is a straight forward process, requiring no prior calibration of the laser diode. However, uncertainty in measuring wavelength and emitted power can result in erroneous junction temperature measurement. In addition, this technique cannot be implemented in wavelength modulation spectroscopy, but is only useful as a characterisation or calibration technique.

The forward voltage method is a better technique for measuring temperature with higher accuracy in comparison to power averaged method and can be easily implemented in wavelength modulation spectroscopy. However, this technique requires a calibration process and an accurate fast current pulse, which can add to the uncertainty in measuring the junction temperature.

In the next chapter, the forward voltage method will be implemented in a control loop to sense and stabilise the laser diode temperature. If the forward voltage based control was successful in stabilising the temperature, then this method will be extended to TDLAS, which is the objective of this project.

4.8 References

[1] Y. Xi and E. Schubert, “Junction–temperature measurement in GaN ultraviolet light-emitting diodes,” Applied Physics Letters, vol. 85, no. 12, pp. 2163 - 2165, 2004.

[2] S. Sze, Physics of Semiconductor Devices, New Jersy: Wiley & Sons, 1981.

[3] P. Mayer, “Pulse testing of laser diodes,” [Online]. Available: www.keithley.co.uk/data?asset=518. [Accessed 18 02 2014].

[4] D. Hodgson, K. Noonan, B. Oslen and T. Orosz, “Pulsing a Laser Diode,” [Online]. Available: http://assets.newport.com/webDocuments-EN/images/AN11_Pulsing_Laser_Diode_IX.PDF. [Accessed 18 02 2014].

[5] E. Kapon, Semiconductor Lasers: Materials and structures, London, Academic Press, 1999.

[6] L. A. Johnson and A. Teh, “Measuring High Power Laser Diode Junction Temperature and Pacakage Thermal Impedance,” . [Online]. Available: http://assets.newport.com/webDocuments-EN/images/AN30_Measure_Laser_Diode_IX.PDF. [Accessed 18 02 2014].

5 Laser Diode series resistance and wavelength control

The temperature dependence of the semiconductor laser diode emission wavelength is 0.25 nm /˚C for AlGaAs lasers and 0.4-0.6 nm/ ˚C [1]. Therefore accurately measuring and controlling the temperature of the laser diode is vital for the wavelength stability of the laser diode. TDLAS requires a long term wavelength stability of better than 10% of the absorption line width of the target gas species. In this chapter the forward voltage of the laser diode is used to accurately sense the temperature of the laser diode and is used as a tool to aid the control of the temperature of the laser diode chip and hence the emission wavelength.

The laser diode forward voltage is the sum of junction voltage and voltage drop across the laser diode as reported in section 573.3, and both are temperature dependent. In chapter 4, the laser diode junction voltage was calculated using forward voltage and the contribution from the laser diode series resistance to the forward voltage was ignored. By ignoring the temperature dependent voltage drop across the laser diode series resistance, Junction temperature calculation for the light sources were compromised as reported in chapter 4.

The aim of this chapter is to refine the forward voltage method by including the influence of laser diode resistance; this is the junction voltage of the laser diode and the novel part of this thesis. This chapter will investigate different methods for calculating the series resistance of a laser diode and the effects of temperature on the laser diode series resistance. Both conventional thermistor temperature control and forward voltage will be investigated for stabilising the laser diode emission wavelength and then the emission wavelength. Then the junction voltage method will be investigated in stabilising the laser diode temperature and then the emission wavelength and compared with the forward voltage and conventional thermistor temperature controlled methods.

In the first part of the chapter the series resistance of two distributed feedback (DFB) lasers; one TO8 Can packaged and the other butterfly packaged are calculated using different techniques. The two lasers have the same gain material (IngaAsP/InP) but different packaging. The aim of this experimental work is to investigate the effects of different packaging on the temperature dependence of the laser diode series resistance.

The 2nd part of this chapter deals with the wavelength control of the laser diode using the voltage drop across the laser diode. Laser diode forward voltage and junction voltage are

investigated for stabilising the laser diode wavelength. Then the performances of these two methods are compared with the conventional thermistor temperature control for stabilising the laser diode wavelength control.

5.1 Laser diode resistance

Laser diode resistance is measured from the current – voltage (I-V) characteristics of the laser diode. The current to the diode can be expressed by Shockly ideal diode equation as reported in section 3.3[2] :

$$I_f = I_s[\exp\left(\frac{eV_f}{\eta kT} - 1\right)] \tag{5.1}$$

Where I_f and I_s are forward and saturation current of the laser diode respectively. V_f is the forward voltage of the laser diode, *e* is the electronic charge, *k* is the Boltzmann's constant, and *T* is the thermodynamic temperature. η is the ideality factor of the laser diode .

Assuming $V_f \gg \eta kT/e$ ($\eta kT/e$ is also called thermal voltage) in equation (5.1)

$$I_f \cong I_s[\exp\left(\frac{eV_f}{\eta kT}\right)] \tag{5.2}$$

Equation (5.2) offers a mean of measuring junction temperature of the laser diode as shown in section 3.2.1.

The voltage of the laser diode can be derived from equation (5.2)

$$V_f = \frac{\eta kT}{e} ln\left(\frac{I_f}{I_s}\right) \tag{5.3}$$

Where

$$I_s = \left[T^3 \exp\left(-\frac{E_g}{kT}\right)\right] T^{\frac{\gamma}{2}} \tag{5.4}$$

E_g is the band gap energy with a unit of volts and γ is a constant. The $T^{\frac{\gamma}{2}}$ term is close to unity. The saturation current can be approximated as

$$I_s = \left[T^3 \exp\left(-\frac{E_g}{kT}\right)\right] C \tag{5.5}$$

Where C is a constant. Substituting equation (5.5) and (5.3) and taking its first derivative in terms of temperature

$$\frac{dV_f}{dT} = \frac{d}{dT}\left[\frac{\eta kT}{e} ln\left(\frac{I_f}{I_s}\right) - \frac{3lnT\,\eta kT}{e} + \frac{\eta E_g}{e}\right] \tag{5.6}$$

The above relationship gives the temperature dependence of the laser diode junction voltage. The forward voltage V_f which is measured across the terminal of the laser diode is given by

$$V_f = V_j + I_f R_s \tag{5.7}$$

Where R_s is the series resistance of the laser diode. Substituting equation (5.7) in equation (5.6), the derivative of junction voltage in terms of forward voltage can be written as

$$\frac{dV_j}{dT} = \frac{d}{dT}\left[\frac{\eta kT}{e} ln\left(\frac{I_f}{I_s}\right) - \frac{3lnT\,\eta kT}{e} + \frac{\eta E_g}{e}\right] - \frac{d}{dT}(I_f R_s) \tag{5.8}$$

Equation (5.8) shows the temperature dependence of the laser diode junction voltage and series resistance.

The junction resistance R_j of the laser diode shown in equation (3.20) can be derived by taking the first derivative of equation (5.3) in terms of forward injection current I_f

$$R_j = \frac{dV_f}{dI_f} = \frac{\eta kT}{e}\frac{1}{I_f} \tag{5.9}$$

Where the saturation current I_s has been ignored as the laser diode is operated with a forward current.

According to equation (5.9), as the injection current is increased, the junction resistance will decrease to zero. However, in practice, the measured resistance with increase in injection current does not decrease to zero and reaches a constant. At this point, the measured resistance is the series resistance of the laser diode, which can be described as [2]:

$$R_s = \frac{1}{A_j}\int_{x_1}^{x_2} \rho(x)dx + \frac{\rho_B}{4r} + R_c \tag{5.10}$$

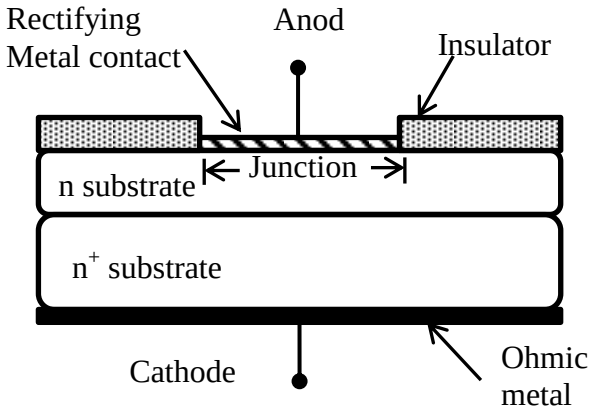

Figure 5.1 Description of a Shottkey diode. Redrawn from [2]

A_j and $\rho(x)$ are the junction area and the series resistance of the quasi-neutral region of the laser diode chip. x_1 and x_2 are the positions of the depletion laser edge and epitaxial layer sub-boundary respectively. ρ_B is the resistivity of the metal-semiconductor substrate and r is its circular area radius. R_c represents the ohmic contact resistance. Equation (5.11) shows the total dynamic resistance,R, of the laser diode

$$R = R_j + R_s \tag{5.11}$$

Both the junction voltage and the series resistance of the laser diode are temperature dependent as shown in equation (5.8). The voltage drop across the laser diode terminals is the forward voltage. The junction voltage of the laser diode is calculated from the forward voltage by subtracting the voltage drop across the series resistance as shown in equation (5.7). The forward voltage of the laser diode decreases with increasing temperature, whereas the laser diode resistance increases with increasing temperature as shown in equation (5.9). Therefore, the temperature dependence of the laser diode series resistance has to be taken into consideration, when the junction voltage is used to stabilise the laser diode.

5.2 Equipment and experimental setup for measuring the laser diode series resistance

Two distributed feedback (DFB) laser diode (Laser Components HHI and NEL NLK1U5EAAA) were used; the first one is packaged in a miniature thermo electric (MTE) T08 Can, while the latter one was butterfly packaged. The thermistors of both laser diodes

had a resistance of 10kΩ at 25 ^{0}C. Both laser diode packages contained a Peltier cooling element to maintain a set temperature.

Both DFB laser were operated above their thresholds and the forward voltage across the laser diode terminals were measured at different thermistor temperatures. The DC injection current to the laser diode was supplied by a current controlled current driver (Thor Labs LDC 202) with an accuracy of ±100μA. The laser diode Peltier temperature was controlled by a temperature controller (Thor Labs TED200) with an accuracy of ±0.1˚C. A digital multimeter (Keithly 195A) was used to measure the voltage drop across the laser diode terminals.

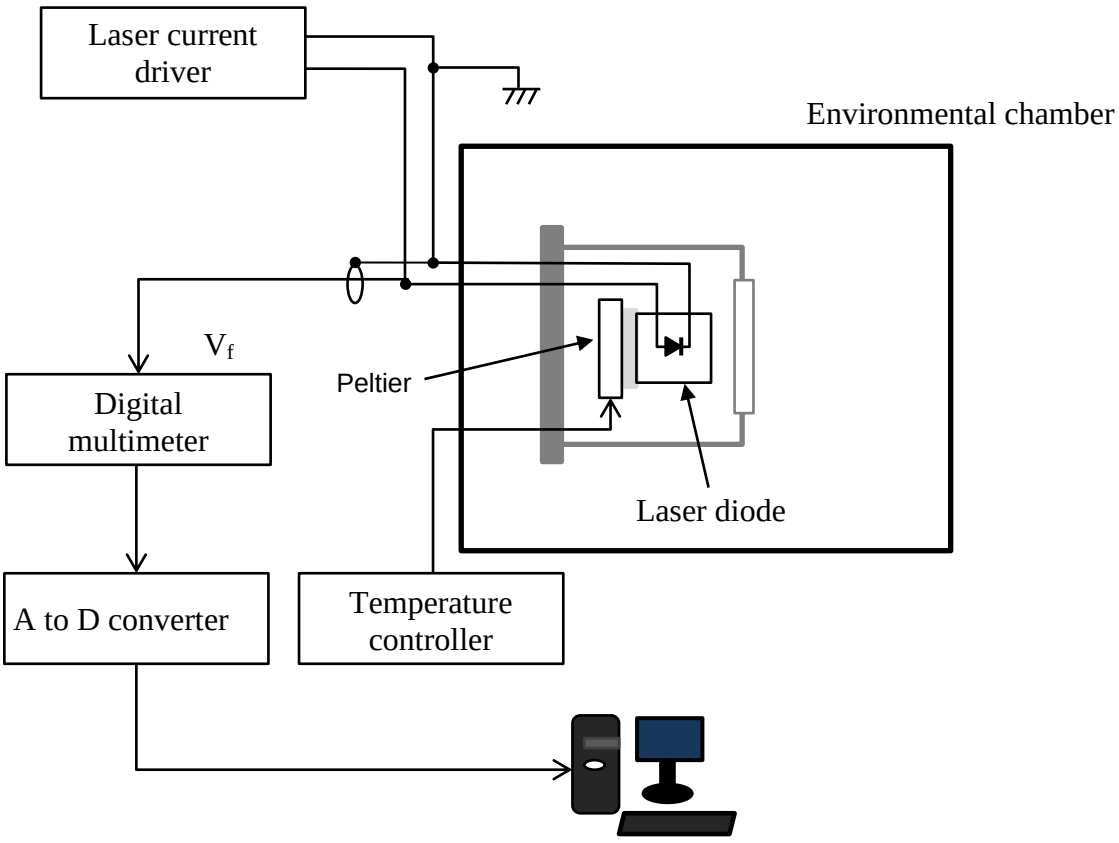

Figure 5.2 Laser diode resistance measurement setup

Figure 5.2 shows the experimental setup used for the laser diode resistance measurement. The laser diode was biased with DC injection current and was operated at a constant temperature using the temperature controller. The voltage drop across the laser diode was acquired with the help of GPIB using LabVIEW software (National Instruments 2013).

5.2.1 **Standard Method**

The laser diode forward voltage V_f is the sum of the junction voltage V_j and the voltage drop across the laser diode series resistance

$$V_f = V_j + I_f R_s \tag{5.12}$$

Substituting equation (5.12) in equation (5.9) [2]

$$\frac{dV_f}{dI_f} = R_s + \left(\frac{\eta kT}{eI_f}\right) \tag{5.13}$$

Where $\frac{\eta kT}{eI_f}$ « R_s Laser diode series resistance was measured by plotting $\frac{dV_f}{dI_f}$ against I_f as shown in Figure (5.3) below

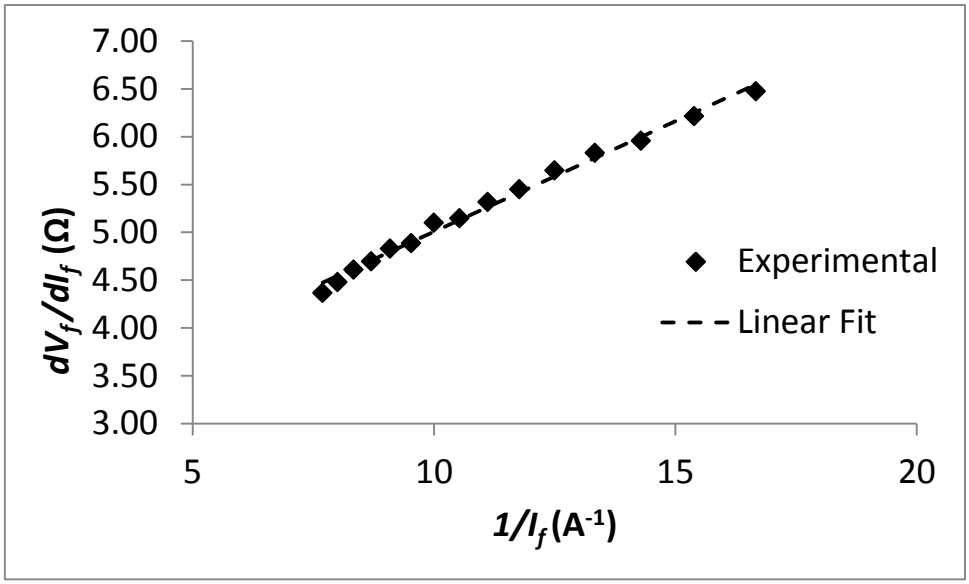

Figure 5.3 Plot of dV_f/dI_f vs $1/I_f$ for MTE T08 Can packaged laser diode at 20˚C thermistor temperature using standard method

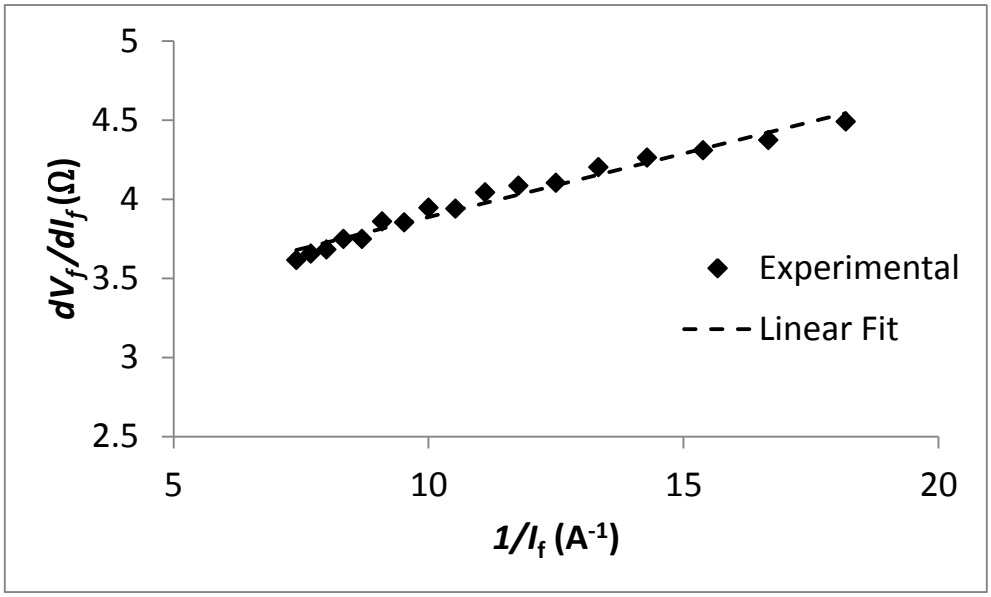

Figure 5.4 Butterfly packaged laser diode dV_f/dI_f vs $1/I_f$ plot at 20˚C thermistor temperature using standard method

Figures 5.3 and 5.4 shows the series resistance measured from the (I-V) characteristics of the MTE T08 Can packaged and butterfly packaged laser diodes. The laser diode was operated in DC conditions in the current range of 55-135mA at different thermistor temperatures. This was an intermediate current voltage range representing the approximately linear region of the I-V relationship. This current range was also selected for the following reasons:

- Operation below threshold will result in a higher series resistance measurement
- Avoiding series resistance change due to heat generation by operating laser high injection current region

The relationship between $\frac{dV_f}{dI_f}$ and $\frac{1}{I_f}$ was approximately linear. The y-axis intercept $\frac{dV_f}{dI_f}$ of the graph gave the measure of the series resistance. The experiment for calculating the series resistance was repeated for a temperature range of 10-40 ˚C Table 5.1 shows the regression parameters for $\frac{dV_f}{dI_f}$ Vs $\frac{1}{I_f}$ relation at different temperatures.

Table 5.1 Regression parameters calculated for the series resistance measurement using standard method

Temperature(˚C)	Slope (m)	Standard error(Δm) (Ω)	Intercept(c) = Rs (Ω)	Standard error(Δc) (Ω)
10	0.23	0.006	2.65	0.06
20	0.23	0.006	2.696	0.06
30	0.23	0.006	2.74	0.07
40	0.22	0.009	2.86	0.1

The resistance of T08 can package diode using the standard method was calculated by using the regression parameters in Table 5.1.

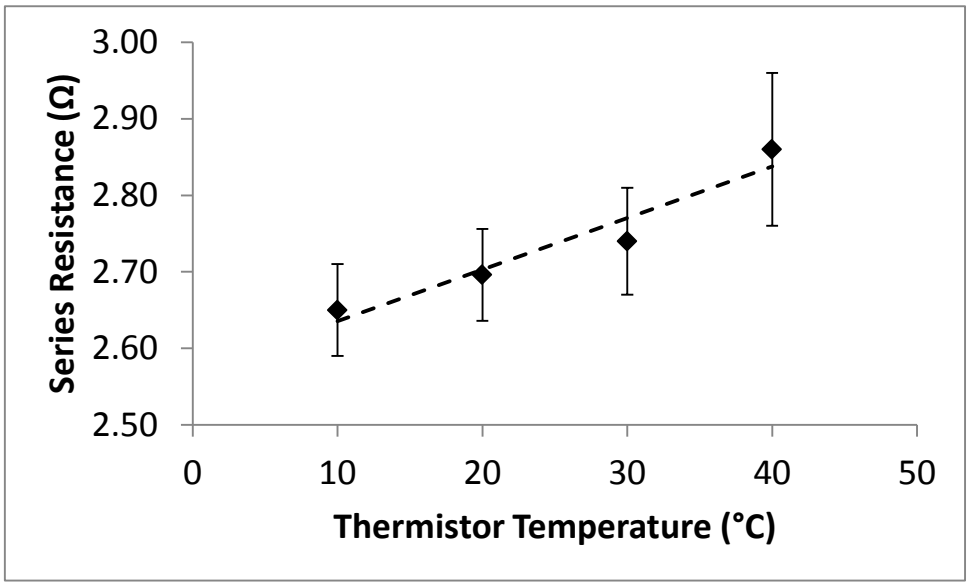

Figure 5.5 T08 Can packaged DFB laser diode resistance at different thermistor temperatures

The series resistance calculated with standard method increased with increasing temperature as shown in Figure 5.5. Table 5.2 shows the regression parameters calculated for the butterfly packaged DFB laser using standard method.

Table 5.2 Regression parameters calculated for Butterfly packaged DFB laser diode series resistance as a function of operating temperature

Temperature (°C)	Slope (m)	Standard error(Δm) (Ω)	Intercept(c) =Rs (Ω)	Standard error(Δc) (Ω)
15	0.08	0.003	3.06	0.04
20	0.08	0.003	3.08	0.04
25	0.08	0.003	3.10	0.04
30	0.08	0.004	3.13	0.04
35	0.08	0.004	3.14	0.04

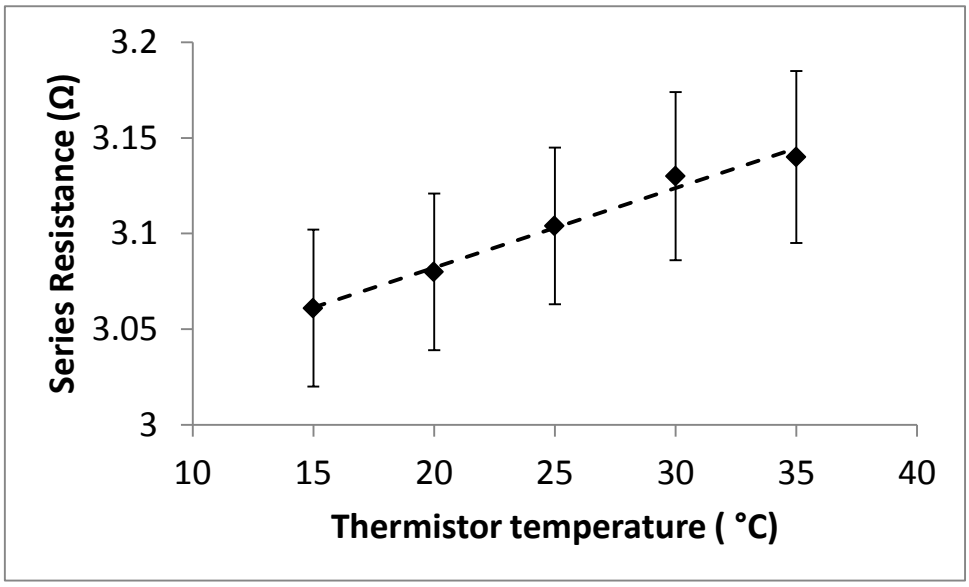

Figure 5.6 Butterfly packaged DFB laser diode resistance calculated with standard method at different thermistor temperatures

Figure 5.6 shows the effect of thermistor temperature on the laser diode series resistance calculated using standard method. Resistance of the laser diode increased with increasing thermistor temperature.

The standard method could be used to calculate the series resistance of both T08 can and butterfly packaged laser diodes. The series resistance of the butterfly packed laser diode was calculated to be higher than the T08 can packed laser diode. The series resistance of both diodes increased with increasing temperature, giving an increase in series resistance of 0.21Ω/°C for T08 and 0.079Ω for Butterfly packaged laser diode in the temperature range 10-40 ˚C.

5.2.2 **Cheung and Cheung Method**

The Cheung and Cheung method [3] is a modified version of the standard method as reviewed in section 3.4.2. In the Cheung and Cheung method the linear relationship between $\frac{dV_f}{dln(I_f)}$ vs I_f is used to measure the resistance of the laser diode, while $\frac{\eta kT}{eI_f} \ll I_f R_s$

$$\frac{dV_f}{dln(I_f)} = RI_f + \left(\frac{\eta kT}{eI_f}\right) \tag{5.14}$$

Both laser diodes forward voltages are measured in a step of 5mA injection current in the current range of 55-135mA. The operating thermistor temperature was varied in the range 10 - 40 ˚C.

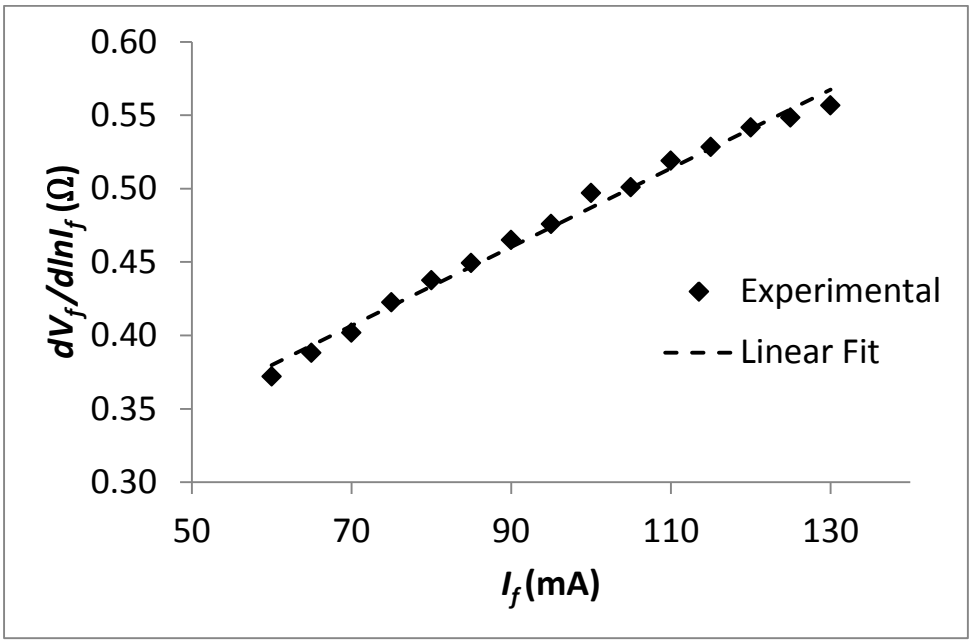

Figure 5.7 MTE T08 Can packaged laser diode plot of $dV_f/dlnI_f$ vs I_f at 20˚C thermistor temperature using the Cheung and Cheung method

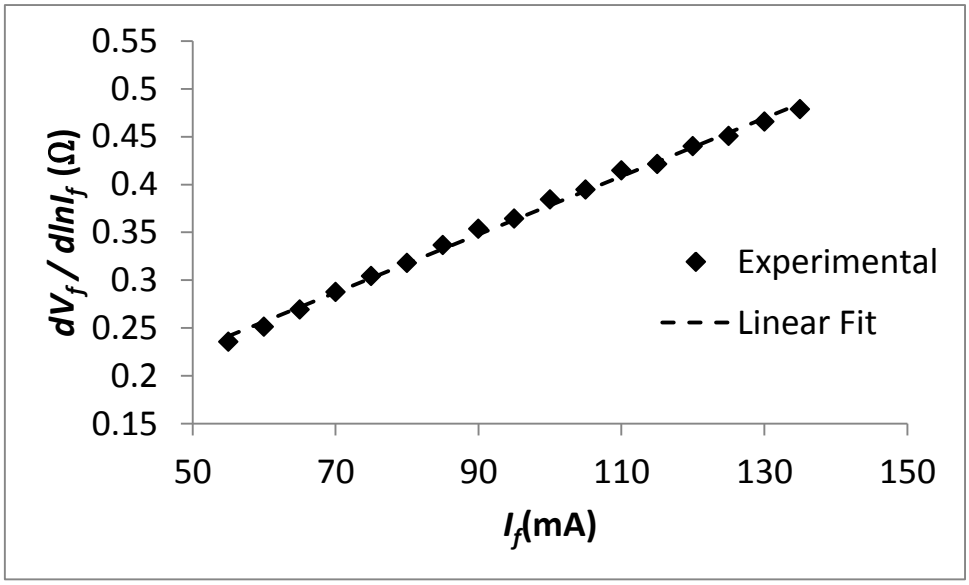

Figure 5.8 Plot of $dV_f/dlnI_f$ vs I_f for Butterfly packaged at 20˚C thermistor temperature using the Cheung and Cheung method

Figures 5.7 and 5.8 show the relationship between $\frac{dV_f}{dln(I_f)}$ vs I_f at 20 ˚C thermistor temperature for the T08 can packaged laser and butterfly packaged laser diode. The relationship between $\frac{dV_f}{dln(I_f)}$ and I_f was approximately linear for both laser diodes as shown by the dashed straight line fit. The slope of the graph between $\frac{dV_f}{dln(I_f)}$ vs I_f gave the measure of the series resistance.

Using calculated regression parameters for the Cheung and Cheung method as tabulated for the standard method in Table 5.1, the series resistance for the MTE laser was calculated as shown in Figure 5.9.

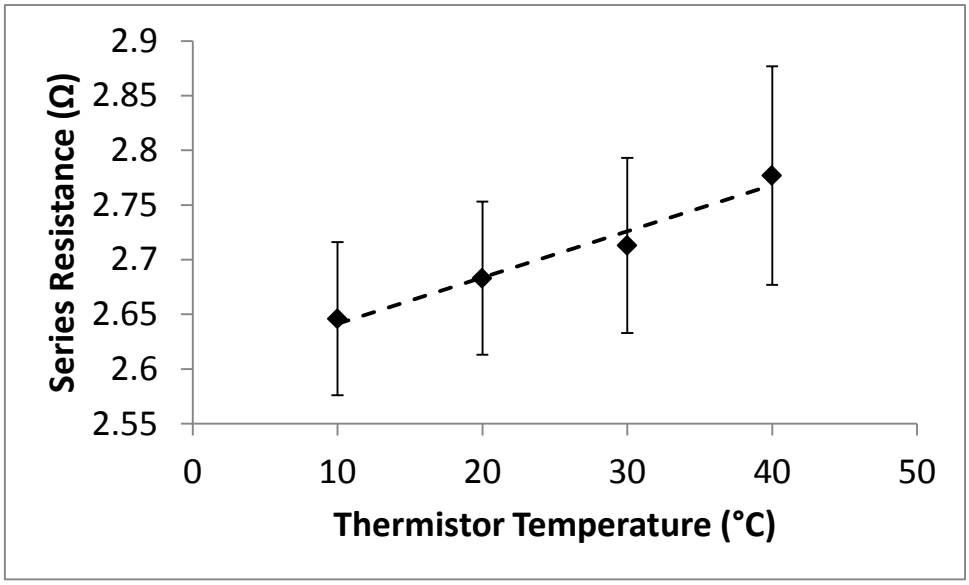

Figure 5.9 T08 Can packaged DFB laser diode series resistance as a function of thermistor temperatures

Figure 5.9 shows the effect of operating thermistor temperature on the series resistance of T08 can packed DFB laser diode. The series resistance for this laser diode was calculated using the Cheung and Cheung method. The series resistance increased linearly with increasing temperature.

By calculating regression parameter as tabulated in the standard method in Table 5.2 , the series resistance of the butterfly packaged DFB laser was calculated as shown in Figure 5.10.

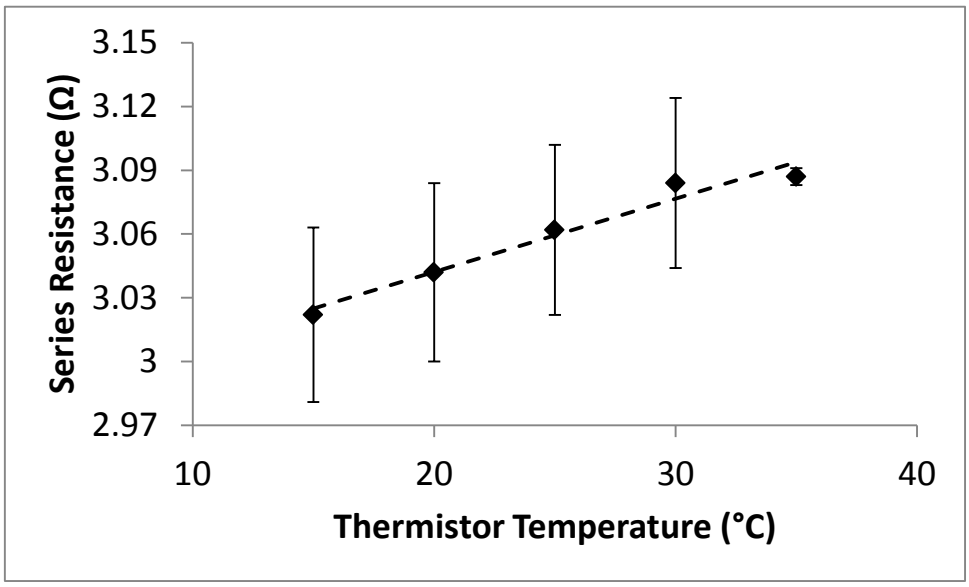

Figure 5.10 Butterfly packaged laser diode series resistance measurement as a function of thermistor temperature

The series resistance of the laser diode increased with increasing temperature. The relationship between the calculated series resistance for the laser diode was approximately linear. More emphasis is given to the lower injection current rage in calculating the series resistance in standard method compared to the Cheung and Cheung method, resulting in higher values for the series resistance. For both T08 and Butterfly packaged, the Cheung and Cheung method gave a lower increase in the series resistance as a function temperature, compared to the standard method.

5.2.3 **Werner method**

Werner [4] used the conductance calculated from the IV characteristics of the diode for measuring the resistance as reviewed in section 3.4.3. By manipulating equation (5.2).

$$\frac{dI_f}{dV_f}\frac{1}{I_f} = \frac{e}{\eta kT} \times [1 - \frac{dI_f}{dV_f} \times R] \qquad (5.15)$$

The relationship between$\frac{dI_f}{dV_f}\frac{1}{I_f}$ and $\frac{dI_f}{dV_f}$ gives a straight line. Both T08 can packaged and butterfly packaged laser diode were operated in the current range of 55-135mA and operating thermistor temperature 10-40 ˚C.

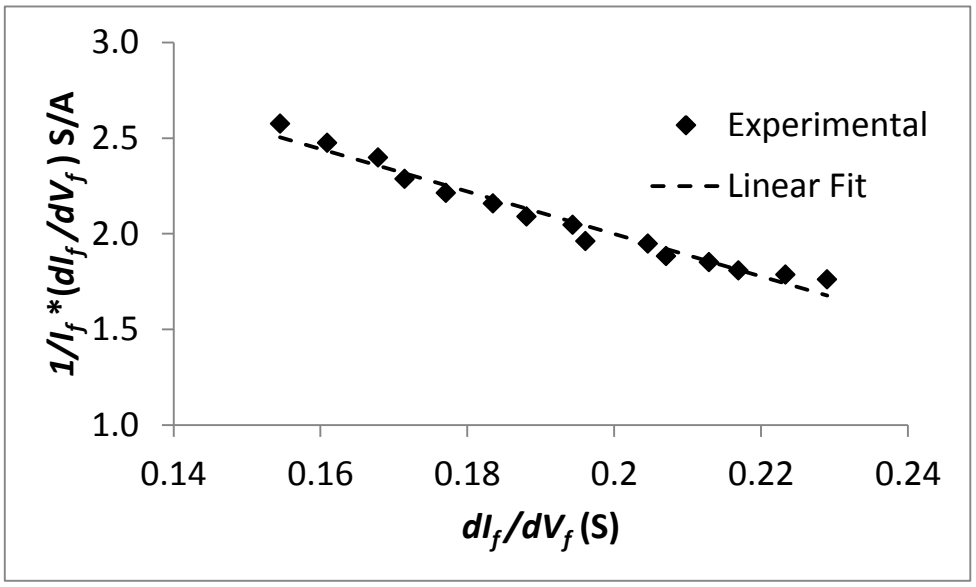

Figure 5.11 MTE T08 Can packaged laser diode plot between $\frac{dI_f}{dV_f}\frac{1}{I_f}$ and $\frac{dI_f}{dV_f}$ at 20˚C using Werner method

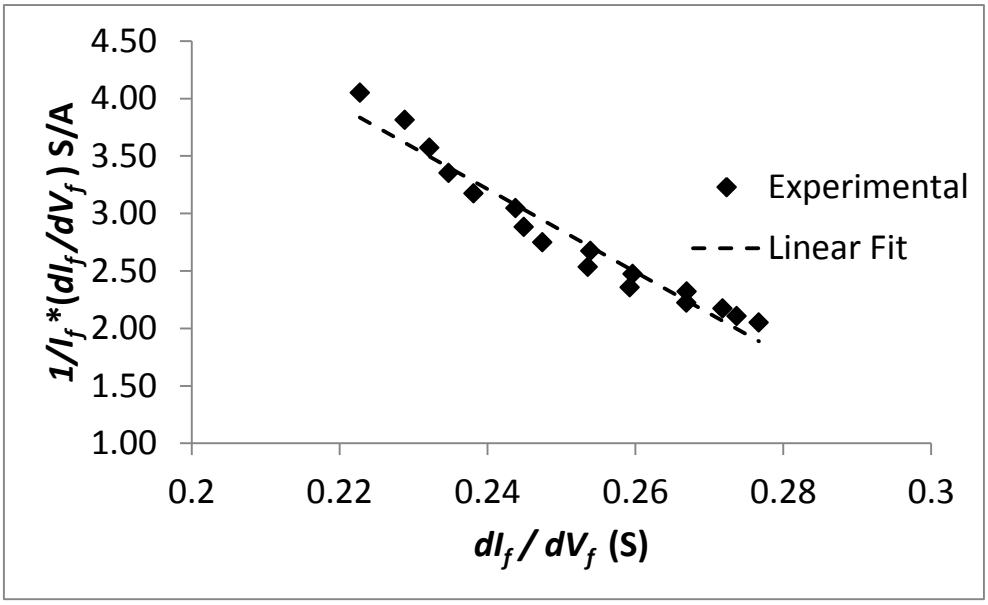

Figure 5.12 Butterfly packaged laser diode plot of $\frac{dI_f}{dV_f}\frac{1}{I_f}$ and $\frac{dI_f}{dV_f}$ at 20˚C thermistor temperature using Werner method

The relationship between $\frac{dI_f}{dV_f}\frac{1}{I_f}$ and $\frac{dI_f}{dV_f}$ was approximately linear for both lasers as shown in Figure 5.11 and Figure 5.12. The series resistance of the laser diode was calculated from the slope of the graph $\frac{R_s.e}{\eta kT}$. The x-axis intercept also gave the measure of resistance $\frac{1}{R_s}$. From the Regression parameters for the relationship between $\frac{dI_f}{dV_f}\frac{1}{I_f}$ and $\frac{dI_f}{dV_f}$, the series resistance of the T08 can packaged laser diode was calculated as shown in Figure 5.13.

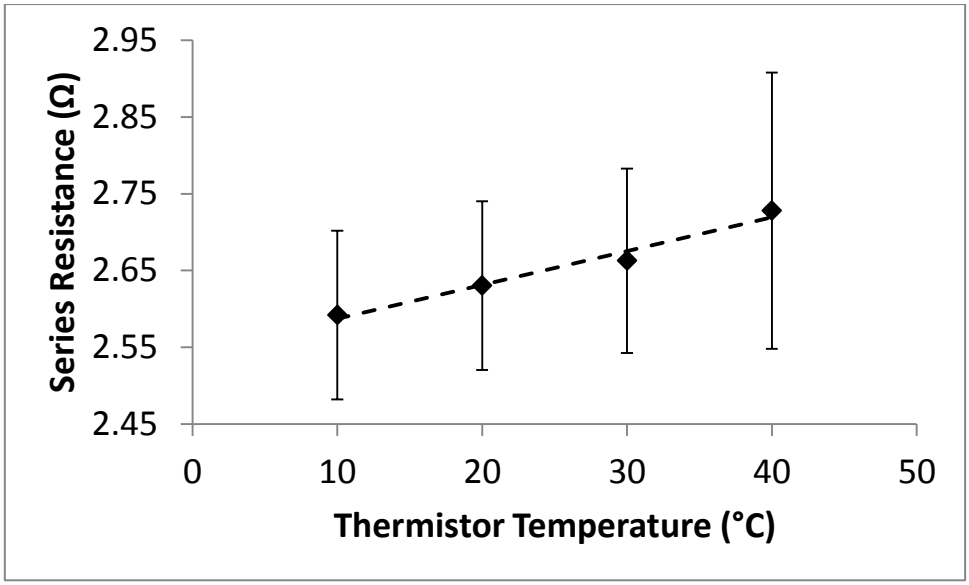

Figure 5.13 T08 can packaged DFB laser diode series resistance as a function of operating thermistor temperature calculated using Werner method

The T08 DFB laser resistance increased with increasing operating temperature as shown in Figure 5.13. The relationship between the operating thermistor temperature and the calculated series resistance was approximately linear.

By using the regression parameters as tabulated for standard method in Table 5.2, the series resistance of the butterfly packaged laser diode was calculated for different operating thermistor temperatures, as shown in Figure 5.14.

The Cheung and Cheung method and the Werner method emphasise high and intermediate voltage range respectively for calculating the series resistance. Both methods revealed similar increases in the laser diode resistance as a function of temperature for both DFB lasers

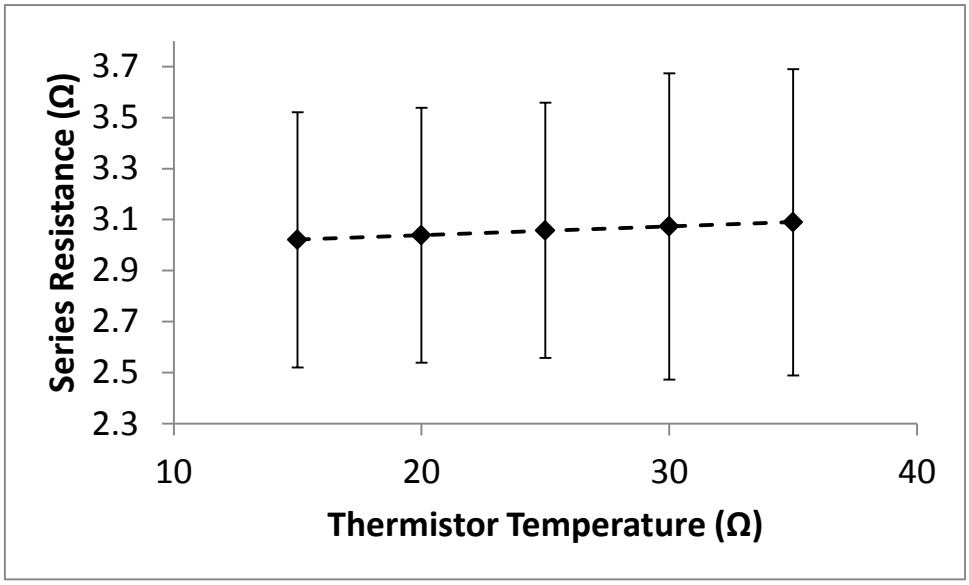

Figure 5.14 Butterfly packaged laser diode series resistance measurement as a function of thermistor temperature

Figure 5.14 shows the resistance of the laser diode as a function of operating thermistor temperatures. The resistance of both laser diodes was increased with increasing temperature. The relationship between the operating thermistor temperature was linear.

Table 5.3 Comparison of methods used for measuring the resistance of T08 Can packaged DFB laser

Temperature(ºC)	Rs according to Method / (Ω)		
	Standard	Cheung and Cheung	Werner
10	2.65±0.06	2.65±0.07	2.59±0.11
20	2.70±0.06	2.68±0.07	2.63±0.11
30	2.74±0.07	2.71±0.08	2.66±0.12
40	2.86±0.1	2.78±0.1	2.73±0.18

Table 5.3 shows the comparison between different methods used to calculate the resistance of the MTE T08 Can package DFB laser. Resistance calculated by the standard method and the Cheung and Cheung method gave similar result (within experimental errors). However, resistance calculation from the Werner method gave lower resistance values for the MTE T08 .can packaged DFB laser diode. This lower resistance calculation could be attributed to the emphasis on the intermediate voltage range by the Werner method, giving a lower measure of the series resistance compared to standard methods. In addition, standard method gave a higher measure of increase in the series resistance (0.21Ω/ ºC) as a function of temperature

for T08 can packaged laser compared to the Cheung and Cheung, and the Werner methods. Both the Cheung and the Werner methods gave similar increase in the laser diode series resistance (0.131Ω, 0.136Ω respectively) as a function of temperature. By analysing the results, error bars for standard method and the Cheung and Cheung method are similar. However, standard method give measure of series resistance, therefore the Cheung and Cheung method will be used to calculate the series resistance.

Table 5.4 Comparison of methods used for measuring the resistance of butterfly packaged DFB laser

Temperature(ºC)	Rs according to Method / (Ω)		
	Standard	Cheung and Cheung	Werner
15	3.06±0.04	3.02±0.041	3.01±0.5
20	3.08±0.041	3.04±0.042	3.04±0.5
25	3.10±0.041	3.06±0.04	3.06±0.5
30	3.13±0.044	3.08±0.04	3.08±0.6
35	3.14±0.045	3.08±0.004	3.08±0.6

Table 5.4 shows resistance values calculated for butterfly packaged DFB laser at different thermistor temperatures. In contrast to Table 5.3, here the Werner and the Cheung and Cheung methods gave similar resistance values (within experimental errors). The resistance values calculated by the standard method were higher in comparison to the Werner and the Cheung and Cheung methods. The emphasis of the standard method is at the lower voltage range in contrast to the Cheung and Cheung and the Werner methods resulting in a higher series resistance calculation. Standard method calculated a higher increase (0.079Ω) in the resistance of the Butterfly packaged DFB laser diode in the temperature range 15-35 ºC compared to the Cheung and Cheng method (≈0.65Ω) and the Werner method (≈0.69Ω). The error bars for the Werner method are higher compared to the standard and the Cheung and Cheung method, however, the standard method gives a higher measure of the series resistance for both lasers. Therefore the Cheung and Cheung method is considered to be the right method for calculating the series resistance of T08 and butterfly packaged laser diodes.

5.3 Laser diode wavelength control

In this section, three different techniques, thermistor based control, forward voltage control and junction voltage based control, were investigated for the stability of the laser diode wavelength. As mentioned in the introduction of this chapter, the laser diode wavelength

temperature coefficient is higher than the current tuning coefficient. To stabilise the laser diode wavelength, it is essential to accurately sense and maintain the operating temperature of the laser diode. In addition, it is essential to maintain short term and long term wavelength stability of the laser diode in applications such spectroscopy and telecommunications.

5.3.1 Laser diode wavelength stability using conventional thermistor based control

In a conventional laser diode temperature control system, the temperature of the laser diode chip is sensed with a thermistor placed from the gain chip at a distance as shown in Figure 5.15.

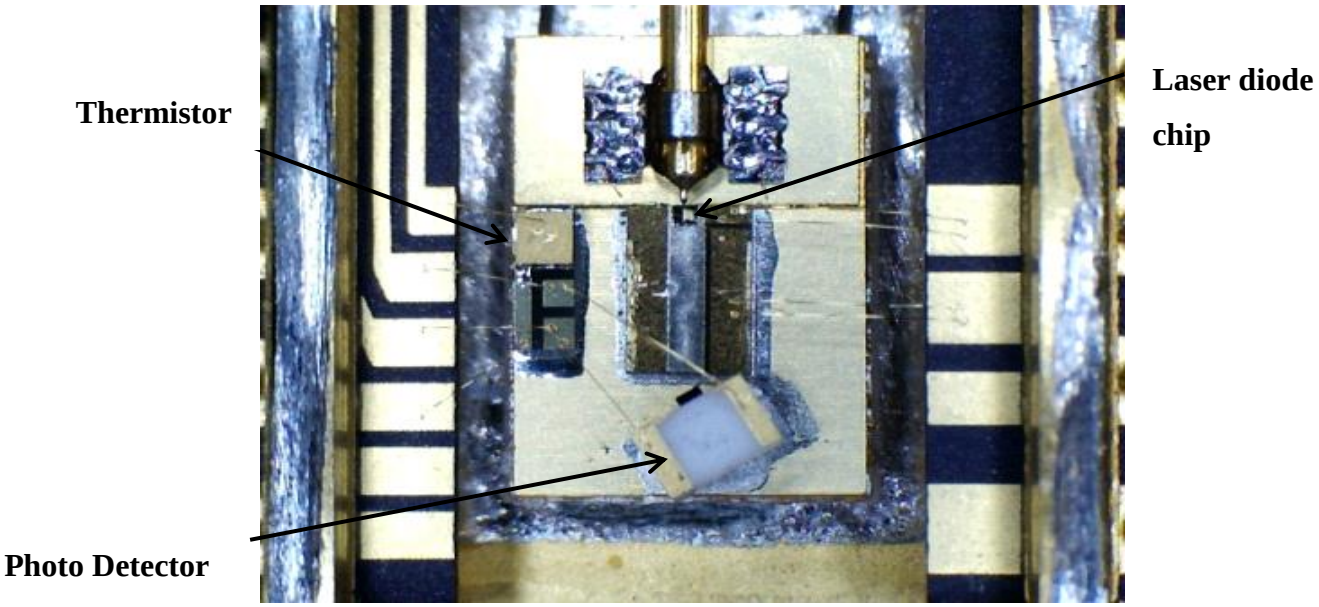

Figure 5.15 Inside view of a DFB laser diode in a butterfly package taken with microscope

5.3.2 Equipment and experimental setup

Conventional thermistor-based temperature control was investigated in order to achieve wavelength stability in an InP ridged waveguide laser (HHI TO8 MTE Module as previously used in section 4.4.1) with a peak wavelength of 1650nm.

The thermistor inside the laser diode package was connected to a temperature controller (Thorlabs TED200), which in turn was connected to the Peltier element in the package in order to control the thermistor temperature. The injection current to the laser diode was supplied using a current driver (Thorlabs LDC200). A custom built environmental chamber was used to maintain constant external ambient temperature, as shown in Figure 5.16. The wavelength of the laser diode was measured with wavelength meter (High Finesse WS6/200IR). The resolution of this wavemeter was 0.45pm and its absolute accuracy was 1.8pm.

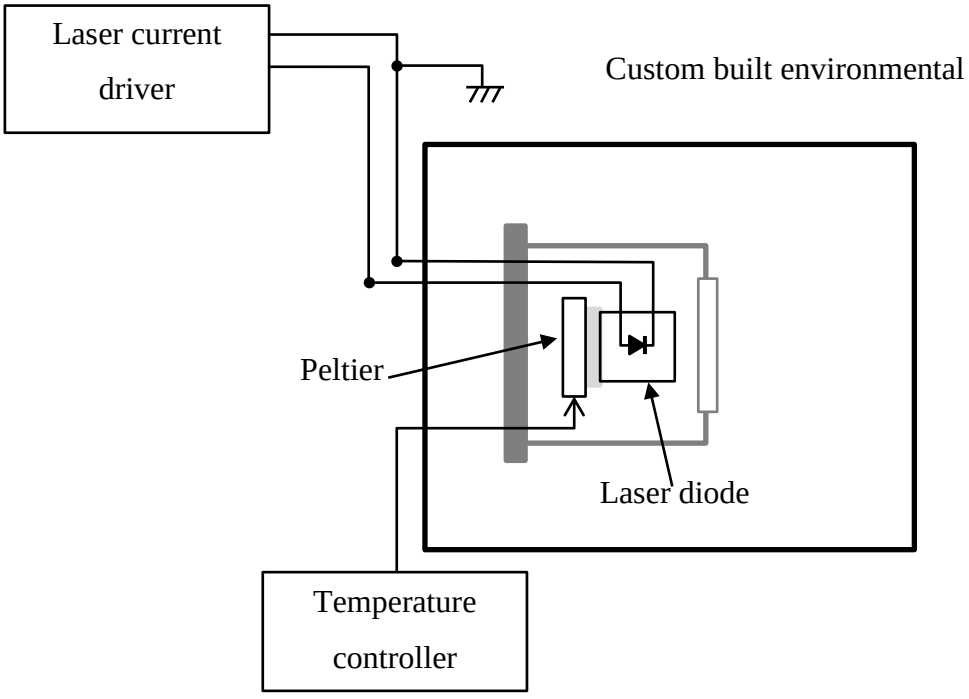

Figure 5.16 Conventional method of laser diode wavelength stabilisation using thermistor

The laser diode placed in an environmental chamber and was operated above threshold at different ambient temperatures, in the range of 15-35˚C. The laser diode injection current was kept constant at 167mA and the thermistor temperature was maintained at 25˚C.

5.3.2.1 Results for conventional control

Figure 5.17 demonstrates the effect of varying ambient temperature on the laser diode wavelength. The laser diode injection current was kept constant at 167mA and the thermistor temperature was maintained at 25˚C, where the laser diode emission wavelength corresponded to methane gas line at 1651nm. The ambient temperature experienced by the

laser diode was varied in 5˚C steps by changing the temperature of the environmental chamber.

As the ambient temperature was increased from 15 ˚C to 35 ˚C, the laser diode emission wavelength drifted to shorter wavelengths, despite having constant injection current and thermistor temperature. This is consistent with the hypothesis that the thermistor was not measuring the actual temperature of the laser diode and that as the ambient temperature was increased, the temperature gradient between the chip and the thermistor was affected. Therefore, the laser diode chip was further cooled down.

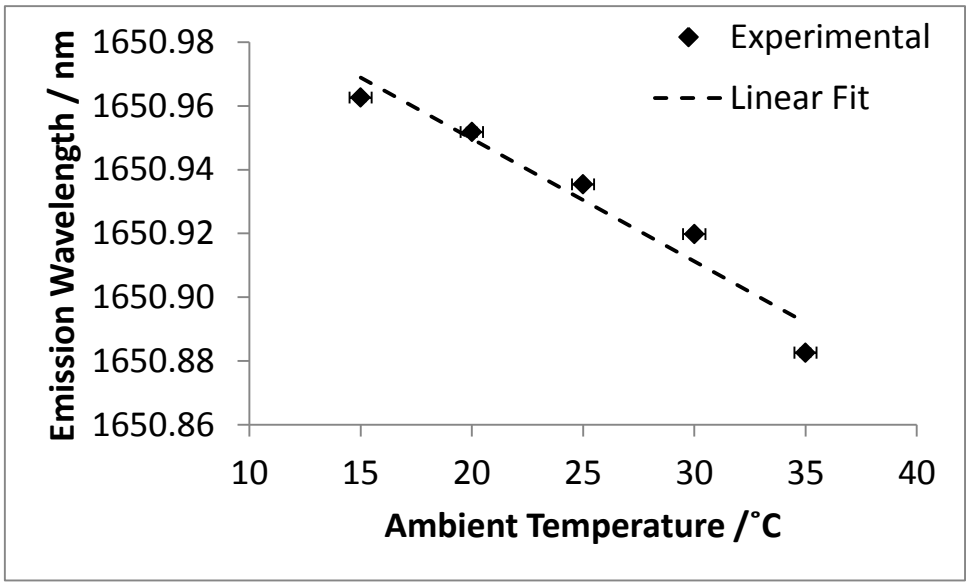

Figure 5.17 Laser diode wavelength drift with ambient temperature while conventionally controlled to a thermistor temperature of 25 ˚C

Thus, the laser diode wavelength drifted towards shorter wavelengths with a total wavelength shift of 80pm over the temperature range of 15-35˚C. The laser diode wavelength had an overall wavelength change with ambient temperature of -3.8pm ±0.55pm /ºC at a constant thermistor temperature.

The conventional thermistor control method was also tested for the long term laser wavelength stability at a single temperature setpoint. The injection current to the laser diode was kept constant at 167mA and the thermistor temperature was controlled to at 25˚C. The ambient temperature was set to 20 ˚C and the wavelength monitored for 60min. Figure 5.18 shows the resulting long term wavelength stability.

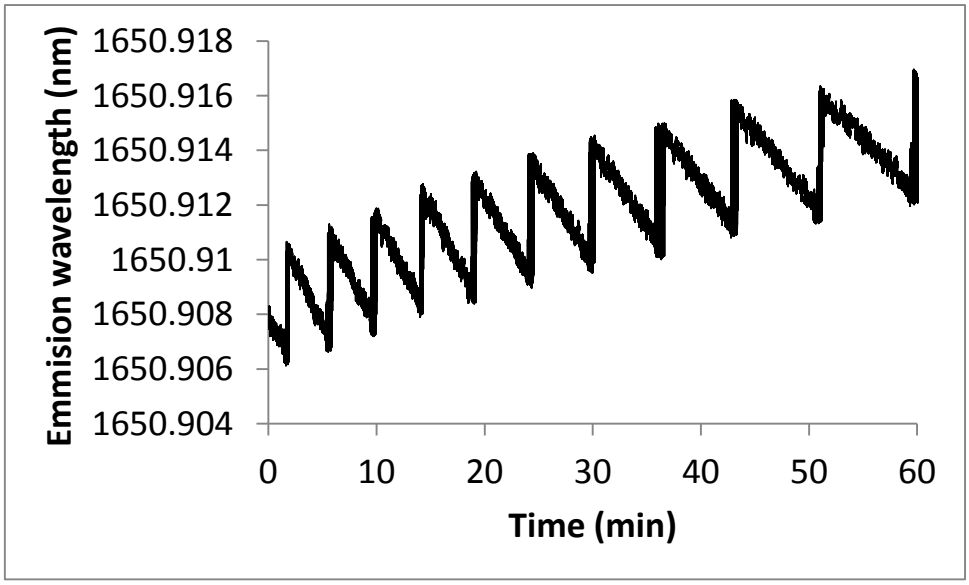

Figure 5.18 Laser diode long term wavelength stability as a function of time at constant ambient temperature of 20 ˚C, thermistor temperature of 25 ˚C and constant injection current of 167mA

The laser diode wavelength drifted over time with a standard deviation of σ=±2.2pm over a time of 60 minutes.

The sawtooth like response could be attributed to mode hops in the laser diode, while maintaining the ambient temperature at 20 ˚C using an environmental chamber. The sawtooth behaviour could also be due to the resetting of the PID to maintain the set thermistor temperature. This mode hop in the laser diode could be the result of the inability of the thermistor to accurately to sense the temperature of the laser diode.

5.3.3 Laser diode wavelength stability using forward voltage based control

The laser diode forward voltage was used as a temperature sensor to stabilise the wavelength of the laser diode according to the method described by Uehara and Katakura[5].

Figure 5.21 shows the I_f-V_f relation for the T08 can packaged DFB laser over the temperature range 10-40 ˚C . The forward voltage (V_f) decreased with increasing operating thermistor temperature. The temperature dependence of the forward voltage of the laser diode was used to stabilise the temperature of the laser diode and thus the emission wavelength.

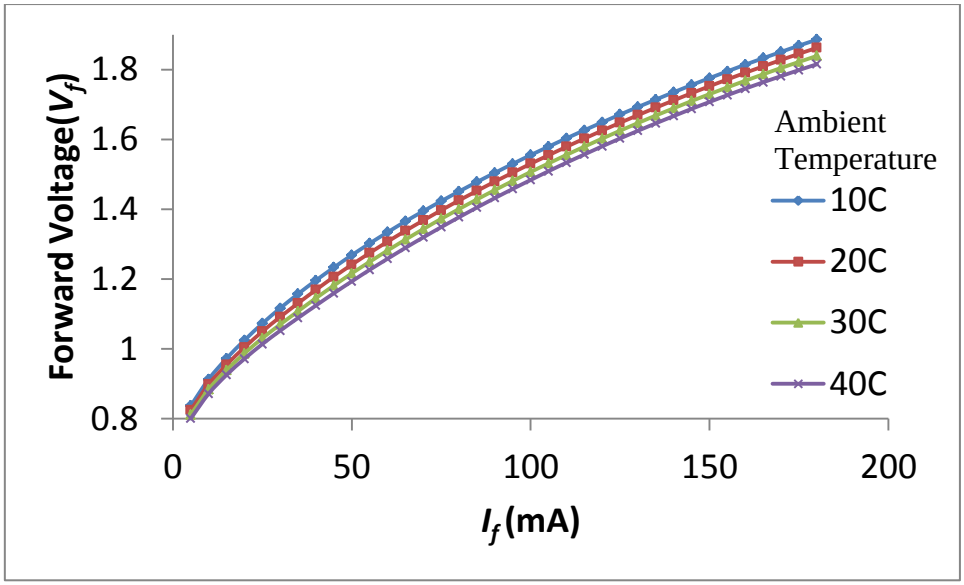

Figure 5.19 V_f -I_f plot of the laser diode operating under thermistor based control at different temperatures

The method of using forward voltage for stabilising the laser diode emission wavelength is described in two sections;

- Equipment and experimental setup
- Results and discussion.

5.3.3.1 Equipment and Experimental setup

The same DFB laser as reported in section 5.3.1 was temperature stabilised using a forward voltage method to achieve wavelength stability. The laser diode was driven using the same current driver (ThorLabs LDC200) and its emission wavelength was monitored using the same wave meter (High Finesse WS6/200IR) as described in section 5.3.1. The laser diode was placed in a custom built environmental chamber with ambient temperature controlled in the range 15-35°C. A LabVIEW (National Instruments) based proportional integral and derivative (PID) controller was used to implement the forward voltage based temperature controller, as shown in the flowchart in Figure 5.20.

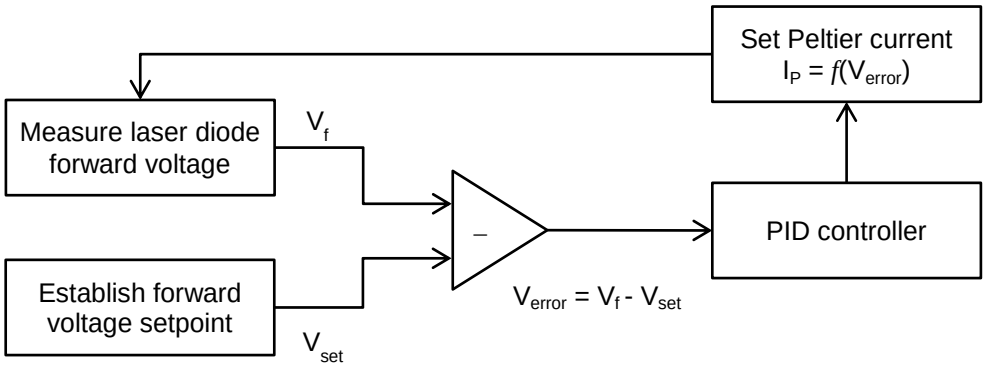

Figure 5.20 Laser diode wavelength stability flow chart using forward voltage based control

The voltage drop across the laser diode was measured and compared to a voltage setpoint, chosen to give a wavelength near the methane gas line (1650.9nm) at specific temperature (for operation at 25˚ C and 167mA). The difference between these voltages acted as an error signal and was fed into the PID controller to stabilise the temperature of the laser diode as described in Figure 5.21. The starting P,I, and D values for the control loop were determined using the method described by Cohen and Coon [6] . Table 5.5 gives the PID values for the forward voltage based control loop.

Table 5.5 PID control values for the forward voltage based control

Control type	Proportional Gain (kc)	Integral time (Ti, min)	Derivative time (Td, min)
PID	5	0.005	0.00005

Appendix B contains the LabVIEW programme written for implementing the forward voltage for stabilising the wavelength of the laser diode.

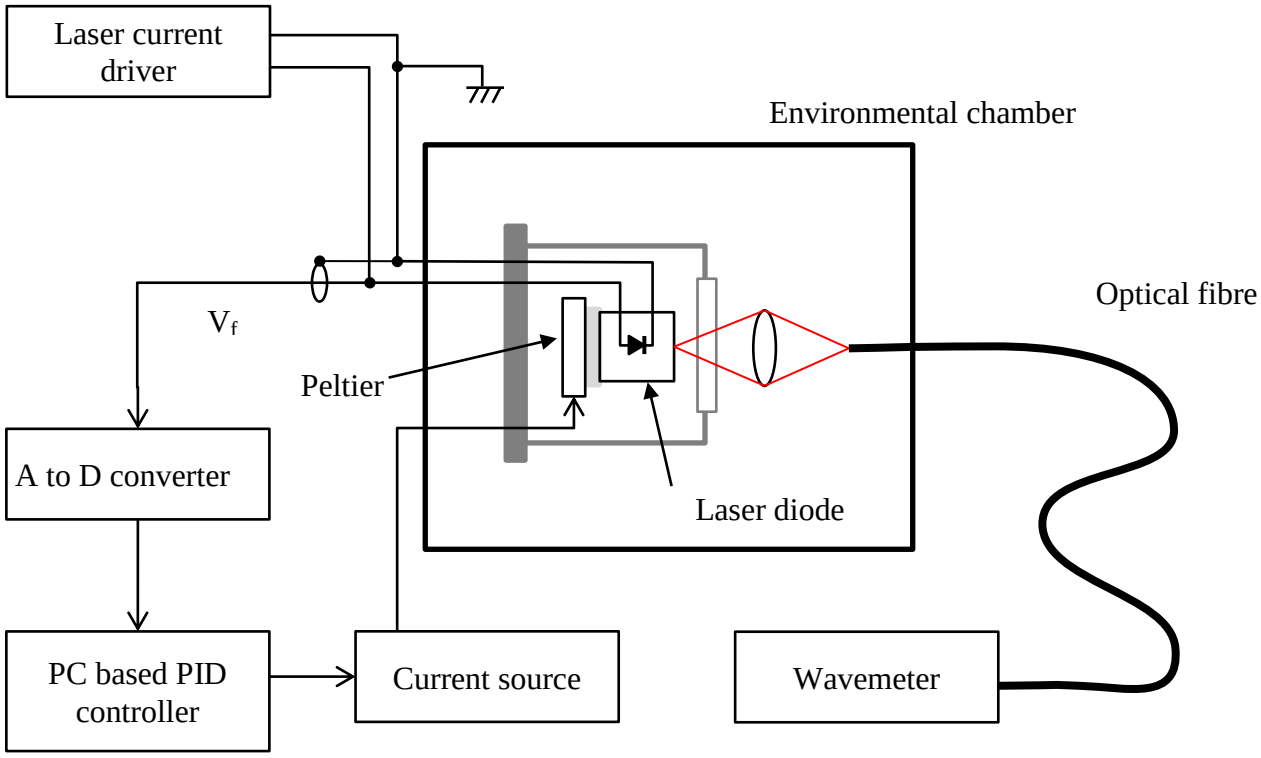

Figure 5.21 Schematic diagram of the forward voltage method to stabilise the laser diode wavelength

5.3.3.2 Results and discussion

The laser diode was driven with a constant injection current of 167mA. The voltage drop was measured while the thermistor was controlled to 25°C ,was used as set voltage for the PID controller, the ambient external temperature of the environmental chamber was then varied in steps of 5°C over the range 15-35°C, while operating under forward voltage control and maintaining the emission wavelength.

Figure 5.22 shows the relationship between ambient temperature and laser diode emission wavelength under forward voltage control. The laser diode wavelength was found to drift towards longer wavelengths at higher ambient temperatures, in contrast to the conventional method using thermistor, where wavelength drifted towards shorter wavelengths as described in section (5.3.1.2). It was found that this technique suffered from a systematic wavelength drift of 4.5pm/°C with varying ambient temperature, as can be observed in the graph in Figure 5.22.

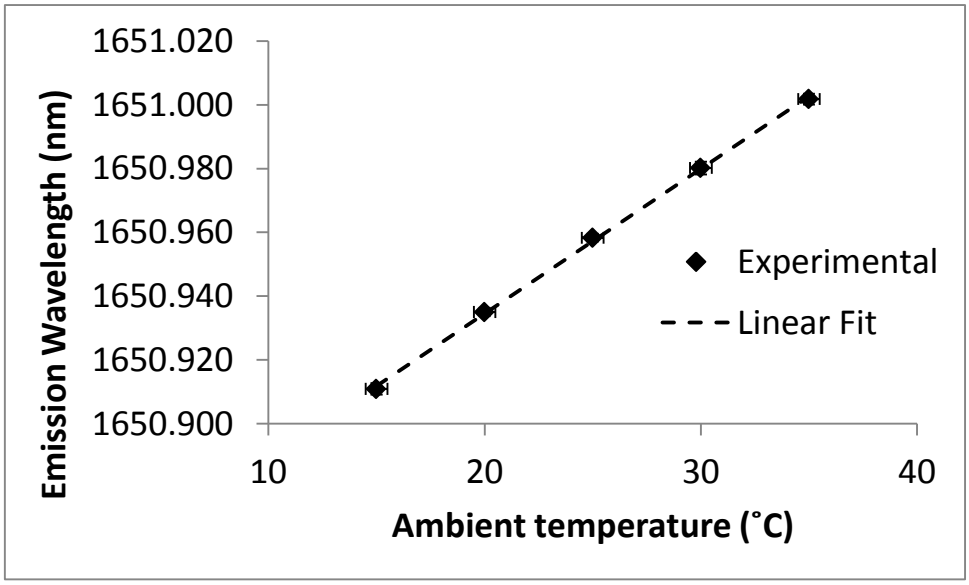

Figure 5.22 Laser diode wavelength stability as a function ambient temperature under forward voltage control.

Figure 5.22 shows that the laser diode wavelength was drifting towards longer wavelength as the temperature was increased, indicating that the forward voltage was influenced by some other parameter, that could influence laser diode junction temperature. The wavelength drift with the forward voltage method over the ambient temperature range (15-35˚C) was 91 pm. The systematic change in wavelength with temperature was 4.5pm/˚C ±0.06pm /˚C. The performance of the forward voltage method in stabilising the wavelength of the laser diode with variable ambient temperature was therefore comparable to that of conventional thermistor-based control

Laser diode long term wavelength stability was assessed by controlling the laser diode temperature using feedback from the forward voltage method. The laser diode was kept in an environmental chamber at a constant temperature of 20 ˚C. The laser diode chip was biased with an injection current of 167mA and the wavelength was measured with the wavemeter (described in section 5.3.1) over a period of 60 minutes.

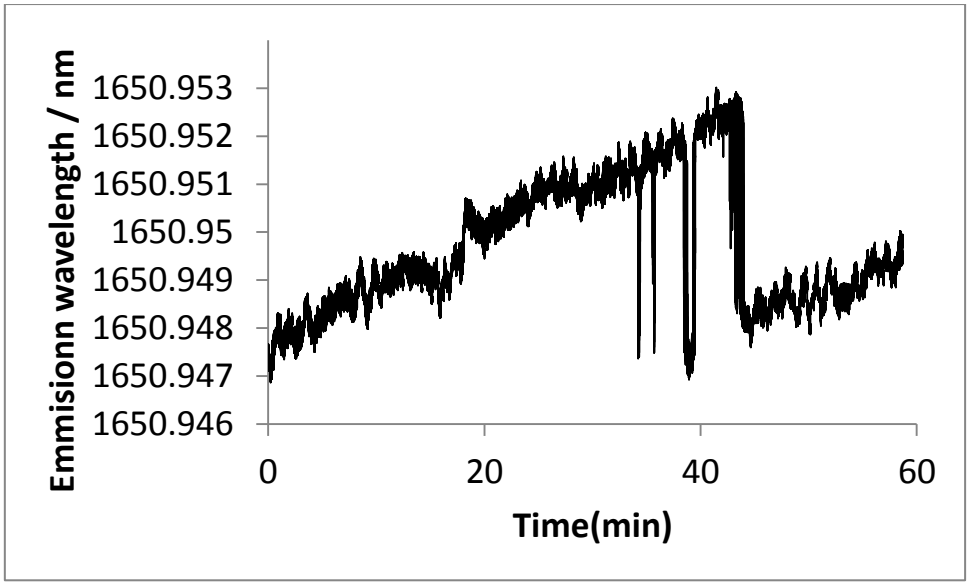

Figure 5.23 Laser diode wavelength stability test as a function of time using forward voltage based control

Figure 5.23 shows the wavelength stability of a laser diode as a function of time diode at constant temperature and injection current. The wavelength stability was σ ±1.32pm, which again was comparable to conventional thermistor based control in section 5.3.2.1. In Figure 5.23, the DFB laser experienced mode hops at approximately 33, 34 and 38min respectively. These mode hops could be attributed to the sudden drop in forward voltage and then the subsequent stabilisation by the forward voltage

The long term wavelength stability and systematic error in wavelength with ambient temperature changes for the forward voltage method were comparable to that of the thermistor. However, tuneable diode laser spectroscopy of gases such as methane, where the absorption line full width half maximum is 50pm (100% methane concentration at atmospheric pressure), requires a more stable laser diode wavelength when faced with varying ambient temperatures. Therefore, an improved wavelength control method is required.

5.3.4 Laser diode junction voltage based control

The forward voltage is the voltage measured across the anode and cathode of the laser diode. The forward voltage is the sum of junction voltage and the voltage drop across the resistance of the laser diode, as described in equation **(**5.7). The laser diode series resistance increased with increasing temperature as shown in section 5.2. The laser diode junction voltage was

investigated for the purpose of stabilising the wavelength of the laser diode over long timescales and in the face of variable ambient temperature.

Figure 5.2 showed that, with increasing temperature, the forward voltage decreased, in contrast to the series resistance of the laser diode as shown in Table 5.3 which increased with increasing temperature.

Table 5.3 confirmed that there was a small additional series resistance within the laser diode, which is temperature dependent. The voltage drop due to the laser diode resistance, will contribute to the forward voltage by adding a small voltage that is dependent on both temperature and injection current, as described in equation (5.7). Therefore, this potentially adds a systematic error to the measurement of the temperature of the laser diode using the forward voltage of the laser diode. This systematic error in temperature sensing using the forward voltage could be observed in Figure 5.22 where, the laser diode emission has drifted towards longer wavelengths due to the increasing ambient temperature.

The junction voltage based control system takes into account the temperature dependence of the laser diode series resistance and its contribution to the forward voltage drop across the laser diode. In the junction voltage control technique, the voltage drop across the series resistance of the laser diode is subtracted from the forward voltage of the laser diode and the resultant voltage is used for stabilising the temperature and wavelength of the laser diode.

5.3.4.1 Equipment and Experimental Setup

The flow chart in Figure 5.24 shows the process used for stablising the laser diode wavelength using laser diode junction voltage. The laser diode series resistance was measured dynamically by modulating the laser diode using a relatively small modulation depth (compared to the DC injection current), while simultaneously applying a DC injection current. The voltage drop across the laser diode was fed into a lock-in amplifier and demodulated at 1f. The demodulated signal gave a measure of the laser dynamic resistance as $\partial V/\partial I$ at the DC current.

The same PID controller was used as described in section 5.3.2.1. The LabVIEW code (Appendix B) used in section 5.3.2.1 was modified by subtracting the voltage drop across the series resistance from the forward voltage measured across the laser diode.

The RMS modulated voltage was measured using a lock-in amplifier and multiplied by an empirically determined factor (A) in Figure 5.24, to give a measure of the series voltage

(I_fR_s). This was subtracted from the DC forward voltage to give a measure of the junction voltage V_j. A setpoint value (Forward voltage at 165mA giving emission wavelength of 165nm minus the calculated voltage across the series resistance at this current) was subtracted from V_j to provide an error signal to the PID. Voltages were measured using a data acquisition card (National Instruments PCI 6259). The voltage compensation and the PID were all implemented in LabVIEW. The output from the PID was sent to the modulation input of the Peltier cooler current diver in order to close the feedback loop.

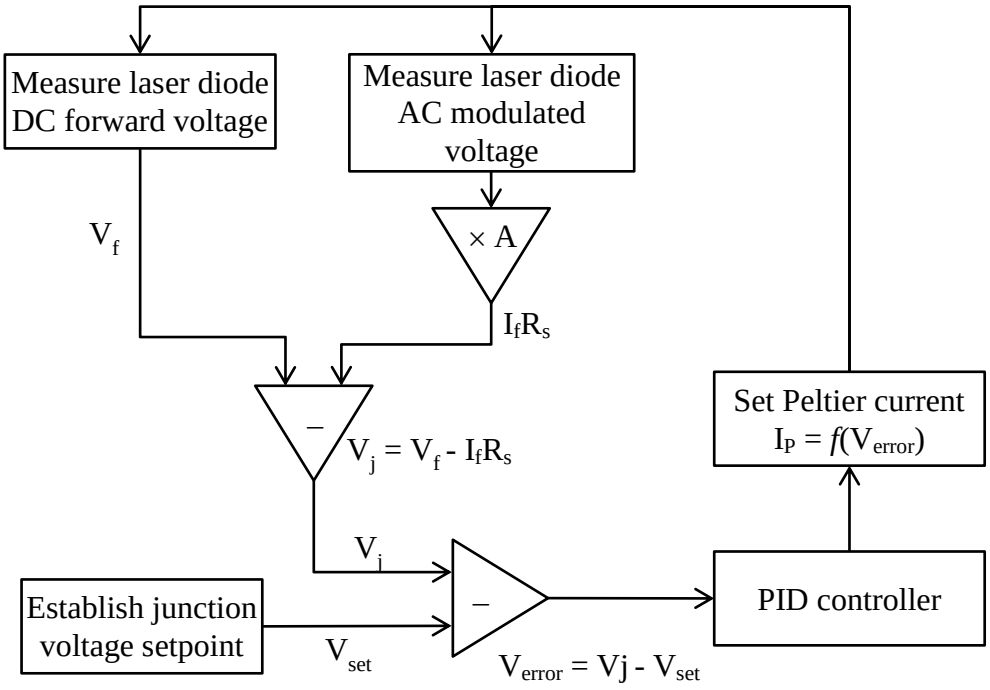

Figure 5.24 Flow chart for the laser diode wavelength stabilisation using junction voltage

The schematic diagram in Figure 5.25 shows the operation of the laser diode wavelength controller using the junction voltage of the laser diode. The laser diode was modulated at 31 kHz with modulation amplitude of $0.08V_{rms}$ (5.2mA current modulation). The smallest modulation amplitude which could be detected by the lock-in amplifier was applied to the injection current in order to reduce contribution to the laser diode resistance by the modulation current. To avoid heating at the gain chip, the laser diode was modulated at a high frequency. The bandwidth of the lock-in amplifier was 100 kHz and to detect 2f and 3f signal, a maximum of 31 kHz modulation frequency was used to modulate the laser diode. A

current driver (Thorlab LDC200) was used to bias the diode at an injection current of 165 mA. A current driver (ThorLab ITC510) was used to drive the Peltier cooler. A lock-in amplifier (Stanford research SR85) was used to measure the 1f modulated forward voltage, providing a dynamic resistance measurement input to the PID which was implemented in LabVIEW. The output error signal from the PID was sent to the modulation input of the Peltier cooler current diver.

The half width half maximum of the methane gas line was ≈ 50pm at atmospheric pressure and 100% concentration. The methane gas was in a gas cell with a short path length of 5mm and methane gas concentration of ≈2.5 / %Vol. The light from the laser diode was coupled into single mode optical fibre and transmitted through the gas cell.

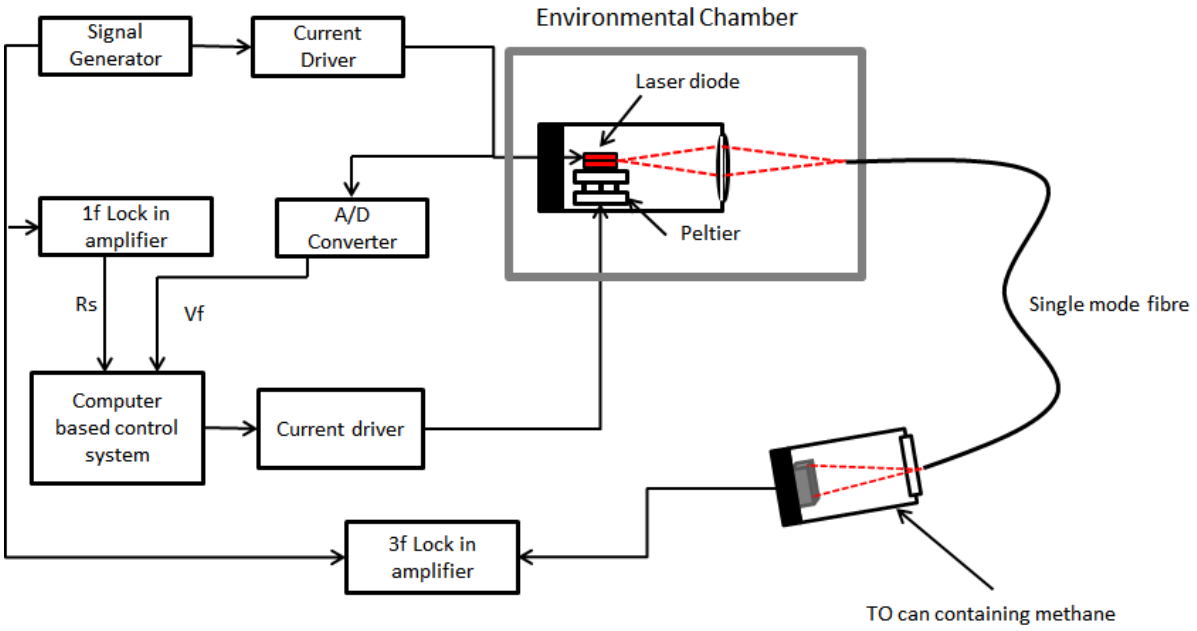

Figure 5.25 Description of the junction voltage method for stabilising the wavelength of the laser diode

The laser diode wavelength stability was measured with the help of a methane gas line at 1650.96nm, due to limited sampling rate of the wavemeter and limited resolution and sampling rate of the optical spectrum analyser. The 3f signal of the detector output from the methane absorption gas line was used to check the wavelength stability of the laser diode.

5.3.4.2 Laser diode wavelength calibration

The laser diode wavelength was calibrated using a methane gas line at 1650.96nm. To achieve this, the laser diode was biased at 165mA with sinusoidal modulation frequency of

31 kHz. The laser diode wavelength change with current was measured to be 23pm/mA by calibrating laser diode wavelength at different injection currents using an optical spectrum analyser. The laser diode modulation amplitude was 5.2mA p-p giving a wavelength tuning of 115pm p-p.

To establish a wavelength calibration, the centre wavelength of the laser diode was scanned across methane gas line while simultaneously applying the sinusoidal dither. The detector output was then fed into the lock-in amplifier and the third harmonic was measured as shown in Figure 5.26 below:

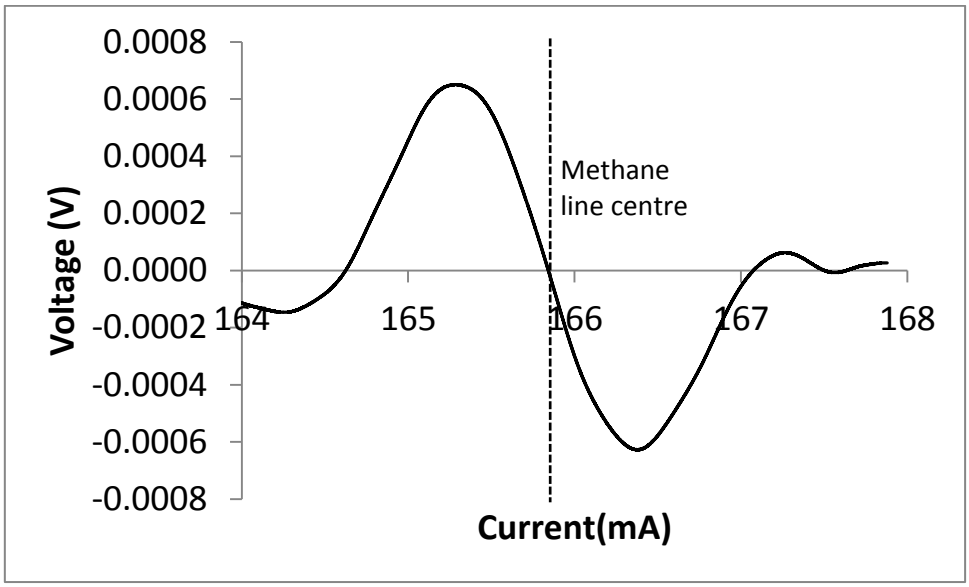

Figure 5.26 Methane 3f signal from gas cell used for wavelength measurement

The zero crossing at y=0 and x=165.8mA, the x-axis of the 3f signal, corresponds to the peak of the methane gas line. To make sure that the line centre had been identified, the calibration process was repeated while observing the 1f, 2f and 3f signals.

The change in laser diode wavelength with injection current in terms of methane gas line can be derived from the relation below

$$\frac{d(3f\ signal)}{d(I_f)} = \frac{d(3f\ signal)}{d(I_f)} \times \frac{d(I_f)}{d(\lambda)} \qquad (5.16)$$

Where, λ is the wavelength and $\frac{d(I_f)}{d(\lambda)}$ is given by the tuning coefficient. The gradient of the linear region of the 3f signal is expanded in the Figure 5.29 below:

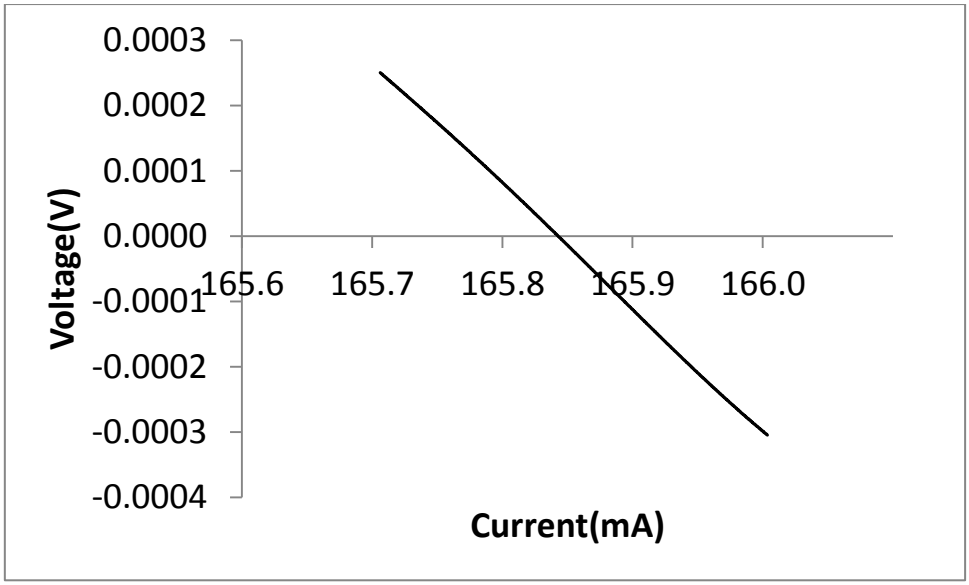

Figure 5.27 Gradient measurement of the 3f signal linear region

The gradient of the 3f signal with injection current was1.904V/mA. By substituting the gradient of the 3f signal linear region and the tuning coefficient, the laser diode wavelength was calibrated in terms of the methane gas line.

By this method, the voltage output from the 3f lock-in amplifier was established to have a calibration coefficient of $\frac{d(3f\ signal)}{d(\lambda)}$ = 83mV/pm

5.3.4.3 Results and discussion

The lock-in amplifier 3f signal was recorded and converted into wavelength using the calibration procedure described above in section (5.3.3.2). Figure 5.28 shows the long-term wavelength stability of the laser diode using junction voltage at 20ºC and injection current of 165.8 mA for duration of one hour. The deviation of the laser diode central peak wavelength from the 3f signal horizontal zero axis gave the measure of the laser diode wavelength stability.

An optical spectrum analyser (Yokogawa AQ6370D) was also used to confirm that there were no wavelength changes that would take the emission outside the linear region of the 3f output /current curve in Figure 5.27.

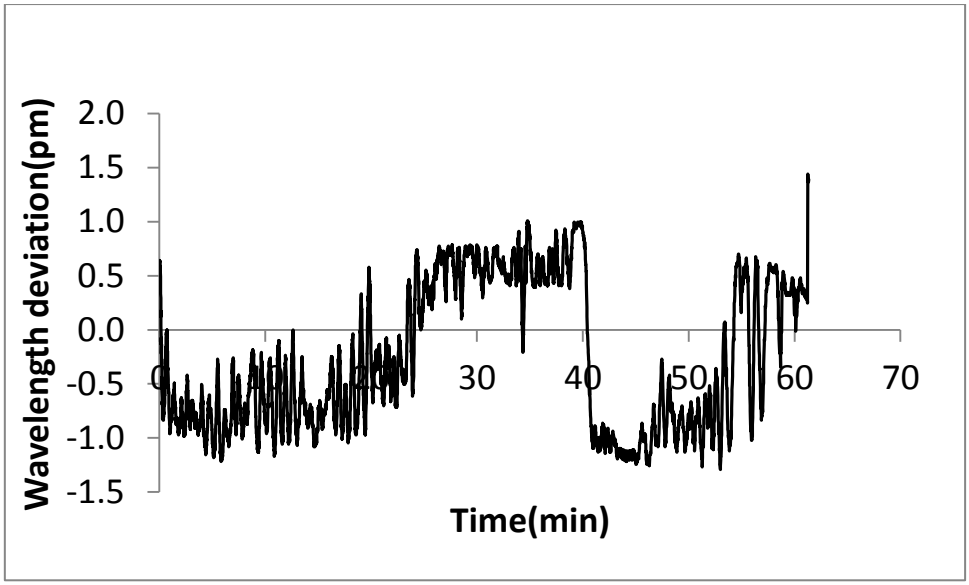

Figure 5.28 Laser diode wavelength stability as a function of time using junction voltage based control

The laser diode remained stable over a period of one hour with a centre wavelength deviation of $\sigma = 0.7$pm. The long term wavelength stability of the laser diode with forward voltage is comparable to that of the thermistor control and forward voltage control methods.

The junction voltage control technique was also tested for wavelength stability with changes in ambient temperature in the range of 15 - 35°C over shorter periods of approximately 5 min.

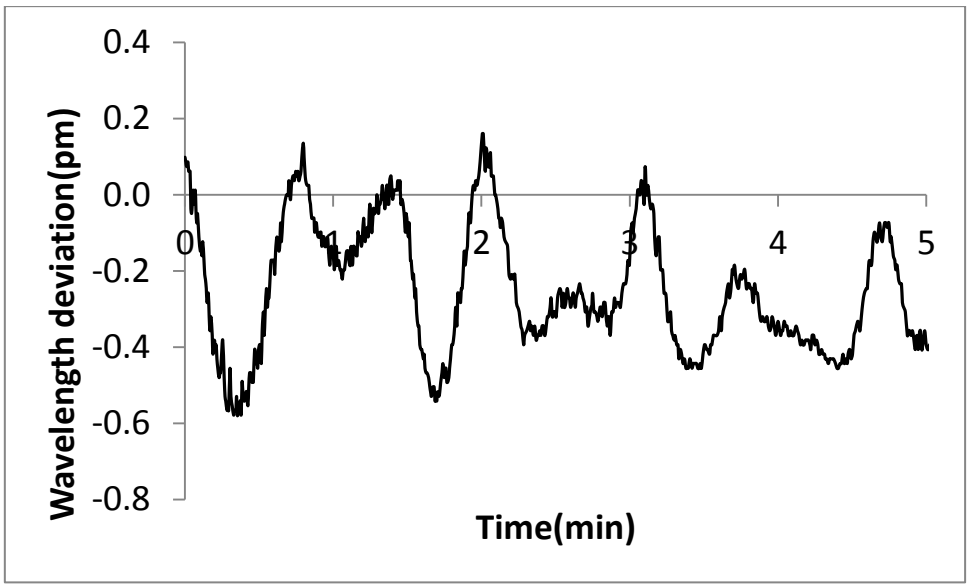

Figure 5.29 Laser diode wave length stability at 15˚C ambient temperature

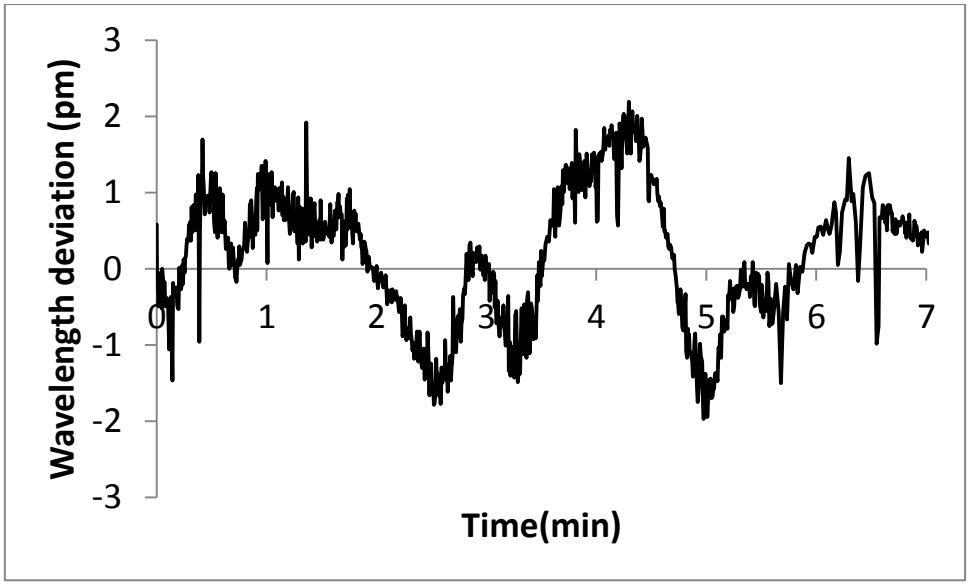

Figure 5.30 The effect of ambient temperature on the laser diode wavelength stability at 35 ˚C

Figures 5.29 and 5.30 shows the effect of ambient temperature on the laser diode wavelength at 15˚C and 30˚C, respectively. In both figures, the laser diode wavelength remained close to the zero crossing point on the x- axis, indicating the laser diode wavelength was near the centre of the methane gas line.

Table 5.6 shows the laser diode wavelength drift with varying ambient temperature. The laser diode wavelength remained stable with an ambient temperature coefficient of less than 0.03pm / °C. The laser diode wavelength stability with ambient temperature using junction voltage is therefore 2 orders of magnitude better than that achieved using conventional thermistor control and using the forward voltage control technique.

Table 5.6 Laser diode wavelength stability with ambient temperature

Ambient Temperature(°C)	Wavelength Deviation (pm)
15	±0.3
20	±0.7
25	±0.8
30	±0.5
35	±0.9

5.4 Discussion and conclusion

Laser diode series resistance can be calculated from the I-V characteristics of the laser diode. The laser diode is operated in DC conditions and the voltage drop across the laser diode terminals is measured with the help of a digital multimeter. By taking the derivative of the laser diode voltage at different operating temperatures, the laser diode resistance of the two DFB lasers (one T08 Can package and the other butterfly packaged) was calculated. Three different techniques were used to calculate to the resistance of these two DFB laser diodes and the results of these techniques were compared. For a T08 Can packaged laser, the standard method, and the Cheung and Cheung method gave approximately similar results whereas the Werner methods gave relatively lower resistance values for this laser. In contrast to the T08 Can package laser, the butterfly packaged showed higher resistance with the standard method, whereas the Werner method, and Cheung and Cheung method gave similar resistance values. The resistance of both laser diodes increased with increasing temperatures using the three different techniques. Both the Cheung and Cheung and the Werner methods show lower increase in the series resistance with temperature compared to the standard method. Based on the calculation results of the series resistance, due to the low error bars, the Cheung and Cheung method was used to calculate the series resistance of the laser diode for use in junction voltage based control.

The laser diode wavelength stability was investigated using three temperature control techniques i.e. the conventional thermistor control, the forward voltage method and the newly developed junction voltage control technique.

In conventional laser diode temperature control, a thermistor placed at a distance from the gain chip is used to sense the temperature of the laser diode chip. The thermistor measures the temperature of its immediate surroundings. However, there is a temperature gradient between the chip and the thermistor resulting in laser diode wavelength drift due to the chip being at a different temperature .It was demonstrated experimentally in the thermistor based temperature control section that with variable ambient temperature the laser diode wavelength decreased with increasing ambient temperature.

The approximately linear relationship between DFB laser diode for voltage and temperature can be used as a temperature sensor and to stabilise the central wavelength of the laser diode. The laser diode forward voltage decreased approximately linearly with increasing operating temperature. It was experimentally demonstrated that the voltage across the laser diode can

be used to stabilise the central wavelength of the laser diode. The performance of the forward voltage control technique was comparable to that of a conventional thermistor control system as tabulated in Table 5.7. However, with variable ambient temperatures the laser diode wavelength drifted due to the temperature dependence of the laser diode series resistance. The laser diode forward voltage decreased with increasing temperature, whereas laser diode resistance increased with increasing temperature. Therefore, when the ambient temperature was increased, the forward voltage decreased, resulting in laser diode wavelength drift towards longer wavelengths.

The laser diode resistance increased with increasing temperature in contrast to a decrease in voltage drop across the laser diode with increasing temperature. Therefore, a new system was developed based on the measurement of the junction voltage of the laser diode to stabilise its wavelength. The laser diode resistance was dynamically measured by modulating the injection current at a DC bias above threshold. The laser diode was modulated at a high frequency (31 kHz) with small amplitude to minimise the additional heat generated due to the modulation current. The 1f demodulated output was scaled and subtracted from the voltage drop measured across the laser diode. The resulting junction voltage was subtracted from a voltage setpoint and the result used as an error signal in a PID loop.

Due to the limited resolution of the spectrum analyser and sampling rate and the fact that the laser diode was modulated, a methane gas line was used to check the wavelength stability of the laser diode. The centre wavelength of the laser diode was checked for long-term stability and under variable ambient temperatures. The laser diode central wavelength remained stable, similar to that of the forward voltage and thermistor in the long term stability testes as shown below in Table 5.7. For wavelength stability with variable ambient temperature, junction voltage control has wavelength stability 2 orders of magnitude better than that of either thermistor or forward voltage control.

Table 5.7 Comparison of laser diode wavelength control stability techniques

Wavelength Control Technique	**Long Term Stability**	**Wavelength Drift with Ambient Temperature**
Thermistor Control	±2.2 pm (±242MHz)	3.8pm/ºC (418MHz/ºC)
Forward voltage Control	±1.32 pm (±145MHz)	4.5 pm/ºC (495MHz/ºC)
Junction Voltage control	±0.7pm (±77MHz)	0.03 pm/ºC (3.3MHz/ºC)

In TDLAS, generally molecular gas absorption lines is used to stabilise the laser diode wavelength as reported in section 2.3.4, where Sudo et al [7] reported a wavelength stability of 500kHz for a DFB laser using an acetylene absorption line. The wavelength stability achieved with this method is higher than the junction voltage control method. However, this wavelength locking method for stabilising laser diode wavelength is tedious and requires an extra reference cell

Tuneable laser diode spectroscopy requires a very stable laser diode wavelength with wavelength stability of better than 10% of the full width half maximum as the gas absorption lines are very narrow, e.g. the methane absorption at 1650.96nm has a linewidth (HWHM) of 50pm for 100% concentration. For an ambient temperature change of 20°C, conventional thermistor control would suffer a wavelength change of 76 pm, greater than the methane gas linewidth at 1650.96nm. Using junction voltage control would bring this down to a more manageable 0.6 pm, which is much smaller than the gas linewidth and similar to the level of wavelength stability over time at a fixed temperature.

This technique has been successfully applied to the TO can – packaged DFB described here. Based on the information here, this technique could be extended to other types of light sources such as VCSEL and UV LED.

5.5 References

[1] T. Ikegami, S. Sudo and Y. Sakai, Frequency stabilization of semiconductor laser diodes, Norwood: Artech House, 1995.

[2] S.Sze, Physics of Semiconductor Devices, New Jersey: Wiley & Sons, 1981.

[3] S. K. Cheung and N. W. Cheung, "Extraction of Schottky diode parameters from forward current voltage characteristics," *Applied Physics Letters,* vol. 49, no. 2, pp. 85 - 87, 1986.

[4] J. J. Werner, "Schottky barrier and pn-junction I/V plots-Small signal evaluation," *Applied Physics A,* vol. 47, pp. 291 - 300, 1988.

[5] K. Uehara and K. Katakura, "New method of frequency stabilisation of semiconductor lasers," *Japanese Journal of Applied Physics*, vol. 27, no. 2, pp. 244 - 246, 1988.

[6] B.W. Bequette, Process control modelling, design and simulation, Prentice Hall International Series, 2003.

[7] S. Sudo, Y. Sakai, H. Yasaka and T. Ikegami "Frequency stabilized DFB laser module using 1.53159μm absorption line of C_2H_2," *IEE Photonics technology Letters ,* vol. 1,no. 10, pp. 281 - 284, 1989.

6 Wavelength control with tuneable diode laser spectroscopy

Tuneable laser diode absorption spectroscopy using wavelength modulation (wavelength modulation spectroscopy) is described in this chapter. The laser diode wavelength stability in wavelength modulation spectroscopy (WMS) is critical in high resolution gas absorption spectroscopy. To achieve wavelength stability several frequency references based on atomic lines, optogalvanic effects, gas molecular absorption lines and interferometers have been implemented as in previous work as reviewed in chapter 2.

In this chapter a novel technique will be described based on measurement of laser diode junction voltage, to stabilise the emission wavelength of the laser diode in WMS, by accurately stabilising the operating temperature of the laser diode. The performance of this junction voltage controlled system is evaluated at different gas concentrations and variable ambient temperatures and is compared with a conventional thermistor controlled system.

In the beginning of this chapter, WMS will be briefly described. Then the basic setup for TDLS using WMS technique will be used to characterise the initial bench top system for WMS.

6.1 Wavelength modulation spectroscopy

Wavelength modulation spectroscopy is a popular gas absorption detection technique with good sensitivity and selectivity. In WMS, the laser diode emission wavelength is modulated with sinusoidal signal and the modulated wavelength is scanned across the gas abortion line using a slowly moving ramp. For optimum WMS, the modulation index should be 2.2 times the full width half maxim (FWHM) of the probed gas absorption line [1]. A detailed description of WMS was given in chapter 2.

The sensitivity of WMS can degrade with temperature and time in the absence of a wavelength locking reference due to the drift in the laser diode emission wavelength.

The laser diode emission wavelength is conventionally locked to a gas absorption line, where the control loop feedback is used to correct the laser wavelength. However, this scheme is extremely sensitive to alignment, is difficult to set up and is bulky.

The wavelength control scheme proposed in chapter 5 has the potential to overcome the challenges of the conventional control locking scheme used in WMS as mentioned above.

The challenges faced in the integration of the wavelength control scheme based on junction voltage were

- The use of a slowly moving current ramp for scanning the modulated laser diode wavelength, which modulated the junction voltage in addition to the junction voltage variation due to the modulating sinusoidal signal
- A synchronisation mismatch between analogue modules such as the lock-in amplifier and filters with the software based module such as the PID loop and averaging filters.

6.2 Equipment for WMS based setup for initial bench top system with thermistor control

The WMS based system comprised the following main elements:

1. Light Source and related drive electronics
    - A 1651nm distributed feedback (DFB) laser diode (Laser Components HHI) miniature thermo electric controller (MTE) module TO8 can packaged mounted on a custom built mount.
    - The injection current to the laser diode was provided using a current driver (Thorlab LDC 200) and the operating temperature was controlled using temperature controller (Thorlabs TED 200).
2. The injection current to the laser diode was modulated at a frequency of 31kHz with a sinusoidal output form SR850 (Stanford) lock-in amplifier. A custom built proportional-integral-differential (PID) circuit was used to add a ramp to the modulation signal to scan the gas lines. The ramp signal at a frequency of 2Hz was provided by a signal generator (Stanford DS345).
3. A gas cell containing methane gas at different concentrations with a path length of 10cm was used to evaluate the bench top WMS system. This gas cell was equipped with conventional wedged (2 degrees beam deviation angle) and anti-reflection coated windows (Thorlabs “c” coating <0.5% at 1650nm) in order to reduce the interference fringes.
4. The detection system comprised an amplified detector (Thorlabs PDA400) and Stanford lock-in amplifier (Stanford SR850) for 1st, 2nd, and 3rd harmonic detection.

5. Data acquisition system was carried out with two data acquisition card (National Instruments PCI 6251 and usb 6281). The data was analysed in the LabVIEW 2013 environment.

6.2.1 Description of the operation of WMS based bench top system

Light from the DFB laser diode was coupled into single mode fibre (SMF28) using three anti reflection (AR) coated aspheric lenses. The light output from the laser diode was elliptical and highly divergent, so an aspheric lens with a short focal length of ≈3mm was used to collect light from the laser diode with a more uniform Gaussian spot, this lens was kept as close as possible to the laser to increase coupling efficiency into the lens. Then a 2nd aspheric lens with focal length of ≈11mm was used to collimate the light from the 1st aspheric lens near the laser diode. The third aspheric lens with ≈18mm focal length was used to couple light into the single mode fibre and then to the gas cell using a fibre coupling system with translation stages as shown in the line diagram and in the picture below in Figure 6.1 and Figure 6.2 respectively.

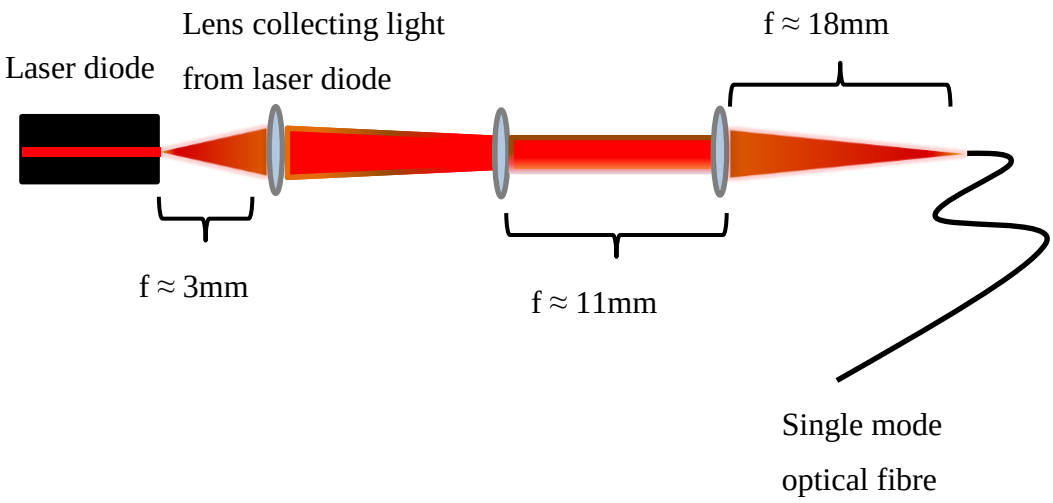

Figure 6.1 Line diagram for the setup of collimating and coupling light from the laser diode into a single mode fibre

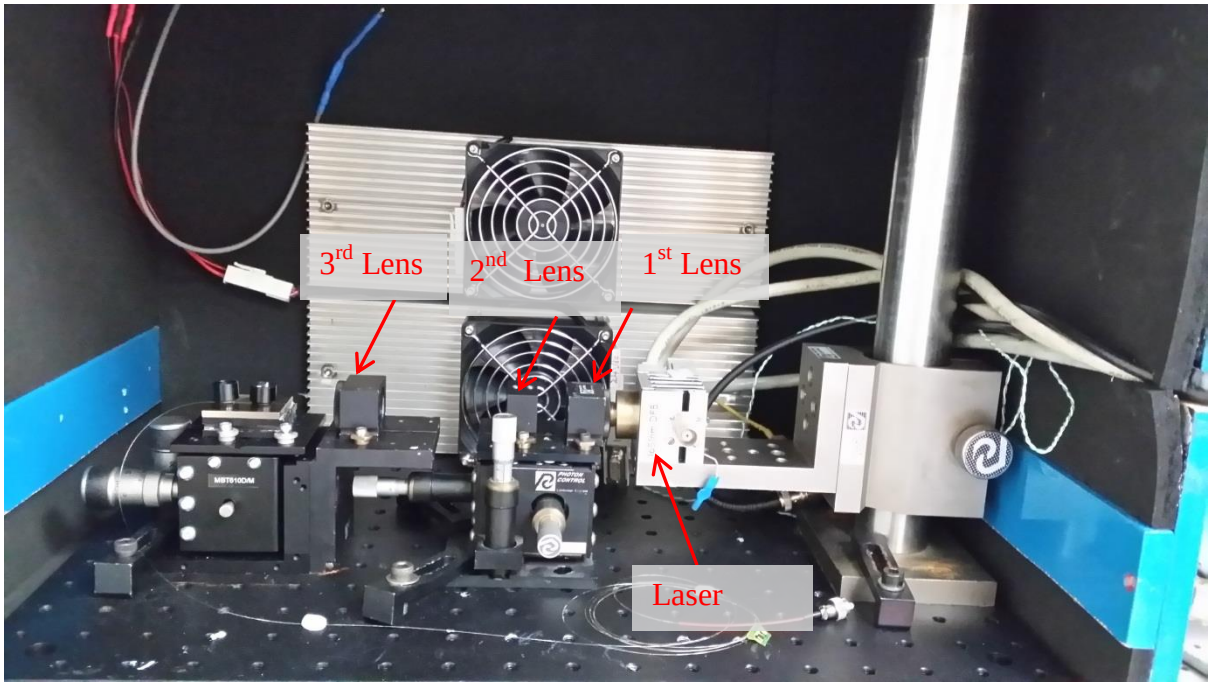

Figure 6.2 Description of the laser diode light collimation and coupling of light into single mode optical fibre

The laser diode was modulated at f = 31 kHz and the modulated light was coupled into a gas cell. The output from the photo detector at the other end of the gas cell was fed into a lock-in amplifier with phase sensitive detection at the 2nd harmonic (2f) of the modulating signal.

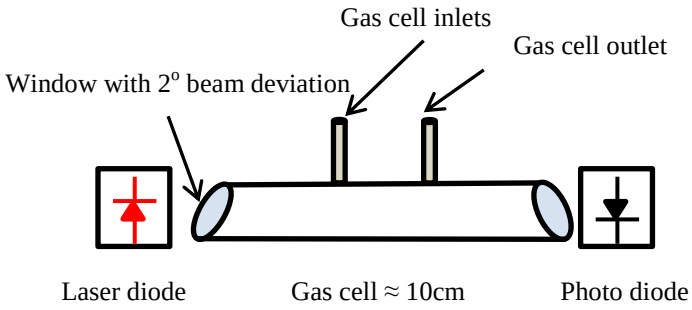

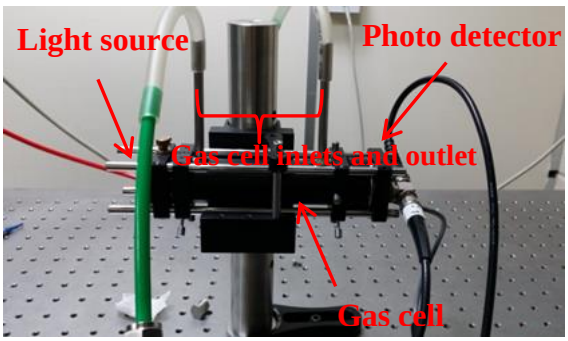

Figure 6.3 Gas cell and its implementation in WMS

Gas to the gas cell was supplied from certified gas cylinders supplied by BOC, one with 100% synthetic air and the other with 2.5% methane concentration. The flow of the gas to the gas cell was controlled with a bank of mass flow controller (Teldyne Hasting HFC-302 and THPS-400 four channel power supplies), as shown in Figure 6.4

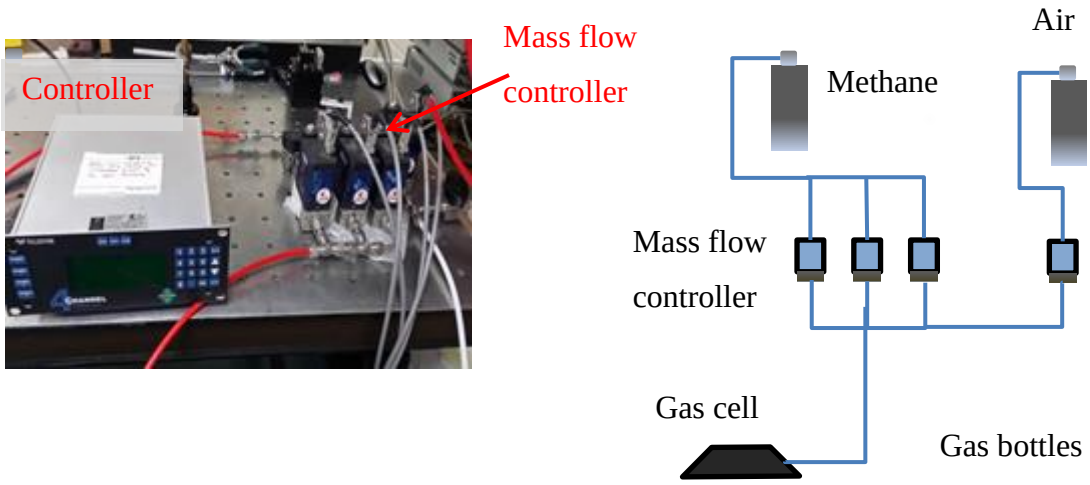

Figure 6.4 Line diagram and picture of the gas flow control system setup

Figure 6.5 represents the experimental setup for evaluation of the initial WMS bench top system.

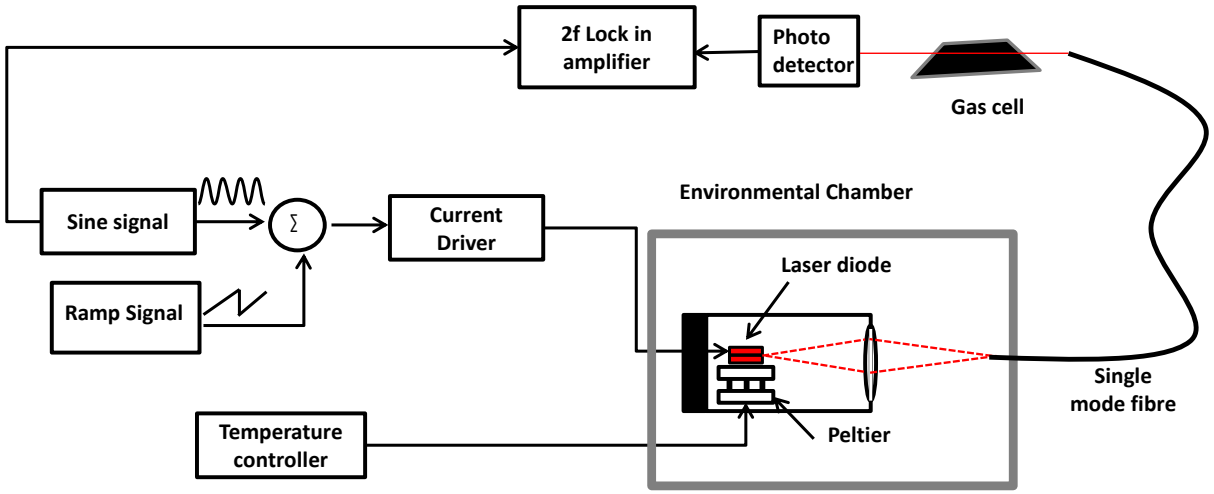

Figure 6.5 Schematic of the experimental setup for wavelength modulation spectroscopy using conventional laser diode control

6.3 Characterisation of the WMS bench top system

The initial WMS bench top system was optimised in two stages. The first stage was to determine the optimum current modulation amplitude for the laser diode and then in the 2nd stage the efficiency of the wavelength modulation coefficient was measured. The final stage of this initial bench top system will be to evaluate the performance of this setup by measuring different concentrations of methane gas.

6.3.1 Optimum current modulation coefficient for WMS bench top system

The bench top WMS based system was used to optimise the current modulation amplitude. The amplitude of the 2f signal is dependent on the modulation index m[1] as reviewed in section 2.4.2

$$m = \frac{i_{mod}}{\delta v} \tag{6.1}$$

Where i_{mod} is the modulation amplitude and δv is the half width at half maximum of the absorption line) [1]**.** For detailed theory on the modulation index refer to chapter 2 of this thesis. The emission wavelength of the laser was varied by adding a sinusoidal signal to the DC injection current of the laser diode. Figure 6.6 shows the 2f signal plotted at different modulation amplitude.

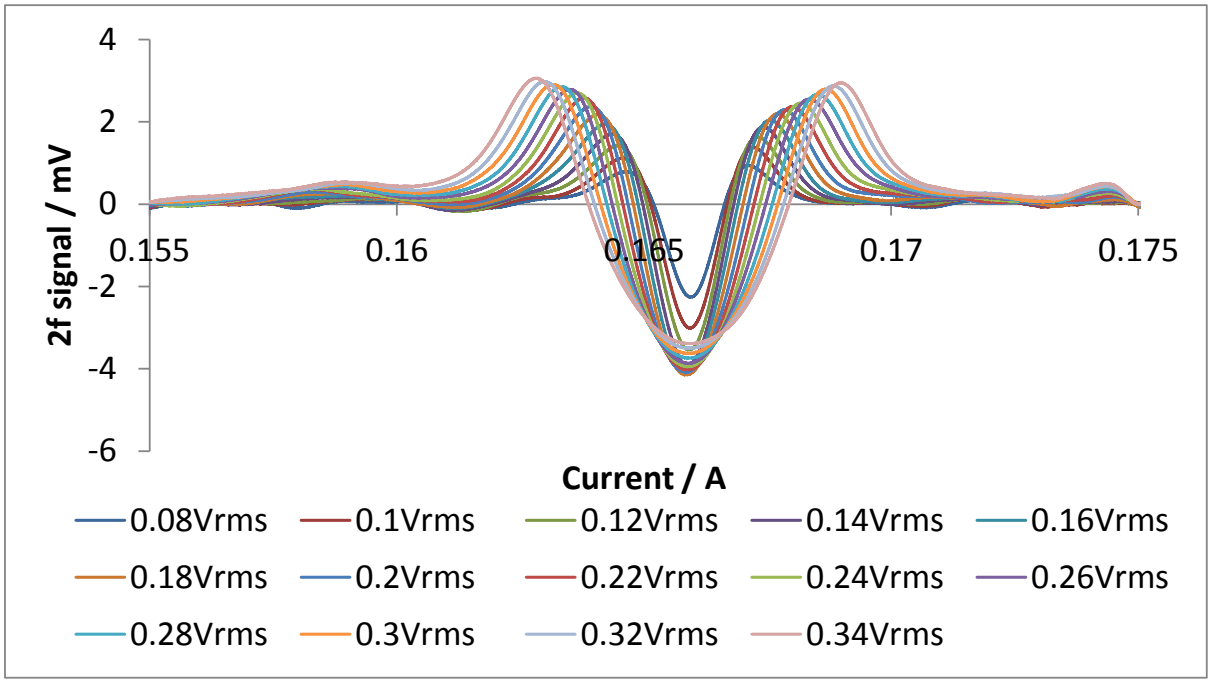

Figure 6.6 2f signal as function current amplitude modulation

By analysing Figure 6.6, it can be observed that the peak of the 2f signal increased with increasing modulation amplitude and the width of the 2f signal remained narrow. However, for modulation amplitudes over 0.180Vrms, the 2f broadened and the peak of the signal decreased. This was the modulation amplitude at which the modulation index was bigger than the half width of the absorption profile and beyond this point, the 2f signal was broad with a low signal to noise ratio. This optimum modulation will scan the laser diode emission wavelength 2.2 times the FWHM of the gas absorption line. The following Tables 6.1and 6.2 show the settings for the ramp signal generator and the lock-in amplifier used in the bench top WMS setup.

Table 6.1 Ramp settings for WMS

Amplitude	Frequency
0.8V	2Hz

Table 6.2 Lock-in amplifier settings for WMS

Time constant(τ)	sensitivity	Sampling rate
3ms	20mV	512Hz

The lock-in amplifier was used as a signal generator to modulate the laser diode and its internal reference was used to achieve the 1f, 2f and 3f signals for the detected light after passing through the gas cell.

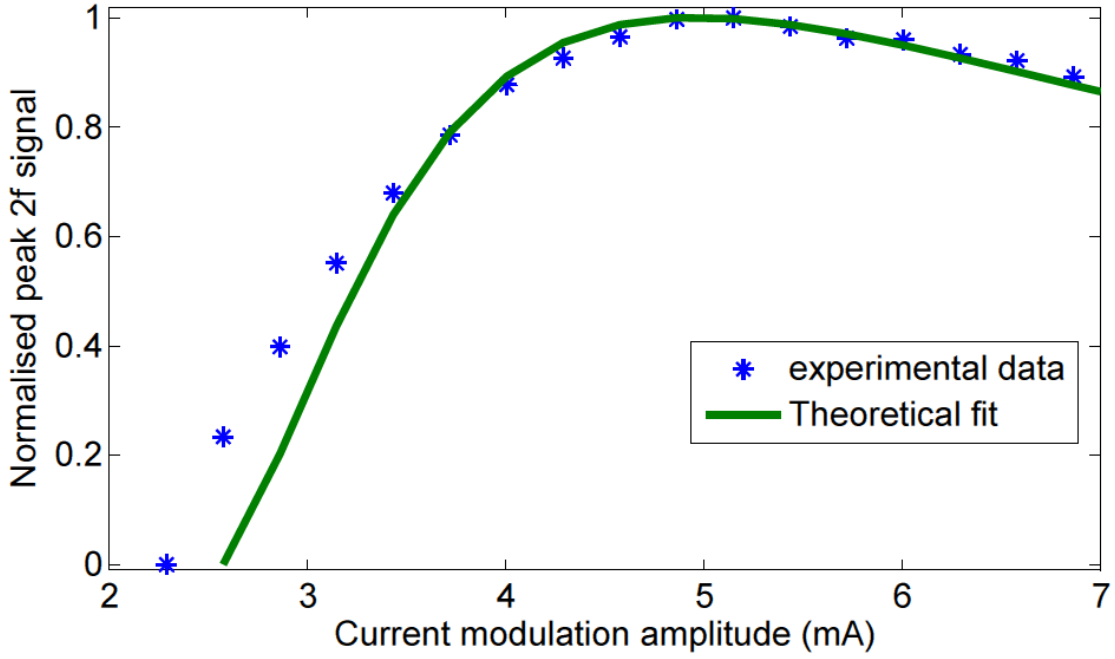

Figure 6.7 2f signal plotted as a function of current amplitude modulation amplitude

Figure 6.7 shows the plot of the peak of each 2f signal against the current modulation amplitude. The curve initially increased linearly with increasing modulation current amplitude and reached its maximum value with current amplitude modulation of 5.1mA. When the current amplitude modulation was increased further, the amplitude of the peak signal reduced. This phenomenon can be compared to the broadening of 2f signal with the reduction of peak amplitude as shown in Figure 6.6. In Figure 6.5, the experimental data was compared with a theoretical data fit to equation 2.34. The experimental curve was following the same pattern as the theoretical curve with the experimental points matching theoretical data points.

6.3.2 Wavelength modulation tuning coefficient efficiency

The laser diode wavelength modulation tuning coefficient is described by the relation $\Delta\lambda/\Delta i$ (pm/mA), where Δi is the current modulation amplitude and $\Delta\lambda$ is the modulated wavelength.

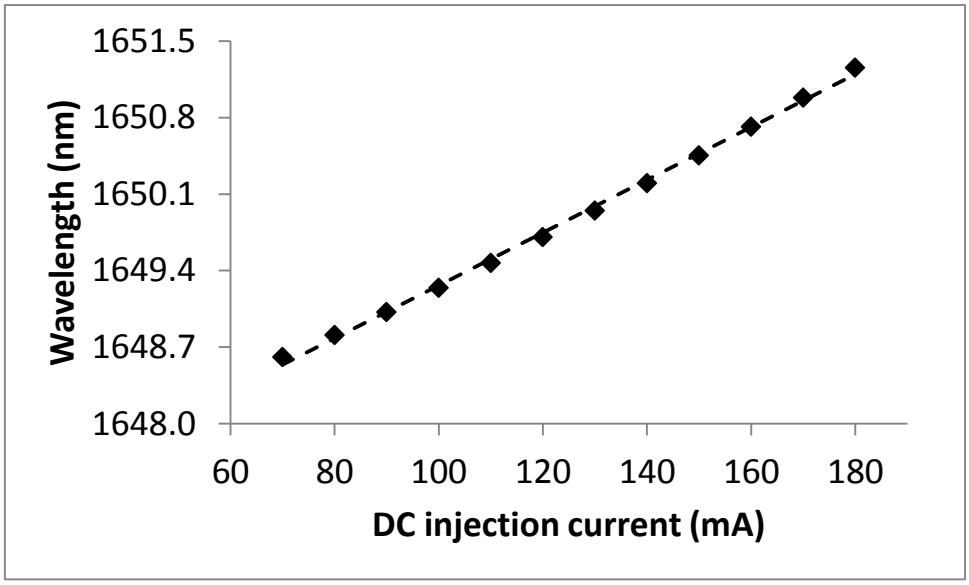

Figure 6.8 Laser diode emission wavelength as a function of injection current at operating thermistor temperature of 25℃

For the laser diode used in this experiment, the $\Delta\lambda/\Delta I$ was 24pm / mA under DC conditions, which was determined experimentally from the slope of laser diode wavelength as a function of DC current as shown in Figure 6.8.

The wavelength tuning coefficient efficiency for this WMS experiment was determined experimentally using an experimental procedure developed by S. Schilt *et al* [2] as described in chapter 2 section 2.4.2. In this experimental procedure, the peak of the 2f signal as a function of current modulation amplitude determines the efficiency of the wavelength modulation.

By plotting the peak 2f signal $s_{2,\,max}$ against the modulation index using a known FWHM of an air broadened methane gas, the optimum modulation index for this bench top system was calculated.

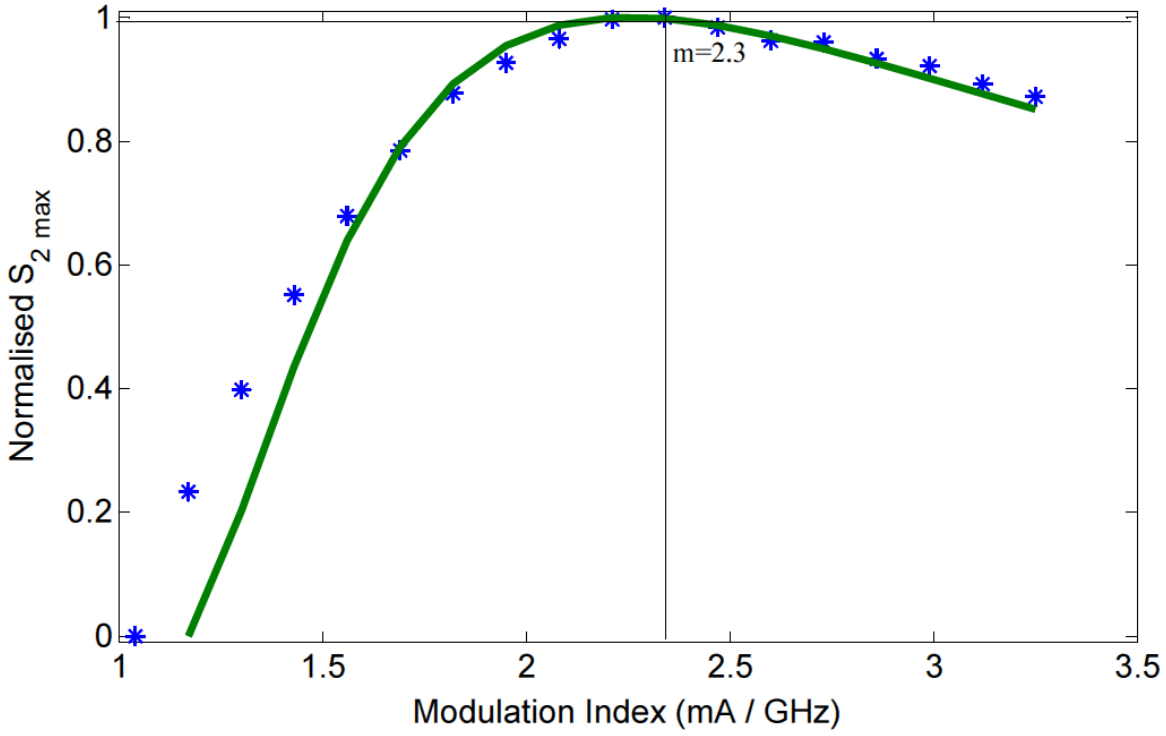

Figure 6.9 Peak 2f signal plotted as function of the modulation index

Figure 6.9 shows a plot of the modulation index and the peak 2f signal $s_{2,\,max}$ .This graph was plotted by modifying the graph in Figure 6.7, where, instead of current modulation amplitude, the 2f signal was plotted against the modulation index. The modulation index for this bench top system was calculated using the known air broadened methane HWHM of 2.2GH [2][3].

The optimum modulation index for this bench top system was calculated to be 2.3 which is close to the theoretical optimum modulation index of 2.2.Therefore the optimum current amplitude modulation was 0.180 vrms (5.15mA).

6.3.3 Gas detection performance

The performance of the initial bench top system which used the thermistor based temperature control, was evaluated by measuring different concentrations of methane gas. Air and methane gas were supplied from BOC cylinders with 100% synthetic air and 2.5% methane respectively. The mixture of air and methane were supplied to the 10cm gas cell using a mass flow controller as described in section 6.2.1.

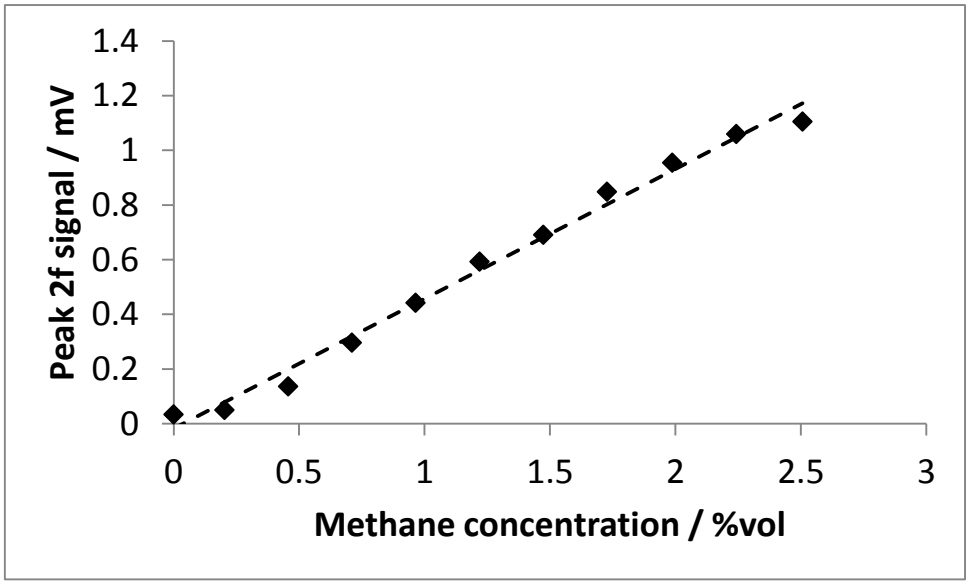

Figure 6.10 2f signal as a function of different methane gas concentration

Figure 6.10 shows the plot of the detected 2f signal at different methane concentrations. The relationship between the measured signal and the concentration of the gas supplied was approximately linear with gas detection in the range of 0.2% to 2.5%.

6.4 Effect of ambient temperature on thermistor controlled based WMS bench top system

The laser diode emission wavelength is highly sensitive to temperature. Therefore a precise control of the temperature is required to stabilise the laser diode wavelength [4]. The temperature of the laser diode is usually stabilised with a thermistor based Peltier with stability of 0.1 ºC. The effect of ambient temperature on the wavelength stability has been previously reported in chapter 5. In this section, the effects of ambient temperature on the performance of the WMS bench top system were investigated. The laser diode was placed in the custom built environmental chamber and the ambient temperature was varied.

The injection current and the thermistor temperature of the laser diode were kept constant. The setup for this experiment was similar to that shown in Figure 6.5. The operating temperature was 26˚C and the DC injection current was 165.28mA.

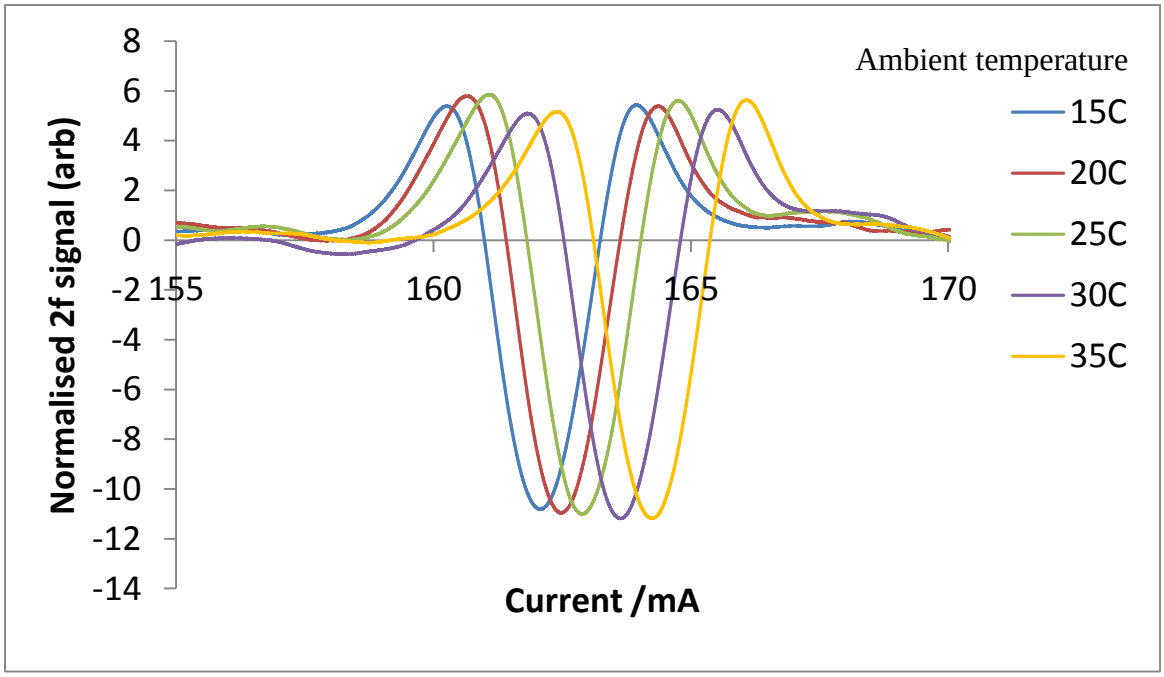

Figure 6.11 The effect of ambient temperature of the 2f signal detection of the WMS bench top system

The ambient temperature was varied in step of 5˚C in the range of 15-35˚C. Figure 6.11 is the plot of the detected 2f signal using WMS bench top system at various ambient temperatures. The 2f signal in Figure 6.11 was normalised with the DC signal at the detector. The detector had a DC offset which was subtracted from the DC signal. By analysing this plot, it can be observed that, with increasing ambient temperature, the detected peak 2f signal shifted toward higher current. The peak of the 2f signal was detected at a ramp current 162.1mA at 15ºC, and as the temperature was increased, the 2f signal was detected at a ramp current 164.3mA at 35ºC. The laser diode drifted 2.2 mA with a drift of σ = 0.11mA / ºC. The laser tuning coefficient for this laser was 24pm / mA, therefore the emission wavelength drift was 53pm. This is larger than the FWHM of the methane line, which is 50pm at 1atm pressure according to the Hitran database [3]. This drift in laser diode wavelength with ambient temperature will potentially limit the detection accuracy for the laser diode using thermistor based temperature controller.

The shift of the peak detected 2f signal with ambient temperature could be attributed to the shift of the emission wavelength to shorter wavelengths due to the overcooling by the thermistor controlled peltier. The graph in Figure 6.11, suggested a thermal gradient between the chip, peltier, thermistor and the ambient temperature.

In chapter 5, the laser diode wavelength drift was calculated to be 3.8pm ±0.6/ ºC, whereas in the WMS, the wavelength drift was calculated to be 2.64 pm / ºC. The higher wavelength drift in chapter 5 could be attributed to interference fringes compared to the results in Figure 6.5.

6.5 WMS based on junction voltage control

This section chapter deals with WMS based gas detection system using the laser diode wavelength control technique as described in chapter 5. The laser diode wavelength control was achieved by using junction voltage of the laser diode as a measure of laser diode chip temperature. The aim of this method was to overcome the wavelength drift of the laser diode with temperature.

The description of the WMS system utilising junction voltage based wavelength control system starts with equipment and description of the system. Then, the performance of this system is evaluated system by detecting different concentration of methane.

This section of the chapter is completed with analysis of the effect of ambient temperature WMS using junction voltage based wavelength control technique.

6.5.1 Equipment

The following are the equipment used in this experiment.

1. Light Source and related drive electronics
    - The light source is similar to the one described in section 6.2.
    - The laser current driver is the same as the one used in previous section. The temperature of the laser diode was controlled with a current source to the Peltier using current driver (Thorlab ITC510).
2. Gas cell was the same as section 6.2
3. The injection current to the laser diode was modulated at a frequency of 31 kHz with a sinusoidal output from a lock-in amplifier (Stanford SR850). A custom built proportional-integral-differential (PID) circuit was used to add the ramp to the modulation signal to scan the gas lines in the gas cell. Another lock-in amplifier (SR850) was used to measure the dynamic series resistance of the laser diode.
4. The detection System was the same as that was used in section 6.2.
5. Data Acquisition system was same that used in 6.2.

6. A low pass filter (Kemo dual variable filter) with attenuation of 48dB/octave and a high pass filter (Stanford SR560) with attenuation of 12dB/octave were used for low frequency and high frequency changes to the forward voltage
7. The ambient temperature of the laser diode was varied with the custom built environmental chamber.

6.5.2 Description and experimental setup of the system

Figure 6.12 shows WMS utilising junction voltage based wavelength control technique. The laser diode was modulated with a 31 kHz sinusoidal signal with amplitude of 10.2mA peak to peak. The modulated signal was scanned across the methane gas line with a ramp signal of 2Hz frequency and amplitude of 16mA peak to peak. The forward voltage drop V_f across the laser anode and cathode terminals was measured and acquired with a data acquisition card in LabVIEW environment. As V_f contained both the ramp signal and sinusoidal signals, V_f was filtered with a high pass filter, where the filtered signal was sent to a lock-in amplifier for dynamic series resistance measurement. V_f signal was also low pass filtered to provide DC forward voltage V_f by averaging out the ramp signal and sinusoidal modulation.

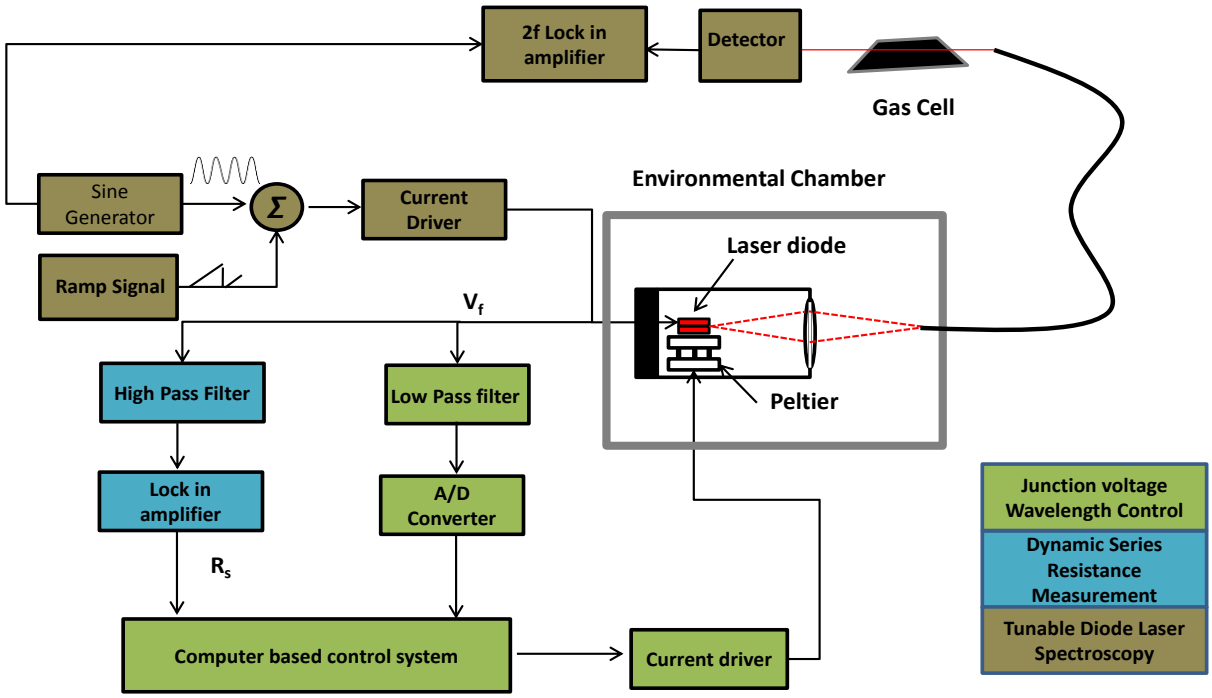

Figure 6.12 TDLS using junction voltage based wavelength control technique

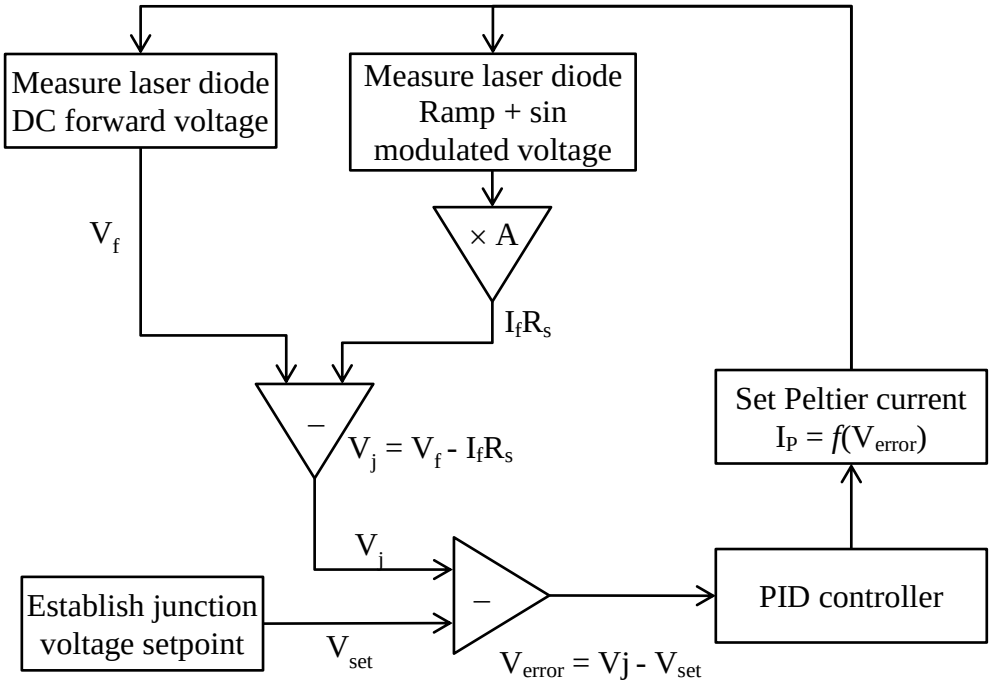

Figure 6.13 Laser diode wavelength stability flow chart using junction voltage based control

Figure 6.13 shows the flow chart for the junction voltage based control system. The laser diode DC injection current was 165.28mA and the forward voltage drop measured at 26 ºC was used as a set point for wavelength control at variable ambient temperature Table 6.3 shows the setting of the low pass and high pass filters for removing the ramp signal from the measured forward voltage V_f.

Table 6.3 Filter setting for WMS using junction voltage based wavelength control system

Filter type	Cut off frequency(3dB point) / Hz
Low pass filter (kemo)	0.1Hz
High pass filter (SR560)	10kHz

Table 6.4 shows settings for the two lock-in amplifier used in the WMS setup, where lock-in amplifier 1 was used for detecting the 2f signal of the detected laser light after passing through a gas cell. On the other hand, Lock-in amplifier 2 was used to calculate the dynamic series resistance of the laser diode.

Table 6.4 Lock-in amplifier settings for WMS using junction voltage based wavelength control system

Type	Application	Time constant	Sampling rate
Lock-in amplifier 1	2f	3ms	512Hz
Lock-in amplifier 2	Dynamic series resistance measurement	1s	512Hz

Table 6.5 contains the LabVIEW based PID control settings. The LabVIEW based code for implementing the junction voltage based wavelength control system could be found in Appendix B.

Table 6.5 PID settings for WMS using junction voltage based wavelength control system

P	I	D
8	0.48s	0 s

Initial PID values were determined using Cohen-Coon method [5] and the optimum values were determined by trial and error.

The performance of this junction voltage based wavelength control system in WMS was investigated by measuring the 2f signal for different methane concentrations and different ambient temperatures.

The next section will deal with the measurement of different concentration of methane gas, followed by analysing the performance of this system at several ambient temperatures while tested for methane gas detection.

6.5.3 Gas concentration measurement

The performance of this WMS system using junction voltage based wavelength control technique was evaluated for detecting different concentrations of methane gas. Mixtures of 100% synthetic air and 2.5% concentration of methane gas were supplied to the gas cell using a mass flow controller as described in section 6.2.1. The optical path length of the gas cell was 10cm as previously described in section 6.5.1.

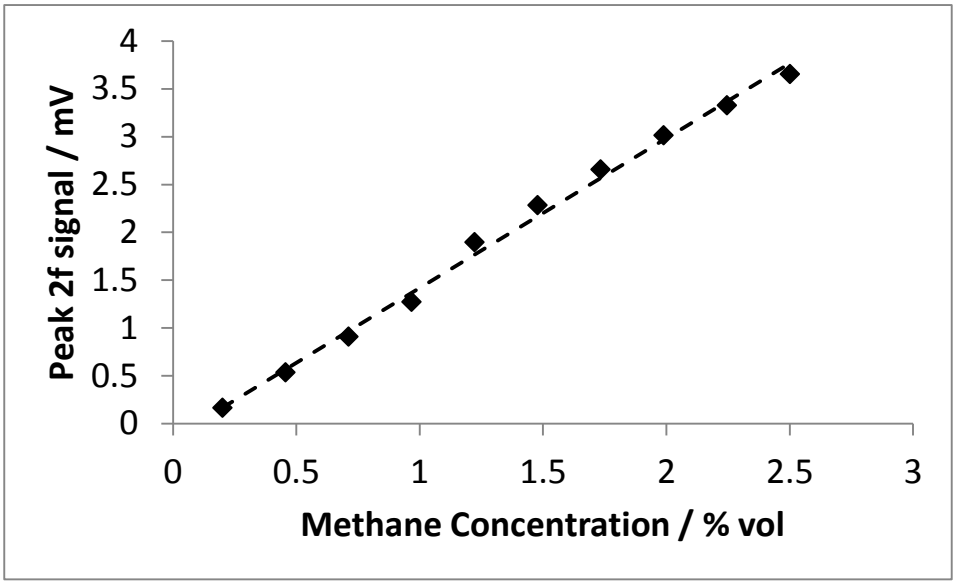

Figure 6.14 2f signal as a function of different methane gas concentration

The peak of the 2f detected signal had a linear relationship with methane concentration as expected. This ability to detect different methane gas concentration while using junction voltage based control suggested that this system could be implemented in WMS.

6.5.4 **Effect of ambient temperature**

The performance of the junction voltage based wavelength control system was investigated by changing the ambient temperature of the laser diode integrated in a TDLAS based WMS setup as shown in Figure 6.13. The temperature of the environmental chamber was varied in steps of 5 ºC, while stabilising the wavelength of the laser diode using junction voltage. The 2f signal of the lock-in amplifier was recorded for constant concentration of methane as shown in Figure 6.15.

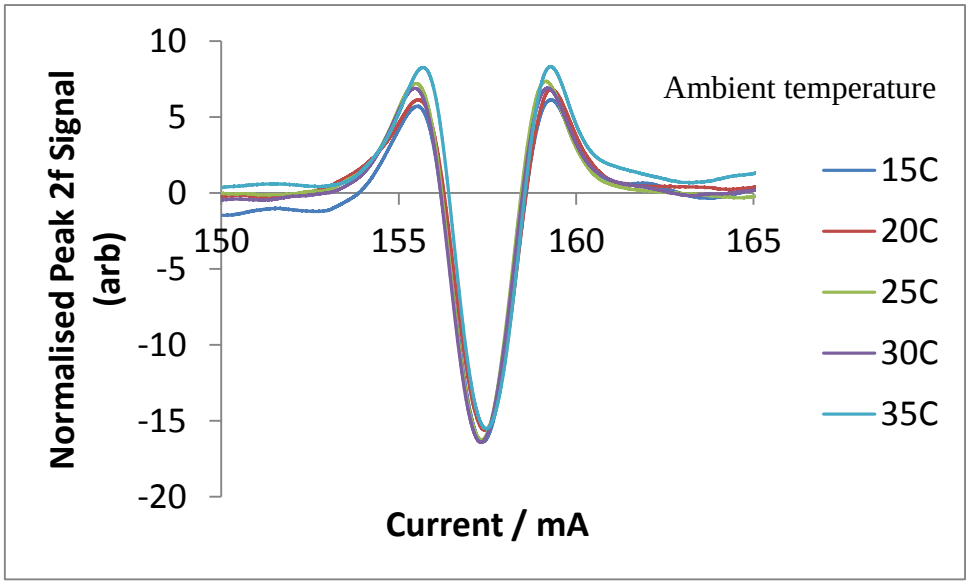

Figure 6.15 Effect of ambient temperature on the 2f detected signal

The peak of the 2f signal for all the temperatures was recorded at injection current of around 157.4 mA with 0.01 mA / ºC, which corresponded to a change in a wavelength with temperature 0.24 pm / ºC . The performance of the junction voltage based wavelength control system in stabilising the wavelength of the laser diode was 10 times better than the conventional thermistor control.

The performance of the junction voltage based control performed well, when this technique was not integrated in WMS resulting in wavelength drift of just 0.03pm / ºC as described in chapter 5 section 5.3.3. However, the laser diode wavelength is still far more stable when it was integrated in WMS than with the conventional temperature controller. The control system was not investigated for detection limit, however the control system should not adversely affect the detection limit

6.6 Summary

WMS bench top system was set up and optimised by choosing suitable amplitude modulation. The wavelength of the laser diode was modulated by modulating the amplitudes of the injection current to the laser. The detected 2f signals were plotted at different modulation amplitude sand the behaviour of 2f signal was analysed. The experimental data was compared with the theoretical predictions. The experimental data followed the same pattern as the theoretical curve in the current range 3.5-7mA. The optimum wavelength modulation tuning coefficient was also calculated by plotting the maximum 2f detected signal

against the modulation index. The calculated modulation index was close to that of the theoretically calculated modulation index with an error of $\Delta m \approx 0.1$ that is within the experimental error

The bench top WMS system was evaluated for detecting different concentration of methane gas. The plot between the methane concentrations and the detected 2f signal was linear in the region 0- 2.5% vol in air.

The effect of ambient temperature on the detection capability of the bench top WMS system was also investigated, where the temperature of the laser diode was controlled by the thermistor based Peltier. The 2f detected signal was recorded at constant injection current and operating temperature, while the ambient temperature was varied. The detected peak 2f signal was recorded at different DC currents, showing that the emission wavelength of the laser diode drifted with the ambient temperature. A drift of 53 pm was recoded over the ambient temperature range 15-35ºC. This drift of the laser diode emission wavelength with variable temperature was larger than the line width of the methane gas absorption molecule, which can potentially limit the detection accuracy for the laser diode used in TDLS.

To overcome the issue of wavelength drift in WMS due to the ambient temperature, a new wavelength control method was introduced. This wavelength control used the junction voltage for measuring accurately the temperature of the gain chip, and then stabilising the wavelength of the laser diode. The laser diode series resistance was measured dynamically to compensate for the change in the laser diode resistance with temperature.

Firstly, the suitability of the junction voltage based wavelength control technique in WMS was investigated by detecting different concentrations of methane gas. The relationship between the different methane concentrations and the detected 2f signal was linear within the range 0-2.5% vol in air.

Then the effect of ambient temperature on the laser diode wavelength stability in WMS system using the wavelength control technique was investigated. The laser diode ambient temperature was varied by varying the environmental chamber temperature in the range 15-35 ºC. The wavelength of the laser diode remained stable with the peak 2f signal detected at the same injection current with a drift of 0.01 mA / ºC, which corresponded to 0.24pm / ºC. The performance of the junction voltage based control system in stabilising the laser diode wavelength was 10 times better than the thermistor conrrol

Based on the performance of the junction voltage based control technique, it can be concluded that this wavelength control technique can be integrated in WMS. In conventional wavelength control, the zero crossing of a gas line 3f signal is used to reduce the drift of the laser diode wavelength in WMS. This method is complicated and requires additional optics. The junction based voltage control technique eliminates the need for reference gas cell. Therefore, this wavelength stability is simple and easy to implement, simplifying the wavelength control in WMS.

6.7 References

[1] J. Reid and D. Labrie, "Second - harmonic detection with tunable diode lasers - comparison of experiment and theory," Applied Physics B, vol. 26, pp. 203 - 210, 1981.

[2] S. Schilt and L. Thevenaz, "Experimental based on wavelength - modulation spectroscopy for the characterization of semiconductor lasers under direct modulation," Applied Optics, vol. 43, no. 22, pp. 4453 - 4456 , 2004.

[3] L. Rothman, R. Gamache, R. Tipping, C. Rinsland, M. Smith, D. Benner, V. Devi, J. Flaud, C. C. Peyret, A. Perrin, A. Goldman, S. Massie, L. Brown and R. Toth, "The HITRAN molecular database: Editions of 1991 and 1992," Journal of Quantitative Spectroscopy and Radiative Transfer, vol. 48, no. 5 - 6, pp. 469 - 507, 1992.

[4] L. Hoolberg, R. Fox, S.Waltman and H. Robinson, Precision spectroscopy, diode lasers, and optical frequency measurement, vol. NIST Technical Note 1504, Diane Publishing CO, 1998.

[5] B.W. Bequette, Process control modelling, design and simulation, Prentice Hall International Series, 2003.

7. Conclusion and Future Work

A laser diode's emission wavelength is strongly dependent on the diodes operating temperature. The operating temperature varies the refractive index and the band gap energy of the gain medium. The change in wavelength due to band gap change is larger than the refractive index change. As the temperature is varied, the resultant change in lasing wavelength is small, however due to the large temperature coefficient of the gain peak wavelength, the lasing mode of the laser jumps from one mode to another mode (i.e. a mode hop). In DFB lasers, the grating selects the lasing frequency; therefore mode hopping in the laser is greatly reduced over wide temperature in contrast to Fabry-Perot laser.

A laser diode can be temperature stabilised with the help of a Peltier element. A thermistor sensor is placed at a distance to sense the temperature of the laser chip. However, the location of the thermistor and the thermal design of the laser package can result in erroneous measurement of the temperature of the chip. The laser diode emission wavelength drifts with the change in ambient temperature, for example, the laser used in this thesis had a drift of 3.8pm/ ºC as discussed in section 5.3.1. The linewidth of the gas absorption line at 1atm pressure and 22 ºC (10cm long path length) is ±36pm. Therefore, a more temperature stable laser is required for TDLAS.

The aim of this thesis was to investigate the performance of a wavelength stabilization system for use in tuneable diode laser absorption spectroscopy (TDLAS). The temperature of a DFB laser was stabilised with a thermistor based Peltier cooler under normal operating temperature and variable ambient temperature. The wavelength stability with ambient temperature was then examined to see whether the drift in wavelength due to the change in ambient temperature will affect the detection capability of TDLAS. It was shown in section 6.4 that the lasing wavelength drifted by ≈ 53 pm over the ambient temperature range 15-35 ºC, which is more than the width of the methane absorption line.

It was proposed in this project, that the laser diode forward voltage could be used to measure the temperature of the laser chip and then to stabilise the laser diode emission wavelength.

In this thesis, an alternative method of measuring the temperature of the junction diode was analysed and investigated. This method has already been used for measuring the junction temperature of light emitting diodes and quantum dot lasers. In this method, the junction

temperature of the distributed feedback laser (DFB) diode was measured, by measuring its pulsed forward voltage as a function of operating temperature. The pulsed injection current had pulse width of 1μs and duty cycle of 0.1- 0.01 % (assuming negligible heat was generated during the pulse current). This method was also extended for measuring the junction temperature of a vertical cavity surface emitting laser, which according to the author's knowledge has not been reported in literature.

Two different pulsed current sources were investigated to measure the junction temperature of the laser diodes from their forward voltage. A voltage - controlled current source provided a variable injection current. The results showed that the pulse voltage measured across the laser diode was deformed and could not be used for measuring the junction temperature. It was noted by the author that in many reported studies, a voltage controlled current source was commonly used to pulse the laser diode for measuring the junction temperature of a diode. This could lead to potentially erroneous results in measuring the junction temperature of the diodes. Instead, a current controlled current source was built to bias the laser and then measure the voltage drop across the laser diode for junction temperature measurement.

A linear relationship was established between the laser diode forward voltage and the operating temperature under the pulse condition. This relationship was used to compare the measured temperature using the forward voltage method and the set operating temperature using a thermistor controlled Peltier.

The effect of ambient temperature changes was investigated by varying the ambient temperature of the laser diode while keeping its pulsed injection current and thermistor Peltier temperature constant. It was confirmed in section 4.6.1that the thermistor did not sense the actual temperature of the laser gain chip as the forward voltage of the laser diode increased with increasing temperature rather than decreasing, indicating that the forward voltage changed while using the thermistor control.

After confirming the inability of the thermistor to sense the actual temperature of the laser diode gain chip, a forward voltage based temperature controller was developed. In this temperature controlled system, the DC forward voltage drop was used to measure the temperature of the gain chip and used in a closed control feedback system to stabilize the temperature of the laser diode and thereby the emission wavelength. This feedback system had similar wavelength stability at constant operating temperature compared to the conventional thermistor control. However, when the ambient temperature was varied, the

laser diode emission wavelength again drifted despite the use of the forward voltage controlled based system. This wavelength drift was of similar magnitude to that of the thermistor controller but in the opposite direction. The wavelength drift measured using this technique was 4.5pm / °C, which is 90pm over the temperature range 15-35°C. The laser diode emission wavelength could potentially miss the gas absorption line which has a line width of 36pm.

This wavelength drift of the laser diode with ambient temperature suggested that another factor was contributing to the junction temperature measured with forward voltage. The technique measured the full voltage drop across the laser diode and did not take into consideration the series resistance of the laser diode. The laser diode series resistance was calculated from the voltage / current relationship of the laser diode. It was shown that the laser diode series resistance was temperature dependent and increased with increasing temperature, in contrast to the forward voltage of the laser diode which decreased with increasing temperature. The change in the series resistance was relatively small (131mΩ over temperature range 10 – 40 °C), though it had profound effect on the wavelength stability of the laser diode with temperature as discussed in the previous paragraph.

The laser diode series resistance was estimated experimentally using different methods such as a standard method, the Werner method and the Cheung and Cheung method. The laser diode series resistance was calculated above the threshold of the laser diode where the voltage drop increased linearly with increasing temperature. This temperature dependence of the laser diode series resistance was then incorporated in stabilising the laser diode emission wavelength in the junction voltage control technique.

A new setup was developed to stabilise the emission wavelength of the laser diode using its junction voltage. In this setup, the voltage drop due to the series resistance of the laser diode was subtracted from the forward voltage of the laser diode. The laser diode dynamic series resistance was calculated from the 1f signal of the lock-in amplifier by modulating its injection current with a sinusoidal signal. The emission wavelength of the laser diode had a wavelength stability ±0.7pm, 2 orders of magnitude better than that of both thermistor and forward voltage control over a period of 1 hour.

In TDLAS, the required wavelength stability of the laser diode emission is stringent. In a conventional TDLAS setup, the laser diode emission wavelength is locked to a reference wavelength such a gas molecular absorption line. The use of such a wavelength reference is

tedious and requires careful alignment of the laser light source to the reference gas cell. Previous work has shown that a wavelength stability of 1.6 kHz using methane and 40 kHz using acetylene gas absorption line can be achieved over a time period of few seconds.

The final goal of the thesis was to develop a new wavelength stability method that was compatible TDLAS using wavelength modulation spectroscopy (WMS). The challenge in integrating the junction voltage based control was the use of a slow ramp (in Hz) and fast sinusoidal modulation (in kHz) which is typical for TDLAS. In addition, the amplitude of the ramp was high making it harder to integrate (High forward voltage and the resultant series resistance) in WMS. By averaging the forward voltage using a low pass filter, the voltage drop across the laser diode was measured, whereas for dynamic resistance measurement the forward voltage was fed into a high pass filter and then to a lock-in amplifier. Thus, the junction voltage was calculated and the error signal was fed in the closed loop to stabilise the wavelength.

The performance of the junction voltage based controller was analysed by detecting different concentration of methane (0-2.5%), confirming its utility in gas detection. In addition, the performance of this wavelength control system was analysed for the effects of variable ambient temperatures. The junction voltage based wavelength control performed 8 times better than the conventional thermistor based setup with a wavelength drift of 0.24pm /°C.

In conclusion, the junction voltage of the laser diode can be used for the accurate temperature measurement of the laser junction temperature and can be used for stabilising laser diode wavelength. This method will overcome the complexity of placing the thermistor near the gain chip. Furthermore, junction voltage based wavelength stabilising technique can be implemented in TDLAS based WMS.

This project was successful in achieving its objective of stabilising the laser diode wavelength for application in TDLAS. This project has resulted in a patent for the newly developed method.

7.1 Future work

The wavelength stability scheme based on junction voltage control described in chapter 5 and 6 used an error signal to vary the temperature of the laser diode to stabilise the wavelength. The response of the feedback loop is relatively slow due to the slow response time of the Peltier cooler (a few Hz). In order to have a faster feedback loop, the error signal could be

fed into the laser diode injection current as reported in the frequency stabilization scheme using Fabry-Perot cavity by Favre *et al* [1] in chapter 2. Atomic transition or molecular absorption line frequency stabilisation schemes stabilise the laser diode frequency by feeding an error signal into the injection current of the laser diode. The current coefficient of a laser diode is smaller than that of the temperature coefficient. The disadvantage of feeding an error signal to the current source will cause the laser diode to operate above its maxing operating current. This may damage the laser diode and shortens its life time.

Synchronising computer based digital signal processing with analogue signals can be complicated. In the junction voltage based wavelength control system, the laser was modulated with the internal signal generator of the analogue lock - in amplifier and averaged in software based moving averaged filter. There was de synchronisation between the two. In addition, the proportional, integral and derivative (PID) feedback loop for wavelength controller was designed in National Instrument software LabVIEW, which also resulted in a synchronisation mismatch between the analogue signal generator of the lock - in amplifier and the PID. Moreover, when the junction voltage base wavelength control was integrated in WMS, two analogue modules of low pass and high pass filters in addition to the software based filters were used for signal conditioning. These analogue and digital signal processing modules further complicated and increased the desynchronisation.

To overcome the problem of the desynchronisation, all the signal processing and modulation module should be designed and implemented in software. To increase the resolution and response time, this could be implemented in a field programmable gate array (FPGA). The use of FPGA will not only overcome the problem of de synchronisation but also reduce the cost and size of the junction voltage control technique. In addition, an FPGA based junction voltage control module could easily be reconfigured for specific applications.

This wavelength stability control technique could be extended to VCSEL and light emitting diodes. An initial investigation has been completed, stabilising the emission wavelength of the laser diode by using the forward voltage method.

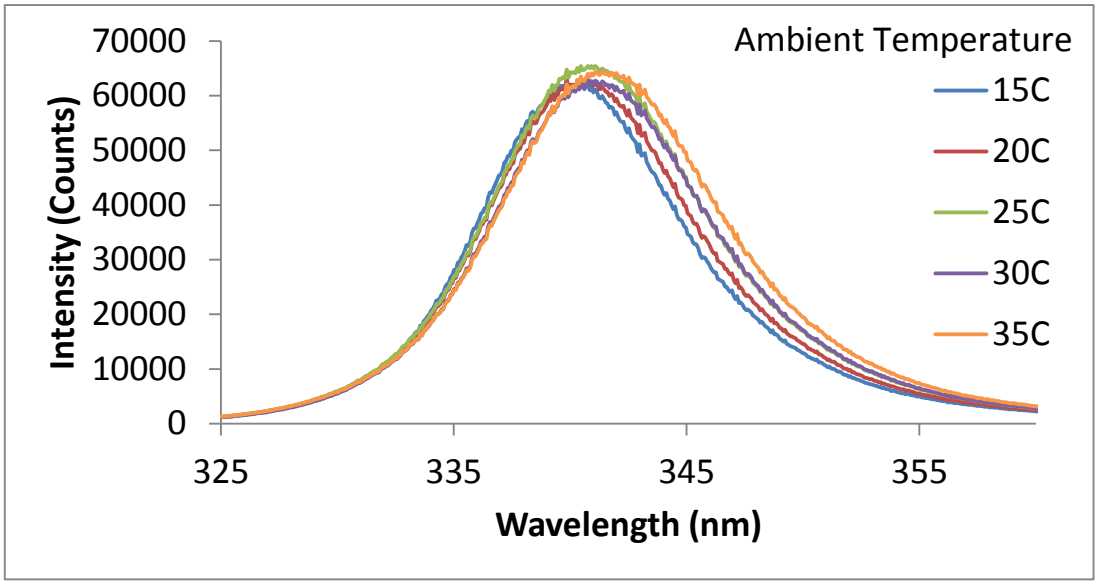

Figure 7.1 Emission wavelength of a light emitting diode with forward voltage based wavelength control

Figure 7.1shows the emission wavelength of LED at various ambient temperatures using a UV spectrometer (Avantes AvaSpec-ULS3648). The laser diode emission wavelength was controlled with forward voltage technique, similar to the one reported for laser diode in chapter 5. The LED emission drifted towards longer wavelength despite the forward voltage technique. This result suggests that, voltage drop due the series resistance of the diode is again contributing towards the forward voltage. Therefore, the contribution due to the series resistance should be subtracted from the forward voltage (resulting in junction voltage) and then used for stabilising the LED wavelength.

The temperature design and location of thermistors with respect to the gain chip is an expensive and difficult part of laser design. As the laser diode electrical characteristics are investigated during the manufacture process so, an FPGA based module, using junction voltage based wavelength control mechanism can be implemented in that stage.

7.2 References

[1] F. Favre and D. L. Guen, “High frequency stability of laser diode for heterodyne communication systems,” Electronics Letters, vol. 16, no. 18, pp. 709 - 710, 1980.

List of Publications

Patents

Laser diode temperature control, application number 1406664.1

A Asmari, J Hodgkinson, R P Tatam, UK

Conference presentations and papers

1. Direct measurement of the junction temperature of a DFB laser diode used in tunable diode laser spectroscopy. A Asmari, F Chen, J Hodgkinson and R P Tatam Proc Photon 12, Durham, UK, Sept 2012

2. Comparison of methods to measure and control the temperature of a distributed feedback laser diode used in tunable diode laser spectroscopy. A Asmari, J Hodgkinson, S Staines and R P Tatam The Celebration of the 50th Anniversary of the Diode Laser, 20-21 September 2012, Coventry, UK

3. A new technique to stabilise the emission wavelength of laser diodes for use in TDLS A Asmari, J Hodgkinson, E Chehura, S E Staines and R P Tatam Presented at FLAIR 2014 (Field Laser Applications in Industry and Research), Florence, Italy, May 2014

4. Wavelength stabilisation of a DFB laser diode using measurement of junction voltage A Asmari, J Hodgkinson, E Chehura, S E Staines and R P Tatam. Proc SPIE 9135, 9135-46, 2014

Planned Publications

1. Wavelength stabilisation of a DFB laser diode using measurement of junction voltage

   A Asmari, J Hodgkinson, E Chehura, SE Staines and RP Tatam

   Target journal. Optical Express (ready for submission)

2. Laser Diode junction temperature measurement method for three different type light sources. A Asmari, J Hodgkinson, S Staines and RP Tatam.

Target journal: Journal of Light wave Technology. (In preparation)

3. Comparing different techniques for measuring laser diode junction temperature measurement. A Asmari, J Hodgkinson, E Chehura, SE Staines and RP Tatam.

Target journal: Journal of Lightwave Technology. (In preparation)

4. Tunable laser diode spectroscopy using a novel method of stabilising laser diode wavelength. A Asmari, J Hodgkinson, E Chehura, SE Staines and RP Tatam.

Target journal: Applied Physics B (In preparation)

5. Laser diode resistance measurement methods. A Asmari, J Hodgkinson, E Chehura, SE Staines and RP Tatam.

Target Journal: Journal of Lightwave Technology. (In preparation)

Appendix A

The following figure shows the circuit diagram for the constant current pulse source used for measuring the forward voltage of the laser diode and light emitting diode.

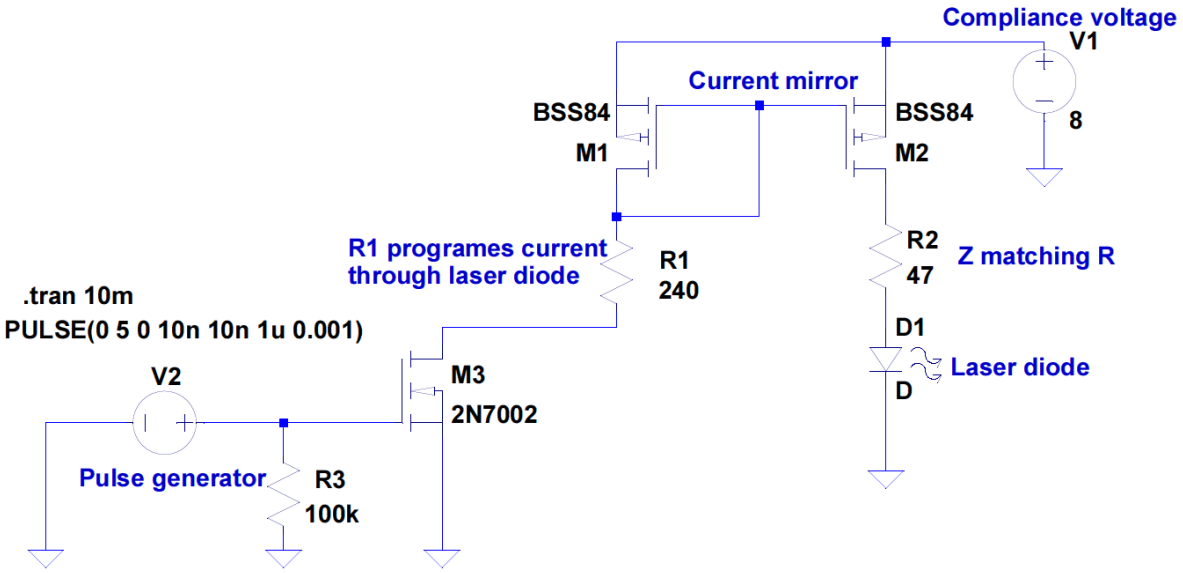

Figure (1) Schematic for the current controlled current pulse sorce used in forward voltage method

Figure (1) is the schematic circuit drawn in LT spice IV. This circuit was then printed and built on a PCB. The two field effect transistors (FET) forming the current mirror circuit ensured a constant current pulse is delivered to the cathode ground laser diode. A BNC 555 pulse generator was used to switch on the FET M3 to allow the current pass through the laser diode and to determine the width and the pulse rate of the current pulse applied to the laser diode.

Figure (2) shows voltage pulse measured across the laser diode. This pulsed voltage was used to calibrate the laser diode for temperature measurement in forward voltage method. Figure (3) is the zoomed in voltage pulse measured across the laser diode. Figure (3) shows that the pulse delivered to the diode maintained its shape; despite the capacitive nature of the diode.

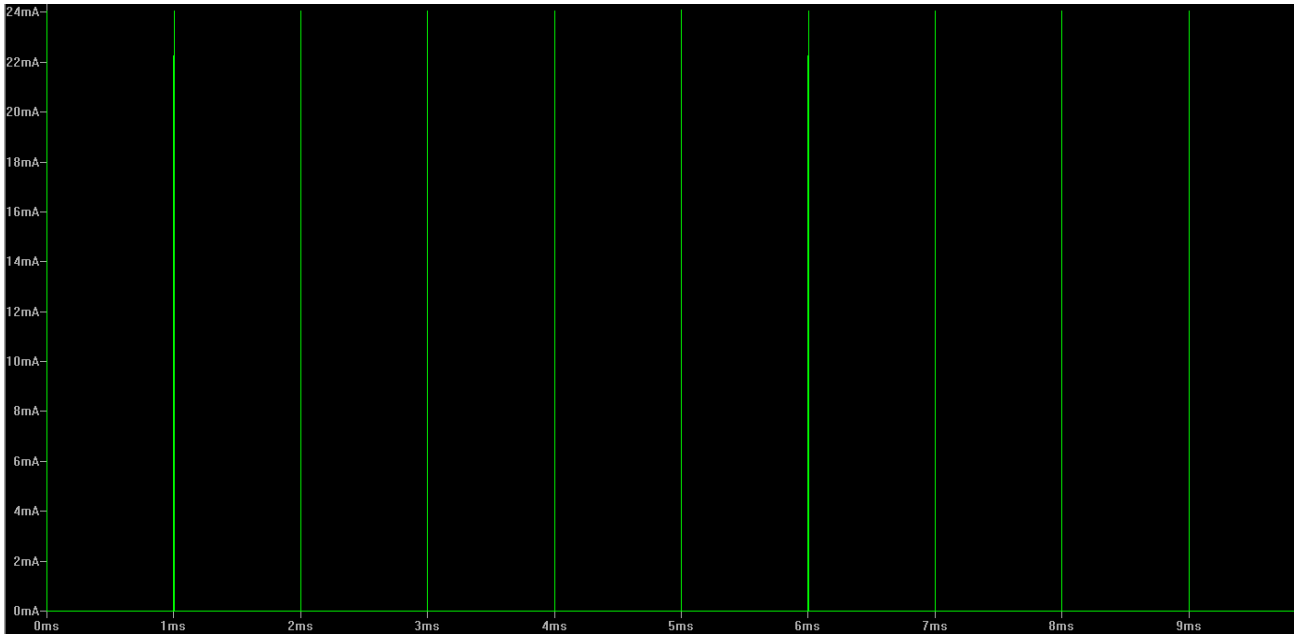

Figure (2) Pulsed voltage measure across ta diode with pulse width of 1us and pulse rate of 1mS

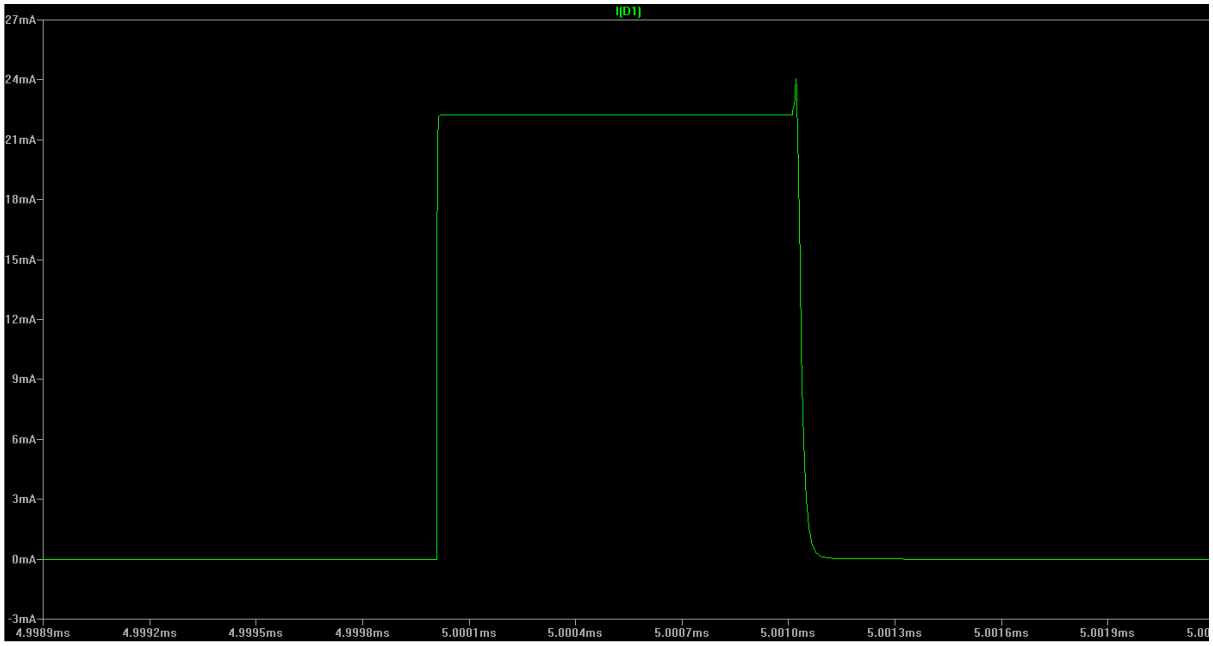

Figure(3) Zoomed in version of the pulsed voltage measured across the diode

Appendix B

LabVIEW Code for Forward voltage

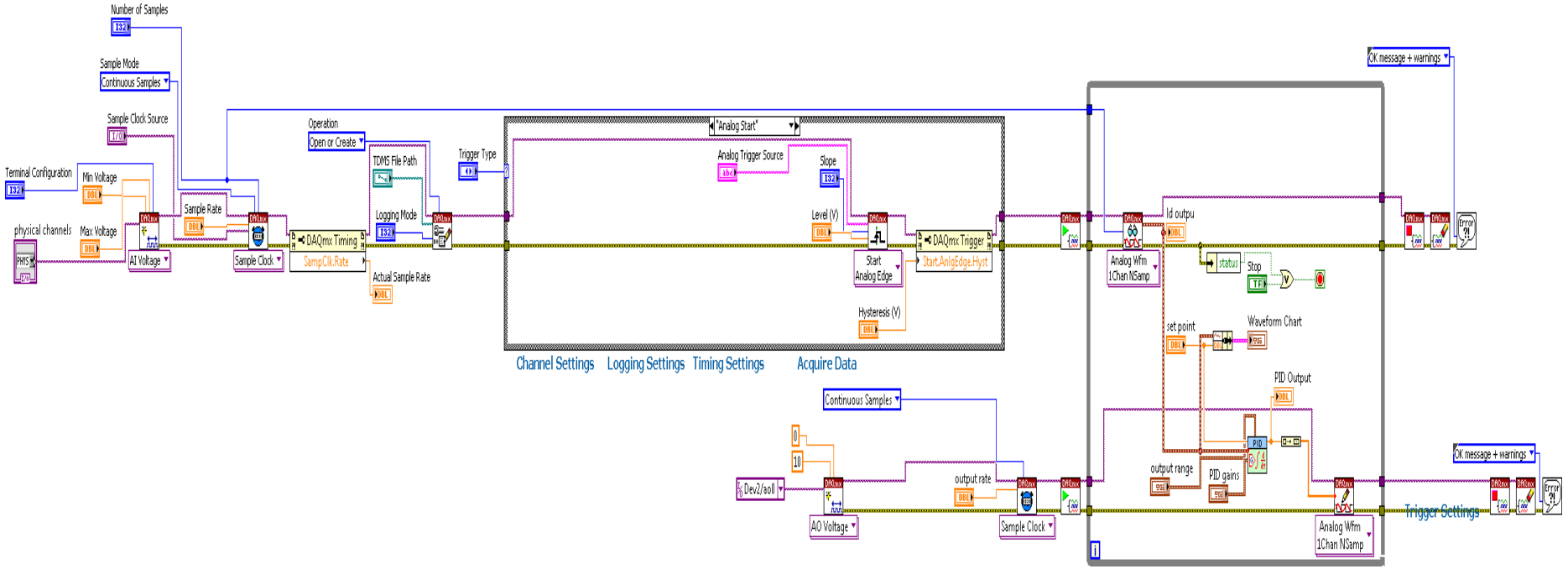

Figure (1) LabVIEW code for Forward voltage method

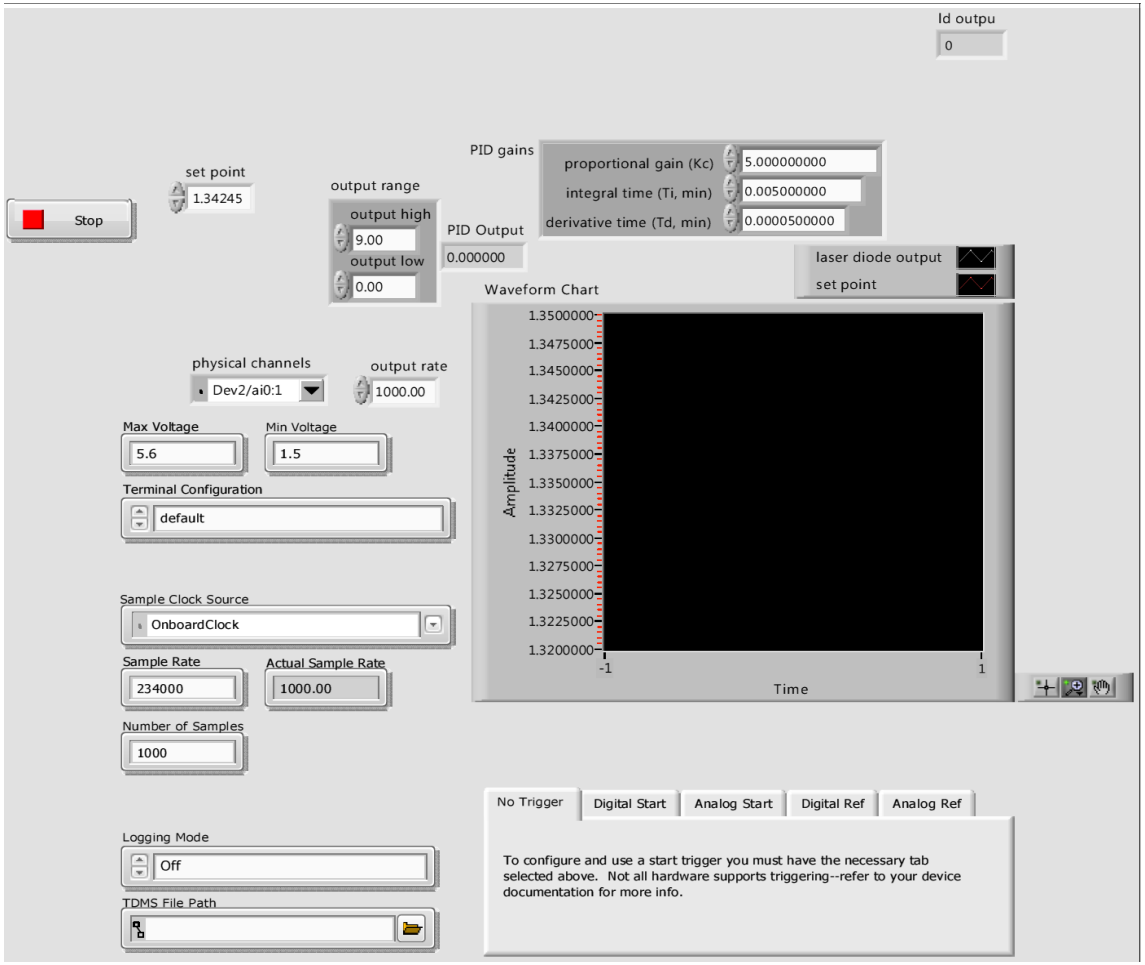

Figure (2) Front panel for the forward voltage method LabVIEW code

LabVIEW code for Junction Voltage control method

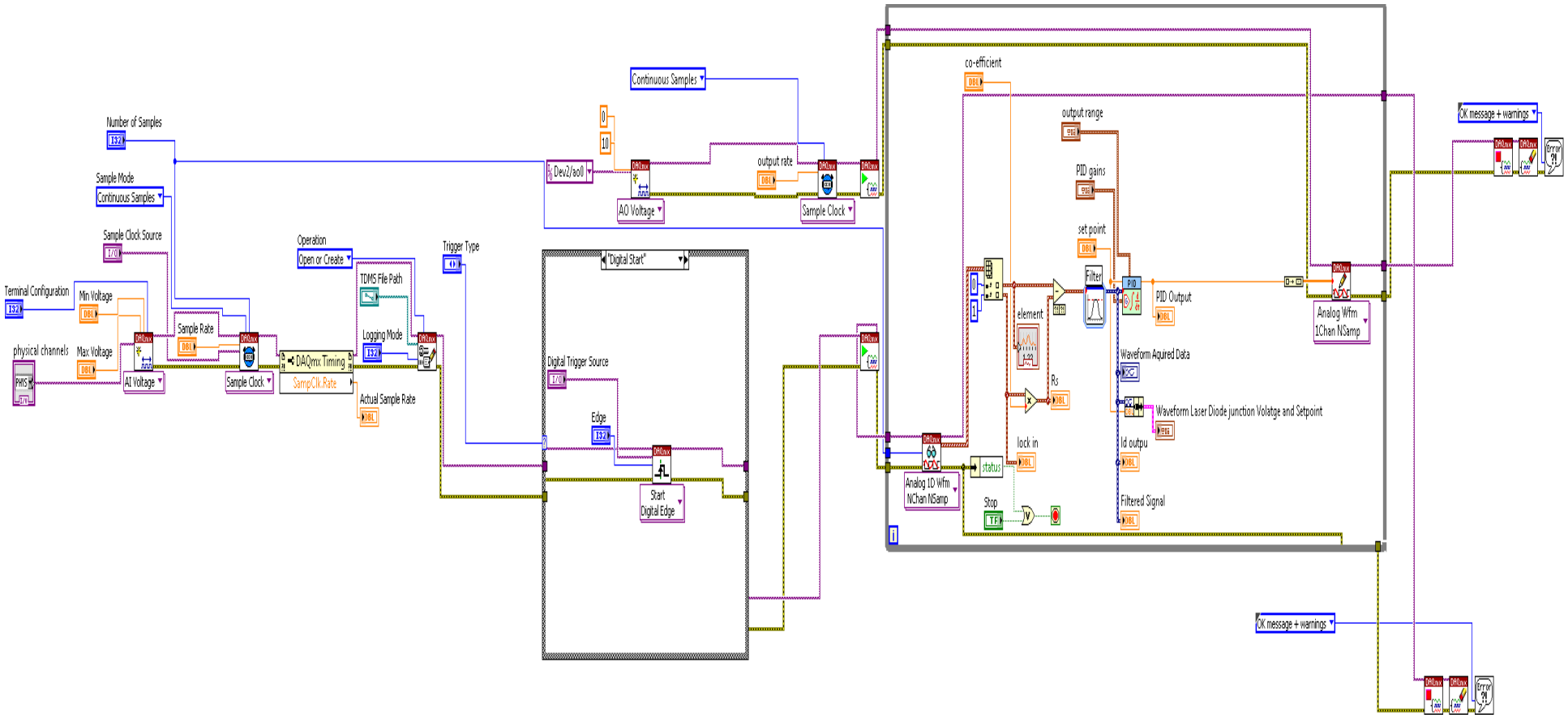

Figure (3) LabVIEW code for junction voltage control technique (block diagram)

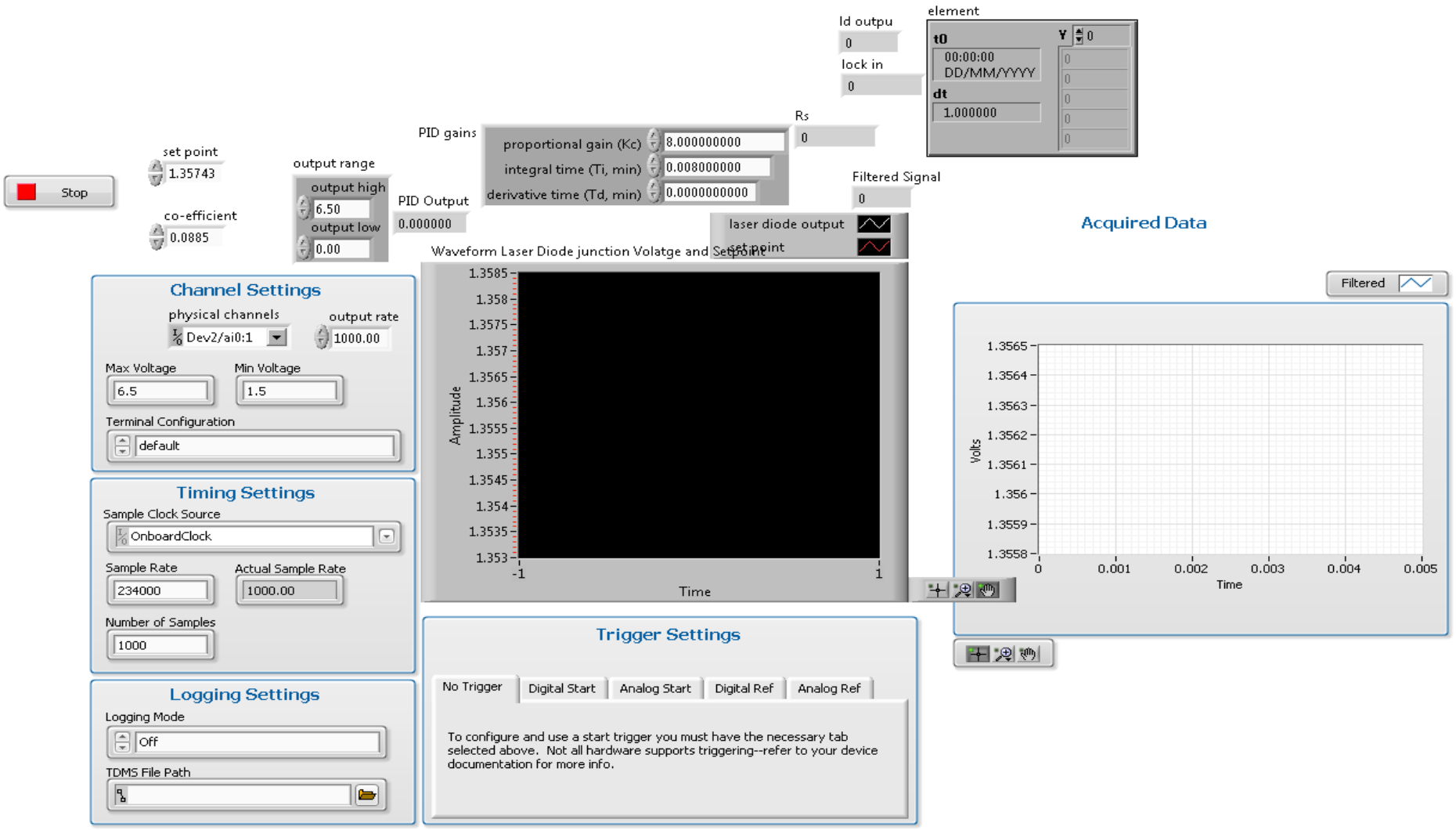

Figure (4) Front panel of the LabVIEW code for junction voltage control technique